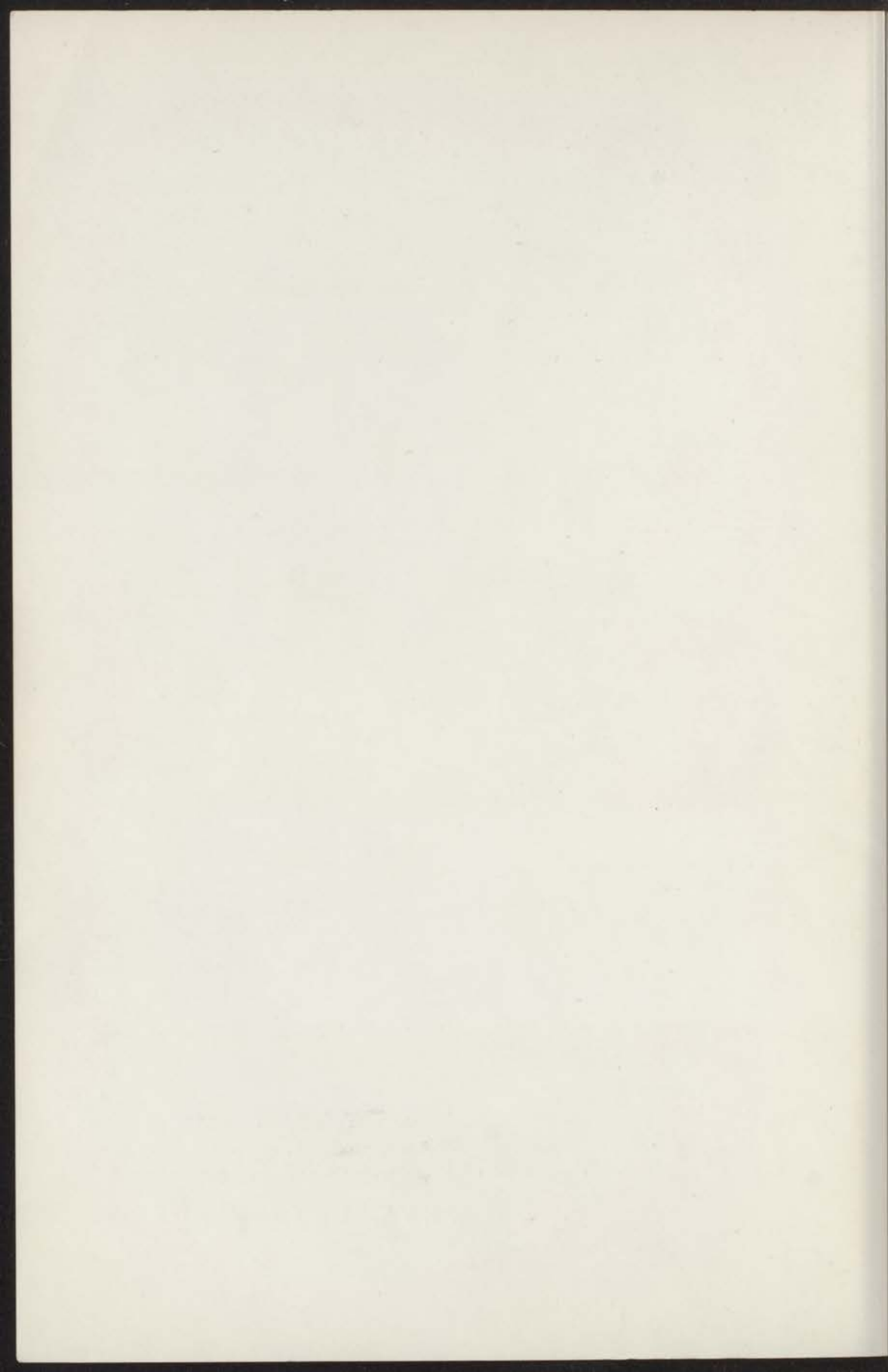


VARIOUS ASPECTS OF
PARAMAGNETIC RELAXATIONS



INSTITUUT-LORENTZ
voor theoretische natuurkunde
Nieuwsteeg 18-Leiden-Nederland

A. J. VAN DUYNVELDT



VARIOUS ASPECTS OF
PARAMAGNETIC RELAXATIONS

19 NOV. 1969

PROEFSCHEFT

DE VERZAMELING VAN DE VRAAG VAN LUSTEN
IN DE WERELD DE EN WAT OVERHOORDE LUSTEN VAN DE
WILDEWISSELSCHAP TE LEIDEN
OP DEZELVE VAN DE RECTOR MAGISTRUS DR. J. H. H. H. H.
HOUTERMAN IN DE FACULTEIT DER WETENSCHAPPEN
TER OORDEELING VAN HEN VERDIENDE OEF DE WERELD
TE VERVOLGEN OP DONNERDAG 7 DECEMBER 1969
TE WAREN 10.14 HUR

ADRIANUS JOHANNES VAN DUYNVELD
LEIDEN TE WAREN 1969

Kast dissertaties

INSTITUUT-LORENTZ
voor theoretische natuurkunde
Nieuwsteeg 18-Leiden-Nederland

last observations

VARIOUS ASPECTS OF PARAMAGNETIC RELAXATIONS

PROEFSCHRIFT

TER VERKRIJGING VAN DE GRAAD VAN DOCTOR
IN DE WISKUNDE EN NATUURWETENSCHAPPEN AAN DE
RIJKSUNIVERSITEIT TE LEIDEN,
OP GEZAG VAN DE RECTOR MAGNIFICUS DR. J. GOSLINGS,
HOGLERAAR IN DE FACULTEIT DER GENEESKUNDE,
TEN OVERSTAAN VAN EEN COMMISSIE UIT DE SENAAT
TE VERDEDIGEN OP WOENSDAG 3 DECEMBER 1969
TE KLOKKE 16.15 UUR

DOOR

ADRIANUS JOHANNES VAN DUYNVELD
GEBOREN TE 'S-GRAVENHAGE IN 1942

INSTITUUT-LORENTZ
voor theoretische natuurkunde
Nieuwsteeg 18-Leiden-Nederland

1969

KONINKLIJKE DRUKKERIJ VAN DE GARDE N.V.
ZALTBOMMEL

PARAMAGNETIC RELAXATIONS OF VARIOUS ASPECTS OF

PROPOSCHRIJFT

DE VERBODING VAN DE GEBOD VAN DOCTOR
IN DE WISSENSCHAP EN NATUURWETENSCHAPPEN VAN DE
HILFSGEWERENDE RECHTS- EN WETENSCAPEN
DE RECHTS- EN WETENSCAPEN VAN DE RECHTS- EN WETENSCAPEN
HOOGESCHOOL IN DE RECHTS- EN WETENSCAPEN
VAN OOSTERLAND VAN DEN GEMENSCHAP VAN DE RECHTS-
EN WETENSCAPEN VAN OOSTERLAND 1 DECEMBER 1947
TE ROTTERDAM

Promotor: PROF. DR. C. J. GORTER

DOOR

ADRIANUS JOHANNES VAN DUYNVELDT
GEBOREN TE GEDAGTE IN 1911

INSTITUUT-LORDS
VAN DE RECHTS- EN WETENSCAPEN
HILFSGEWERENDE RECHTS- EN WETENSCAPEN

ROTHSCHEDE BOEKRIJST VAN DE GARDIE VAN
ROTTERDAM

CONTENTS

PREFACE		vii
CHAPTER I. THE RELATIONSHIP OF THE TWO SEXES		1
1. Introduction		1
2. Theoretical background		10
3. Empirical studies		15
4. Conclusions		25
a. Summary		25
b. Recommendations		26
CHAPTER II. PSYCHOLOGICAL DEVELOPMENT OF THE CHILD		27
1. Introduction		27
2. Theoretical background		30
3. Empirical studies		35
a. The role of the mother in the child's development		35
b. The role of the father in the child's development		40
c. The role of the child in the family		45
d. The role of the child in society		50
e. The role of the child in the world		55
4. Conclusions		60
a. Summary		60
b. Recommendations		65
c. Further research		70
5. Appendix		75
CHAPTER III. THE PSYCHOLOGICAL DEVELOPMENT OF THE ADULT		76
1. Introduction		76
2. Theoretical background		80
3. Empirical studies		85
a. Psychological growth		85
b. Physical growth		90
c. Social growth		95
4. Conclusions		100
a. Summary		100
b. Recommendations		105

*Aan Marijke
en de kinderen*

Presented by PROF. DR. C. J. GORTER

1952
1953

CONTENTS

INTRODUCTION	9
CHAPTER I. CROSS RELAXATION IN DILUTED NICKEL FLUOSILICATE AND CHROMIUM CESIUM ALUM CRYSTALS	
1. Introduction	13
2. Samples	15
3. Experimental technique	16
4. Experimental results	18
5. Discussion	25
a. External fields	25
b. Internal fields	26
c. Relaxation times	31
CHAPTER II. PARAMAGNETIC RELAXATION PHENOMENA IN NICKEL-LANTHANUM DOUBLE NITRATE	
1. Introduction	35
2. Samples	36
3. Results	37
a. 100% $\text{Ni}_3\text{La}_2(\text{NO}_3)_{12} \cdot 24\text{H}_2\text{O}$, external magnetic field $H_e // c$ axis	37
b. 100% $\text{Ni}_3\text{La}_2(\text{NO}_3)_{12} \cdot 24\text{H}_2\text{O}$, external magnetic field $H_e \perp c$ axis	39
c. 60% $\text{Ni}_3\text{La}_2(\text{NO}_3)_{12} \cdot 24\text{H}_2\text{O}$, $H_e // c$ axis	40
d. 20% $\text{Ni}_3\text{La}_2(\text{NO}_3)_{12} \cdot 24\text{H}_2\text{O}$, $H_e // c$ axis	40
e. 7% $\text{Ni}_3\text{La}_2(\text{NO}_3)_{12} \cdot 24\text{H}_2\text{O}$, $H_e // c$ axis	41
f. b/C values	42
4. Discussion	42
a. Cross relaxations in 7% $\text{Ni}_3\text{La}_2(\text{NO}_3)_{12} \cdot 24\text{H}_2\text{O}$	42
b. Fast relaxation processes in 100% and 60% $\text{Ni}_3\text{La}_2(\text{NO}_3)_{12} \cdot 24\text{H}_2\text{O}$	44
c. b/C values	47
5. Conclusion	48
CHAPTER III. SPIN-LATTICE RELAXATION IN MANGANESE FLUOSILICATE	
1. Introduction	49
2. Experimental methods, samples	50
3. Experimental results	51
a. Nondiluted samples	51
b. Diluted samples	54
c. b/C values	55
4. Discussion	56
5. Conclusions	59

CHAPTER IV. SPIN-LATTICE RELAXATION IN ERBIUM ETHYLSULPHATE	60
1. Introduction	60
2. Experimental results	61
a. Erbium ethylsulphate; $H_c \perp c$ axis	64
b. Erbium ethylsulphate; powdered samples	65
c. Erbium ethylsulphate; $H_c // c$ axis	67
3. Discussion	67
4. Conclusion	68

CHAPTER V. THE INFLUENCE OF NONMAGNETIC IMPURITIES ON THE PARAMAGNETIC SPIN-LATTICE RELAXATION IN COPPER TUTTON SALTS	70
1. Introduction	70
2. Experimental results	73
3. Discussion	78
4. Conclusion	81

CHAPTER VI. RELAXATION MEASUREMENTS ON $MnCl_2 \cdot 4H_2O$ AND $MnBr_2 \cdot 4H_2O$	82
1. Introduction	82
2. The field-step method and the character of the results to be expected	83
3. Experimental results	84
3.1. Relaxation measurements	84
3.2. Measurements of the adiabatic susceptibility χ_{ad}	87
4. Discussion of the relaxation measurements	89

SAMENVATTING	92
------------------------	----

INTRODUCTION

Paramagnetic relaxation is the name for the processes which occur when the magnetization of a paramagnetic crystal tends toward equilibrium after a small change in one of the external conditions.

A theoretical paper by Waller¹⁾ in 1932 and the positive experimental result described by Gorter, *et al.*²⁾ in 1936 were the first of many publications on this subject. In Leiden paramagnetic spin-lattice and spin-spin relaxation phenomena have been observed using various experimental techniques. Difficulties in correlating the results obtained at different temperatures, using different equipment, lead De Vries in 1963³⁾ to construct a bridge with which one could measure the differential susceptibility for the frequencies intermediate between the range covered by the Hartshorn bridges ($\nu < 1$ kHz) and by the high frequency methods ($\nu > 1$ MHz). All the results described in this thesis were obtained with this apparatus. A selection has been made from the results of three years of experimental research. Many different aspects of paramagnetic relaxation come into the discussion, which may be somewhat confusing for readers who are not familiar with the topic, but which does underline the great flexibility of the equipment.

Three recent publications^{4, 5, 6)} give an almost complete description of the existing paramagnetic relaxation theories. As these reviews are available now for every interested research worker we shall just mention the relaxation processes which come into the discussion in this thesis.

In the theory one usually considers the behaviour of isolated ions in contact with the lattice modes (phonons). Though experiments are not performed on isolated ions the theories describe the results adequately.

A paramagnetic ion with energy eigenstates E_1 and E_2 can change states by creating or annihilating a phonon $\omega = |E_1 - E_2|/\hbar$. This mechanism leads to the so-called direct relaxation process. The energy $E_1 - E_2$ can also be exchanged with two phonons if a phonon ω_1 is created and a phonon ω_2 is destroyed so that $\hbar\omega_1 - \hbar\omega_2 = E_1 - E_2$. In the case of a quasi-Raman relaxation process this energy exchange takes place via a virtual intermediate state. If the two-phonon process occurs via a real intermediate state one gets a resonance type process, the so-called Orbach process. The different

processes can be recognized by their different dependence on temperature and external magnetic field. If the phonon modes allowed are given by the Debye distribution, the theoretical predictions can be summarized as follows:

- 1) Spin-lattice relaxation in a salt containing ions with an even number of electrons (non-Kramers salt), with two low-lying energy levels and with a third energy level at $\Delta \gg kT$. For low temperatures and large external magnetic fields the simplified expression for τ_L becomes:

$$\tau_L^{-1} = \underset{\text{(dir. pr.)}}{a_1 H^2 T} + \underset{\text{(Ram. pr.)}}{b_1 T^7} + \underset{\text{(Orbach pr.)}}{c_1 \exp(-\Delta/kT)} \quad (1)$$

- 2) Spin-lattice relaxation in salts containing ions with an odd number of electrons (Kramers salts). The expression for τ_L , if $\Delta \gg kT$, is:

$$\tau_L^{-1} = \underset{\text{(dir. pr.)}}{a_2 H^4 T} + \underset{\text{(Raman processes)}}{b_2 T^9} + \underset{\text{(Orbach pr.)}}{c_2 H^2 T^7} + d_2 \exp(-\Delta/kT) \quad (2)$$

while if $\Delta \ll kT$ the expression for τ_L becomes:

$$\tau_L^{-1} = \underset{\text{(dir. pr.)}}{a_3 H^4 T} + \underset{\text{(Raman processes)}}{b_3 T^5} + c_3 H^2 T^7 \quad (3)$$

The coefficients in the above expressions are such that the direct process dominates at the lowest temperatures.

In some cases an equilibrium population of energy levels of a paramagnetic ion can be reached by cross-relaxation processes. These relaxations occur at values of the external magnetic field where neighbouring ions can change states while causing only a relatively small variation in the total energy. The times of the cross-relaxation processes show an exponential behaviour ($\tau \propto \exp \beta(H - H_0)^2$) around the field value H_0 where the variation in total energy is zero. The associated magnetic moment may change considerably, so if one measures the susceptibility as a function of the external magnetic field, the cross relaxations appear as increases in the χ' vs. H_c curves with corresponding changes in χ'' . With the present equipment it is possible to determine many of the field values where the minima of the cross-relaxation times occur, to measure the actual cross-relaxation times, and also to obtain information on the specific heat of the various systems.

Chapter I of this thesis deals with cross-relaxation processes in diluted crystals of $\text{NiSiF}_6 \cdot 6\text{H}_2\text{O}$ and $\text{CrCs}(\text{SO}_4)_2 \cdot 12\text{H}_2\text{O}$. For both salts it has been possible to identify the energy transitions in neighbouring ions causing the observed cross relaxations. The exponential field dependence of the cross-relaxation time has been verified for some of the processes. The internal field values agreed with those obtained from other measurements.

In Chapter II relaxation phenomena in $\text{Ni}_3\text{La}_2(\text{NO}_3)_{12} \cdot 24\text{H}_2\text{O}$ are discussed. In diluted samples we demonstrated the occurrence of cross

relaxations between exchange-coupled nickel ion pairs. In the concentrated samples these cross relaxations are intermixed with the spin-lattice relaxation; as a result one observes a relaxation with an anomalous dependence on the external magnetic field.

In chapters III to VI measurements of the spin-lattice relaxation times in manganese fluosilicate, manganese chloride, erbium ethylsulphate and various copper Tutton salts are reported.

$\text{MnSiF}_6 \cdot 6\text{H}_2\text{O}$ (Ch. III). The occurrence of the T^5 dependence of the inverse relaxation time above 10 K (*cf.* eq. (3)) is demonstrated. At helium temperatures a direct relaxation process has been observed in a powdered specimen, but single crystals show more complex temperature dependences. The relaxation processes observed can be described with the assumption that the spin-lattice and the phonon-bottleneck relaxation times are of approximately equal magnitude at helium temperatures.

$\text{Er}(\text{C}_2\text{H}_5\text{SO}_4)_3 \cdot 9\text{H}_2\text{O}$ (Ch. IV). Above 4.2 K the spin-lattice relaxation time could be described by an exponential temperature dependence (Orbach process). At the temperatures of liquid helium and at external magnetic fields $H_e > 3$ kOe double relaxation processes have been observed. A detailed explanation of the relaxation mechanism cannot yet be given, but the results indicate that the poor heat contact between the sample and the liquid helium may have an important influence. The relaxation times show temperature dependences intermediate between those characteristic of an Orbach process and of a direct relaxation process.

Copper Tutton salts (Ch. V). In an extension of the work of De Vries *et al.*⁷⁾ the influence of nonmagnetic impurities on the place of the monovalent cation in the copper Tutton salts was studied. The observed fast relaxations have been related to irregularities in the orientation of the tetragonal symmetry axis in the mixed crystals and with the difference in ionic radii between impurity ions and replaced monovalent cations. The short relaxation times show an exponential temperature dependence ($\tau \propto \exp(\Delta/kT) - 1$) which might be explained if one would assume that low frequency phonons of energy Δ have an enhanced effect in the perturbation hamiltonian.

$\text{MnCl}_2 \cdot 4\text{H}_2\text{O}$ and $\text{MnBr}_2 \cdot 4\text{H}_2\text{O}$ (Ch. VI). In these samples the spin-lattice relaxation has been studied not only in the paramagnetic region but also in the antiferromagnetic state. For the chloride a relative maximum of the relaxation time at the transition temperature has been found, though below this temperature no single relaxation times have been observed. The thermodynamical relation $\tau = c_{\text{H}}/\alpha$ describes the maximum reasonably well if the heat transfer coefficient α does not vary at the transition temperature. The complete behaviour of antiferromagnetic spin-lattice relaxation cannot yet be understood. Above helium temperatures no evidence for a T^5 dependence of τ_{L}^{-1} has been found, the relaxation times are best described by $\tau_{\text{L}}^{-1} \propto T^7$

but the expected dependence on external magnetic field could not be verified. From the results obtained on the bromide it was not possible to get more insight into the antiferromagnetic spin-lattice relaxation.

REFERENCES

- 1) Waller, I., Z. Physik **79** (1932) 370.
- 2) Gorter, C. J., Physica **3** (1936) 503.
- 3) De Vries, A. J. and Livius, J. W. M., Commun. Kamerlingh Onnes Lab., Leiden No. 349a; Appl. sci. Res. **17** (1967) 31.
- 4) Manenkov, A. A. and Orbach, R., Spin-lattice relaxation in ionic solids, (Harper and Row, New York 1966).
- 5) Stevens, K. W. H., Reports on progress in physics, Vol. **XXX-1** (1967) 189.
- 6) Verstelle, J. C. and Curtis, D. A., Handbuch der Physik Bd **18/1** (1968).
- 7) De Vries, A. J., Curtis, D. A., Livius, J. W. M., Van Duyneveldt, A. J. and Gorter, C. J., Commun. Leiden No. 356a; Physica **36** (1967) 65.

CROSS RELAXATION IN DILUTED NICKEL FLUOSILICATE AND
CHROMIUM CESIUM ALUM CRYSTALS**Synopsis**

Paramagnetic cross-relaxation phenomena have been studied in nickel fluosilicate and chromium cesium alum crystals. Measurements were made at frequencies from 660 Hz to 1 MHz. In order to avoid spin-lattice effects temperatures as low as 2 K were chosen. In the nickel salt one-, two- and three-spin cross-relaxation processes were found. Their contributions to the paramagnetic susceptibilities were not very large but it was possible to determine some cross-relaxation times. The chromium alums were examined more closely. A wide variety of cross-relaxation processes was found, a five-spin process being the most complicated one. These processes had a considerable effect on the paramagnetic susceptibility. The cross-relaxation times were studied as a function of field in some detail. Comparison with theoretical predictions was satisfactory.

1. *Introduction.* In chromium potassium alum De Vrijer¹⁾ (1951) observed a new relaxation mechanism which he suggested to be a relaxation between two types of spin system. In a paper by Verstelle, *et al.*²⁾ measurements on diluted chromium alums were analysed; in these salts the "De Vrijer's third relaxation" was more pronounced and it was attributed to simultaneous upward and downward energy transitions in neighbouring ions. Bloembergen³⁾ classified these relaxation processes among his cross relaxations. However, earlier investigators never analysed the details of their results in terms of simultaneous energy transitions. In this paper measurements of cross-relaxation phenomena in diluted crystals of nickel fluosilicate and of chromium cesium alum are reported. For both salts it was possible to identify the energy transitions in neighbouring ions causing the cross relaxation.

The paramagnetic relaxation behaviour was studied by observing the two components of the complex susceptibility. Therefore the sample is placed in a constant magnetic field H_e and a parallel oscillating field of amplitude h such that the total field H is given by:

$$H = H_e + h \sin \omega t.$$

If the system is linear the magnetic behaviour can be described by the complex susceptibility, $\bar{\chi} = \chi' - i\chi''$. To describe spin-lattice relaxation the paramagnetic salt is usually supposed to consist of two or more systems. The so-called "spin-system" is connected with all the magnetic properties of the paramagnetic salt. At frequencies at which spin-lattice relaxation occurs the spin system is supposed to be in internal equilibrium, characterized by a spin temperature T_s (Casimir-du Pré⁴). Supposing that the energy transfer per second between spin-system and lattice, bath *etc.* is proportional to the temperature difference ($T_s - T_L$) one can derive the frequency dependence of $\bar{\chi}$:

$$\begin{aligned}\chi' &= \chi_{ad} + \frac{\chi_0 - \chi_{ad}}{1 + \tau_L^2 \omega^2} \\ \chi'' &= (\chi_0 - \chi_{ad}) \frac{\tau_L \omega}{1 + \tau_L^2 \omega^2}\end{aligned}\quad (1)$$

τ_L is the relaxation time of the energy transfer between the two systems. χ_0 is the static value of $\bar{\chi}$, which means $\bar{\chi}$ measured at frequencies being so low that the spin temperature is constant and thus does not follow the field variation. χ_{ad} is the value of $\bar{\chi}$ at frequencies where the spin-system follows the field variation without losing energy to the lattice. $\bar{\chi}$ has an analogous frequency dependence as derived by Debye⁵) for the case of dielectric relaxation. If the susceptibility has a frequency dependence as given in eq. (1) it is said to have a good Debye-shape with a relaxation time τ_L .

All processes occurring within the spin-system (spin-spin processes) reduce χ' to values less than χ_{ad} and lead to an increased value of χ'' in the same frequency range. In this paper we are interested in cross relaxation in which neighbouring ions are concerned. These processes are possible if we have ions with $S > \frac{1}{2}$ and if the splittings between the energy levels are of equal or almost equal magnitude. At certain magnetic fields H_0 two - or more - spin flips in neighbouring ions conserve energy while a considerable change of magnetic moment occurs. Also at field values close to H_0 these spin flips are possible, the dipole-dipole interactions of the whole spin-system being able to compensate small energy differences. If the possibility of cross relaxation is zero the spin-system is thought to consist of separate parts without direct interactions.

In analogy to Casimir and Du Pré's idea of spin-lattice relaxation, we may now consider the separate spin-systems to have equal temperatures if $\omega \ll \tau_{cr}^{-1}$ and to be isolated from each other at frequencies $\omega \gg \tau_{cr}^{-1}$. The susceptibility again has a Debye form (eq. (1)) but now $\bar{\chi}$ starts ($\omega \ll \tau_{cr}^{-1}$) at the value χ_{ad} and goes to a lower value χ_1 if $\omega \gg \tau_{cr}^{-1}$. τ_{cr} may then be considered as the time constant of the cross-relaxation process connecting the spin-systems.

The theoretical work of Bloembergen³⁾ gives a final expression for $\bar{\chi}$ which shows that the description given above is useful.

In this paper the number of spins characterising a cross-relaxation process will refer to the number of spin transitions involved.

2. *Samples.* a) The complexity of the earlier results on chromium potassium alum was the reason to search for cross relaxation in nickel fluosilicates. These salts have a simple magnetic structure so there is a better chance of understanding the effects observed. The nickel fluosilicate crystal has a hexagonal structure and the unit cell contains only one paramagnetic ion⁶⁾. The Ni²⁺ ion is surrounded by six water molecules which cause a crystalline field of nearly cubic symmetry with a trigonal distortion parallel to the *c* axis of the crystal. In most of the investigations the external field was parallel to the *c* axis; the lowest energy levels in this case are shown in fig. 1⁷⁾.

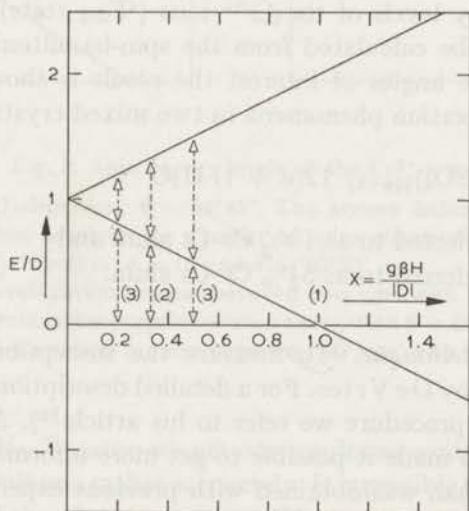
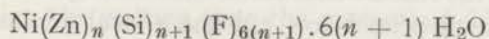


Fig. 1. Spin energy levels of the Ni²⁺-ion; H_e parallel to the tetragonal axis of the crystal ($\theta = 0^\circ$). The arrows indicate possibilities for cross-relaxation processes; within brackets the number of spins involved in the process.

In our frequency range cross-relaxation phenomena are found only in diluted samples. Crystals were grown from a solution of NiSiF₆ and ZnSiF₆ in water. The magnetic susceptibility of the crystals was compared with that of a nondiluted sample, which gave approximate determination of the concentration. We studied two samples, which are supposed to be mixed crystals:



one with $n = 4.5$, referred to as 18% NiSiF₆·6H₂O and one with $n = 16$, referred to as 6% NiSiF₆·6H₂O.

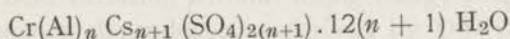
b) For comparison with the earlier work we also studied the chromium alums. Instead of the potassium alum the cesium alum was chosen, this crystal is more stable while no different splittings of the lowest energy levels are known.

In the alums the Cr³⁺ ions are placed in a face centered cubic lattice. The ion is surrounded by eight water molecules, causing an electric field of cubic symmetry with small trigonal distortions along the body diagonals of the cube. There are four ions in a unit cell⁸). Measurements were carried out with the magnetic field H_c in two different crystal directions:

i) the [100]-direction, giving an identical position of the four ions with respect to the magnetic field, the angle θ between H_c and the trigonal axis being 54°45' for all ions.

ii) the [111]-direction, giving $\theta = 0^\circ$ for one ion and $\theta = 70^\circ30'$ for the other three.

The lowest energy levels of the Cr³⁺ ions (⁴F_{3/2} state) as a function of magnetic field can be calculated from the spin-hamiltonian (e.g. Schulz-Dubois⁹). For the angles of interest the result is shown in fig. 2. We measured cross-relaxation phenomena in two mixed crystals:



one with $n = 9$, referred to as 10% Cr-Cs alum and one with $n = 17$, referred to as 5½% Cr-Cs alum.

3. *Experimental technique.* To measure the susceptibility we used the apparatus designed by De Vries. For a detailed description of the equipment and the measuring procedure we refer to his article¹⁰). A few points may be mentioned which made it possible to get more information about cross-relaxation effects than was obtained with previous experimental methods.

a) One bridge may be used in the wide frequency range from 500 Hz to 1 MHz.

b) The overall sensitivity of the bridge permits us to carry out measurements with diluted single crystals.

c) Measurements normally are made with a slowly varying magnetic field H_c . On a dual channel X-Y writer the horizontal signal is proportional to the field H_c , the two vertical ones are proportional to χ' and χ'' respectively. By assuming that at the measuring frequency $\chi'(H_c=0)$ is equal to χ_0 one easily finds χ'/χ_0 vs H_c and χ''/χ_0 vs H_c . If χ'' is small, it is still possible to get information about cross relaxation, just by looking for minima in the curve χ'' vs H_c . So, if at a field H_0 the relaxation is faster than in neighbouring fields, then the absorption at frequencies below τ_{cr}^{-1} has a local minimum

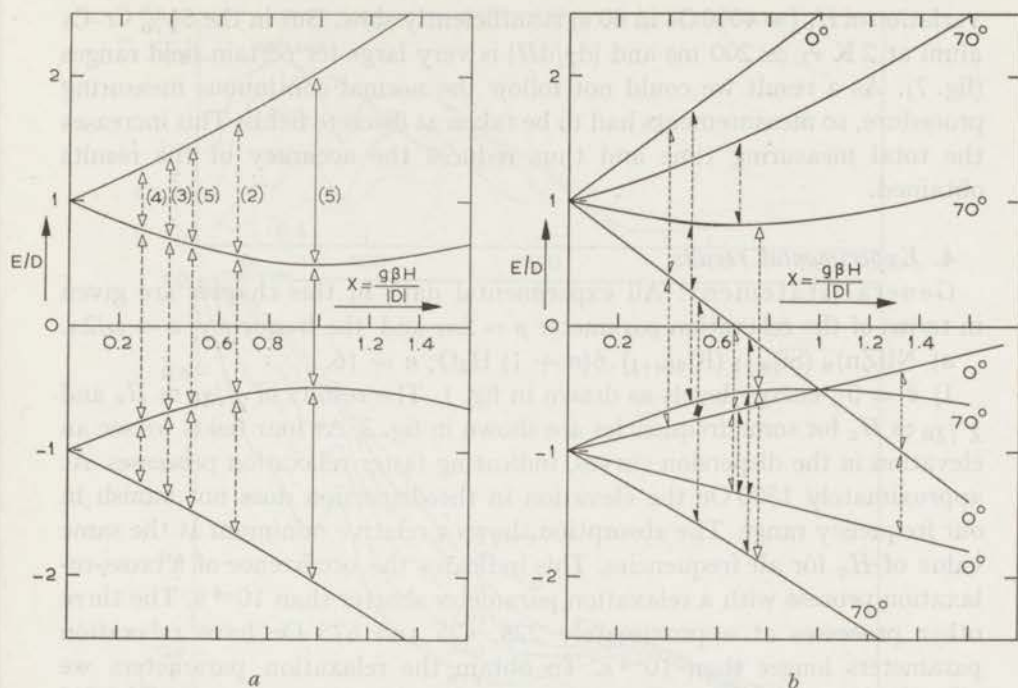


Fig. 2. Spin energy levels of the Cr^{3+} -ion.

a) H_c parallel to the [100]-direction; $\theta = 54^\circ 45'$. The arrows indicate possibilities for cross-relaxation processes; within brackets the number of spins effectively involved in the process.

b) H_c parallel to the [111]-direction; $\theta = 0^\circ$ and $\theta = 70^\circ 30'$.

↳ possibility for a cross-relaxation process between two ions with $\theta = 0^\circ$,

▲ possibility for a cross-relaxation process between an ion with $\theta = 0^\circ$ and one with $\theta = 70^\circ 30'$,

⧧ possibility for a cross-relaxation process between two ions with $\theta = 70^\circ 30'$.

around the value H_0 . Because we get our results as continuous functions of H_c we can localize minima rather accurately. It is possible in this way to detect cross relaxations if they have a very small intensity or even if they occur at frequencies far above 1 MHz. To measure cross relaxation within the spin-system we prefer conditions in which the spin-system is isolated from the lattice so that the cross relaxation is not influenced by spin-lattice relaxation. Decreasing the temperature makes spin-lattice relaxation slower; cross relaxation is temperature independent. Taking all measurements at approximately 2 K we sufficiently fulfilled this condition in many cases. For the $5\frac{1}{2}\%$ Cr-Cs alum this had the disadvantage that we could not do measurements with the slowly varying magnetic field. After a change in magnetic field the susceptibility χ goes to its equilibrium value χ_e with a time constant τ_L so we had to wait a time $t \gg \tau_L$ before we could measure the value χ_e . During the waiting time the magnetic field must not alter. Normally the

variation of H_c (≈ 4000 Oe in 60 s) is sufficiently slow. But in the 5½% Cr-Cs alum at 2 K $\tau_L \approx 200$ ms and $|d\chi/dH|$ is very large for certain field ranges (fig. 7). As a result we could not follow the normal continuous measuring procedure, so measurements had to be taken at discrete fields. This increases the total measuring time and thus reduces the accuracy of the results obtained.

4. Experimental results.

General statement: All experimental data in this chapter are given in terms of the relaxation parameter $\rho = 2\pi\tau$ and the frequency $\nu = \omega/2\pi$.

a) $\text{Ni}(\text{Zn})_n (\text{Si})_{n+1} (\text{F})_{6(n+1)} \cdot 6(n+1) \text{H}_2\text{O}$; $n = 16$.

1) $\theta = 0^\circ$, energy levels as drawn in fig. 1. The results of χ'/χ_0 vs H_c and χ''/χ_0 vs H_c for some frequencies are shown in fig. 3. At four fields we see an elevation in the dispersion curves, indicating faster relaxation processes. At approximately 1300 Oe the elevation in the dispersion does not vanish in our frequency range. The absorption shows a relative minimum at the same value of H_c for all frequencies. This indicates the occurrence of a cross-relaxation process with a relaxation parameter shorter than 10^{-6} s. The three other processes at approximately 225, 425 and 675 Oe have relaxation parameters longer than 10^{-6} s. To obtain the relaxation parameters we plotted χ'/χ_0 and χ''/χ_0 vs $\log \nu$ for a series of fields. The curves obtained did not have the Debye shape. This indicates that the times of the three cross-relaxation processes are too close together. The absorption and dispersion curves at each field should be interpreted as a sum of three Debye curves. We made an estimate of the relaxation parameters near the field values where they are shortest. Close to a field value where an energy-conserving spin jump is possible, $\Delta\chi'$ of the connected cross-relaxation process is at its maximum value³). Other cross relaxations, if they still occur at this field, give much lower contributions to the susceptibility. We therefore determined the frequency ν_{top} where χ'' is a maximum as a function of ν at a series of H_c -values. This ν_{top} merely has a simple meaning if H_c happens to be situated near one of the fields H_0 where energy-conserving spin jumps can occur. It then may be equal to $(\rho_{\text{cr}})^{-1}$. Fig. 4 demonstrates that in this way a clear estimate of ρ_{cr} as well as of the fields H_0 is possible. The resulting values of H_0 and ρ_{cr} are given in Table I.

It is interesting to compare the fields H_0 with the energy level scheme. The three values and the minimum of the fast relaxation at 1340 Oe give four field values H_0 at which cross relaxation occurs. The ratio between them is 0.17 : 0.32 : 0.50 : 1.00. If we look at the energy level scheme in fig. 1, the four simplest possibilities for an energy-conserving spin jump are found at field values in the ratio 0.20 : 0.33 : 0.50 : 1.00. The agreement is good, particularly if one takes into account that the sample orientation was not too accurate. A value of θ of a few degrees affects the low field behaviour

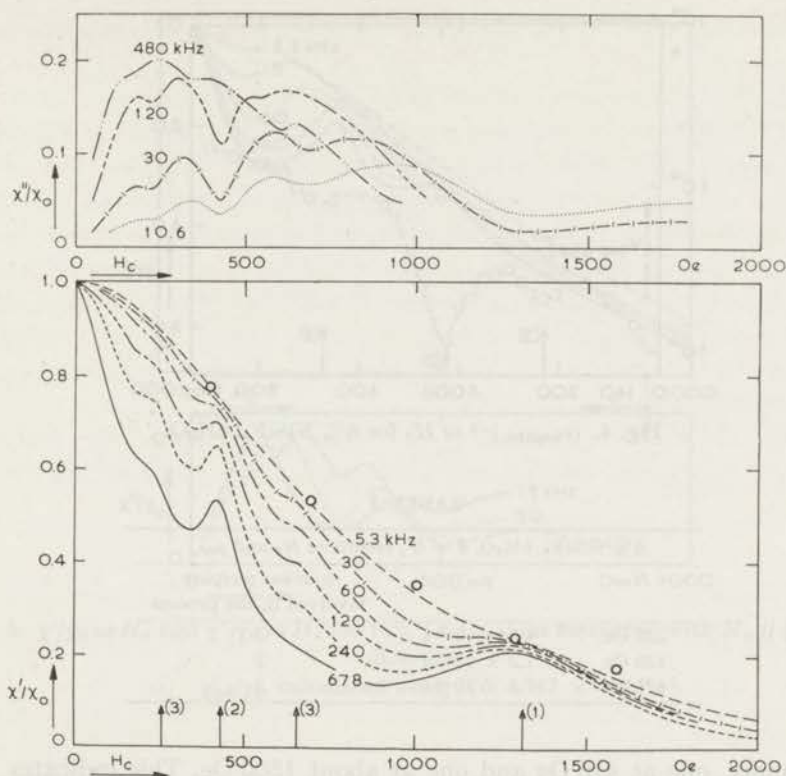


Fig. 3. χ'/χ_0 vs H_c and χ''/χ_0 vs H_c for 6% NiSiF₆·6H₂O measured with $\theta = 0^\circ$.
 ○: χ''_{ad}/χ_0 calculated using $b/C = 55 \times 10^4 \text{ Oe}^2$.

rather strongly. The energy levels become slightly curved near zero field and the cross relaxation at $x = 0.20$ (fig. 1) moves down.

From our results one finds for the zero field energy level splitting $D = -0.13 \text{ cm}^{-1}$ which is close to the value measured by resonance techniques¹¹).

General comparison of the relaxation parameters confirms the expectation that the cross-relaxation process becomes slower if more spins are involved in the energy-conserving process.

II) Measurements with $\theta = 90^\circ$ did not show any cross-relaxation processes. The energy level scheme in fact does not permit an energy-conserving one or two-spin jump. Above 2000 Oe more complicated processes are possible. Taking into account the results obtained at $\theta = 0^\circ$ it may be expected that it will be very difficult to detect such high-field low-frequency cross relaxations.

b) Ni(Zn)_n(Si)_{n+1}(F)_{6(n+1)}·6(n+1)H₂O; $n = 4\frac{1}{2}$. We only studied this salt parallel to the c axis ($\theta = 0^\circ$). For high frequencies χ''/χ_0 vs H_c showed

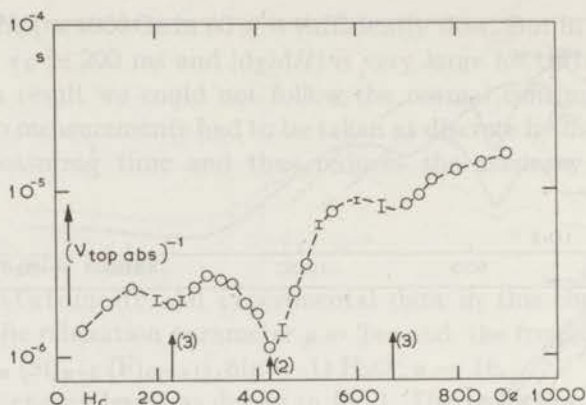


Fig. 4. $(v_{\text{topabs.}})^{-1}$ vs H_c for 6% NiSiF₆·6H₂O.

TABLE I

6% NiSiF ₆ ·6H ₂ O, $\theta = 0^\circ$, results of H_0 and ρ_{cr}		
H_0	ρ_{cr}	number of spins involved in the process
225 Oe	4.2×10^{-6} s	3
425 Oe	1.2×10^{-6} s	2
675 Oe	7.5×10^{-6} s	3

two minima, one at 475 Oe and one at about 1500 Oe. This indicates the occurrence of two cross-relaxation processes being too fast to be measured in our frequency range. These processes clearly correspond to those occurring at 425 Oe and 1340 Oe in the more diluted nickel fluosilicate and the D -value must be accordingly somewhat higher: $D \simeq -0.14 \text{ cm}^{-1}$.

c) Cr(Al)_{*n*}(Cs)_{*n*+1}(SO₄)_{2(*n*+1)}·12(*n*+1)H₂O; $n = 9$.

1) $H_c \parallel [100]$ -direction; $\theta = 54^\circ 45'$ for all ions. In fig. 2a the Cr³⁺ energy levels and the possibilities for energy-conserving spin jumps are presented.

For a few frequencies the results of χ'/χ_0 vs H_c and χ''/χ_0 vs H_c are shown in fig. 5. Around two field values $H_c = 300 (\pm 5)$ Oe and $H_c = 505 (\pm 5)$ Oe a considerable influence of cross-relaxation processes is noticeable. Zimmerman¹²⁾ kindly studied paramagnetic resonance at about 9 GHz in one of our crystals and found $D = -0.0715 \text{ cm}^{-1}$ at liquid helium temperatures. From this D -value one expects two- and three-spin jumps to occur at 307 Oe and 515 Oe. These values are slightly higher than those found in the present research (see also section 5).

The process at $H_c = 505$ Oe has a relaxation parameter $< 10^{-6}$ s. In order to obtain the relaxation times in the lower field range we plotted χ'/χ_0 vs $\log \nu$ and χ''/χ_0 vs $\log \nu$. Near the minimum of the relaxation time at 300 Oe the curves approach a Debye shape with $\rho_{\text{cr}} = 0.9 \times 10^{-6}$ s. At other field values the curves have to be described as a sum of more relaxation

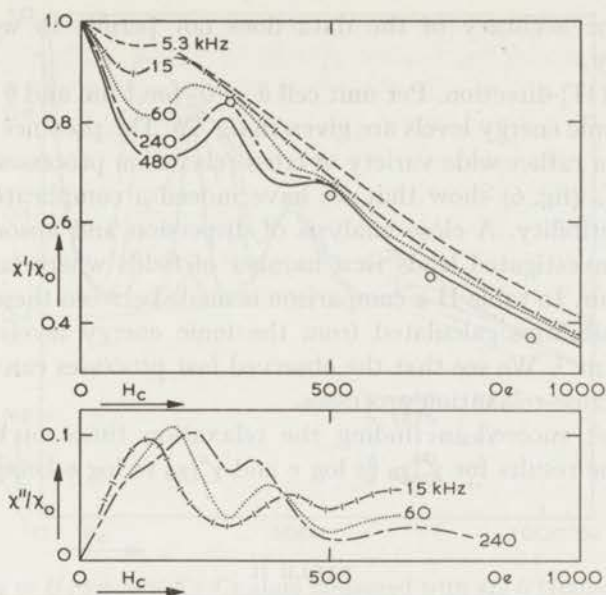


Fig. 5. χ'/χ_0 vs H_e and χ''/χ_0 vs H_e for 10% Cr-Cs alum measured with $H_e // [100]$ -direction.

○: χ_{ad}/χ_0 , calculated using $b/C = 47 \times 10^4 \text{ Oe}^2$.

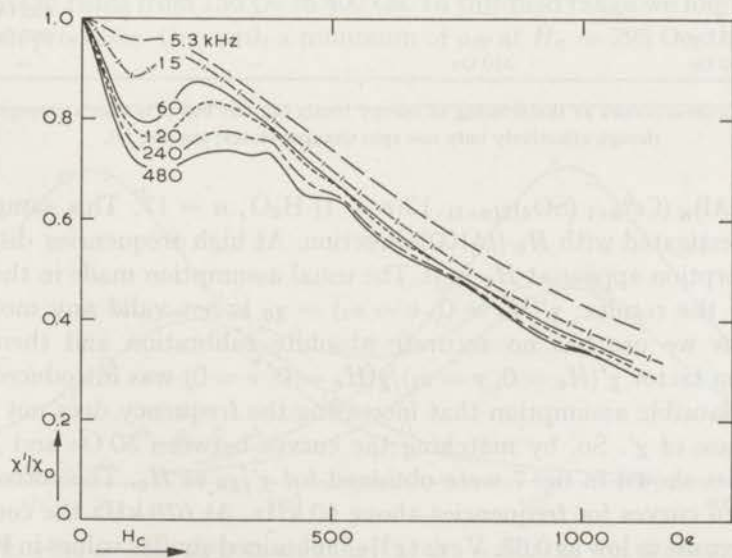


Fig. 6. χ'/χ_0 vs H_e for 10% Cr-Cs alum measured with $H_e // [111]$ -direction.

processes. The accuracy of the data does not permit to work this out quantitatively.

II. $H_c // [111]$ -direction. Per unit cell $\theta = 0^\circ$ for 1 ion and $\theta = 70^\circ 30'$ for 3 ions. The ionic energy levels are given in fig. 2b. The presence of two kinds of ions gives a rather wide variety of cross-relaxation processes. The results of χ'/χ_0 vs H_c (fig. 6) show that we have indeed a complicated behaviour of the susceptibility. A close analysis of dispersion and absorption for all frequencies investigated leads to a number of fields where fast relaxation processes occur. In table II a comparison is made between these field values and the possibilities calculated from the ionic energy levels using $D = -0.0715 \text{ cm}^{-1}$. We see that the observed fast processes can be explained by two-spin cross-relaxation processes.

We did not succeed in finding the relaxation times of the processes concerned, the results for χ'/χ_0 vs $\log \nu$ and χ''/χ_0 vs $\log \nu$ being too complicated.

TABLE II

10% Cr-Cs alum, H_c parallel to the [111]-direction			
Comparison between the fields where a fast cross-relaxation process is observed and those expected for 2-spin processes if $D = -0.0715 \text{ cm}^{-1}$			
measurements	expectations		
	2 ions with $\theta = 0^\circ$	2 ions with $\theta = 70\frac{1}{2}^\circ$	1 ion with $\theta = 0^\circ$ 1 ion with $\theta = 70\frac{1}{2}^\circ$
1010 Oe	1030 Oe	—	—
755 Oe	775 Oe*	—	—
570 Oe	—	590 Oe	570 Oe
530 Oe	515 Oe	—	535 Oe
—	—	—	405 Oe
385 Oe	—	—	385 Oe
300 Oe	310 Oe	—	—

*) This process occurs at the crossing of energy levels (fig. 2b) but it is also a two-spin process though effectively only one spin changes states; see also ¹³⁾.

d) $\text{Cr}(\text{Al})_n(\text{Cs})_{n+1}(\text{SO}_4)_{2(n+1)} \cdot 12(n+1) \text{H}_2\text{O}$; $n = 17$. This sample was only investigated with $H_c // [100]$ -direction. At high frequencies dispersion and absorption appear at $H_c = 0$. The usual assumption made in the calculation of the results: $\chi'(H_c = 0, \nu = \nu_1) = \chi_0$ is not valid any more. The apparatus we use has no accurate absolute calibration and therefore a correction factor $\chi'(H_c = 0, \nu = \nu_1)/\chi(H_c = 0, \nu = 0)$ was introduced based on the plausible assumption that increasing the frequency does not lead to an increase of χ' . So, by matching the curves between 50 Oe and 150 Oe, the results shown in fig. 7 were obtained for χ'/χ_0 vs H_c . The correction is applied to curves for frequencies above 60 kHz. At 678 kHz the correction factor became as low as 0.88. Verstelle²⁾ obtained similar values in Fe-NH₄ alum.

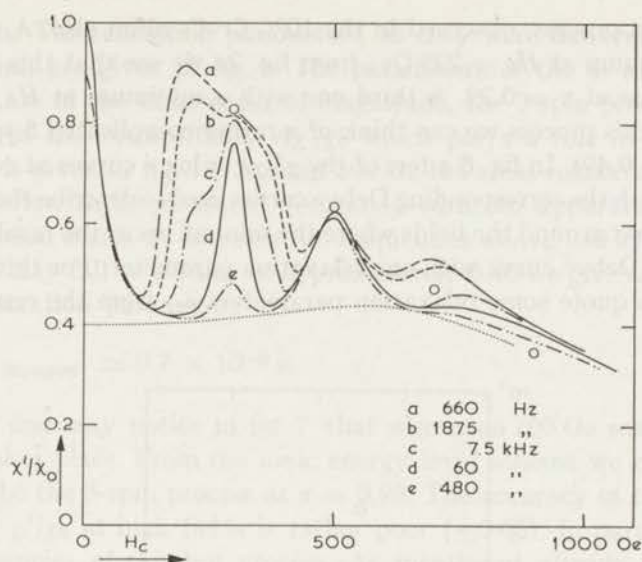


Fig. 7. χ'/χ_0 vs H_e for 5½% Cr-Cs alum measured with $H_e // [100]$ -direction.

○: χ_{ad}/χ_0 calculated using $b/C = 44 \times 10^4 \text{ Oe}^2$.

.....: χ_{is}/χ_0 as calculated by Verstelle¹⁵).

From the shape of the χ'/χ_0 vs H_e curves one may note immediately that cross relaxation again occurs near $H_e = 300 \text{ Oe}$ and $H_e = 500 \text{ Oe}$. The further dilution did increase the fraction of the susceptibility which participates in the cross-relaxation processes. This makes description of χ'/χ_0 vs $\log \nu$ and χ''/χ_0 vs $\log \nu$ with more than one standard Debye curve possible for a series of fields from 150 Oe to 400 Oe. In this field range we found three relaxation processes. One with a minimum of ρ_{er} at $H_e = 295 \text{ Oe}$, this must

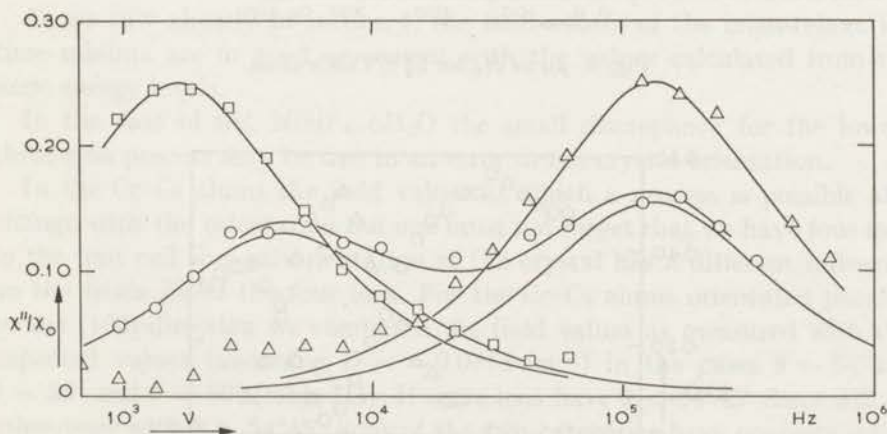


Fig. 8. χ''/χ_0 vs ν for 5½% Cr-Cs alum; Δ : $H_e = 310 \text{ Oe}$, \circ : $H_e = 270 \text{ Oe}$, \square : $H_e = 170 \text{ Oe}$; the lines show the standard Debye curves.

be the 3-spin process, observed in the 10% Cr-Cs alum also. A second one with a minimum at $H_c = 225$ Oe; from fig. 2a we see that this can be the 4-spin process at $x = 0.29$. A third one with a minimum at $H_c = 350$ Oe; to describe this process we can think of a rather complicated 5-spin process (fig. 2a, $x = 0.49$). In fig. 8 a few of the χ''/χ_0 vs $\log v$ curves at constant H_c are shown with the corresponding Debye curves used to describe the processes. We notice that around the fields where the minima occur the results are very close to one Debye curve with one relaxation parameter. For this reason we were able to quote some relaxation parameters ρ_{cr} from the results on the

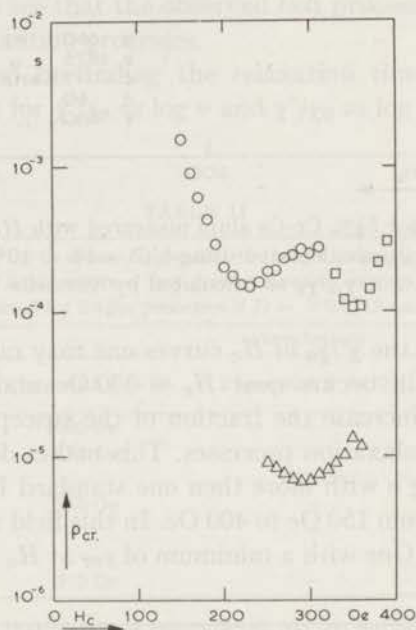


Fig. 9. ρ_{cr} vs H_c for 5½% Cr-Cs alum.

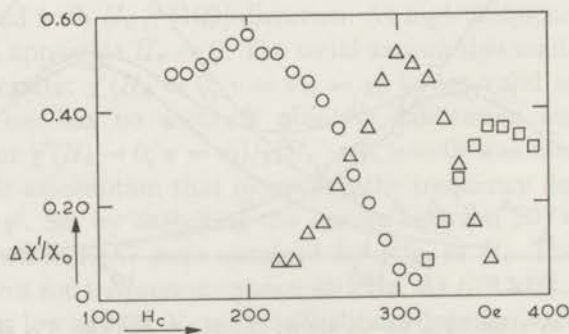


Fig. 10. $\Delta\chi/\chi_0$ vs H_c for 5½% Cr-Cs alum.

other salts. The relaxation parameters, as they were derived for the 5½% Cr-Cs alum, are given in fig. 9. The parameters of the 4- and the 5-spin processes are of the same order of magnitude, the 3-spin process is faster. The part of the susceptibility $\Delta\chi'/\chi_0$ which plays a role in the different processes is given in fig. 10. Around 500 Oe the cross-relaxation parameter is still too low to be measured accurately with our apparatus. At 500 Oe the dispersion starts to decrease for frequencies above 340 kHz. Assuming that χ'/χ_0 may fall to a value of approximately 0.40 we give as an estimate of the relaxation parameter:

$$(\rho_{cr})_{H_0=500} \simeq 0.7 \times 10^{-6} \text{ s.}$$

Finally one may notice in fig. 7 that also near 700 Oe some relaxation process takes place. From the ionic energy level scheme we conclude that this may be the 5-spin process at $x = 0.98$. The accuracy of the curves for χ'/χ_0 and χ''/χ_0 at high fields is rather poor (± 0.05), in particular at the low frequencies of this last process. As mentioned already in section 3, this is mainly due to the increase of measuring time in this highly diluted salt with its slow spin-lattice relaxation. The accuracy and the small effect of the cross relaxation on the susceptibility together do not allow us to derive ρ_{cr} vs H_c for a series of fields around 700 Oe. An estimate gives:

$$(\rho_{cr})_{H_0=700} \simeq 1.5 \times 10^{-3} \text{ s.}$$

5. *Discussion.* a) External fields. If a cross-relaxation process between neighbouring ions is possible, the fastest process occurs at the field H_0 where the spin jumps conserve energy exactly. At field values close to H_0 the process is only possible because the interaction in the spin-system can balance small energy differences; in this case the process becomes slower.

As we saw already in section 4, the field values of the cross-relaxation time minima are in good agreement with the values calculated from the ionic energy levels.

In the case of 6% NiSiF₆.6H₂O the small discrepancy for the lowest three-spin process may be due to an error in the crystal orientation.

In the Cr-Cs alums the field values at which a process is possible also change with the orientation but one must not forget that we have four ions in the unit cell so a misorientation of the crystal has a different influence on the fields H_0 of the four ions. For the Cr-Cs alums orientated parallel to the [100]-direction we compared the field values as measured with the expected values (assuming $D = -0.0715 \text{ cm}^{-1}$) in the cases $\theta = 54^\circ 45'$, $\theta = 50^\circ$ and $\theta = 60^\circ$ (table III). If some ions have $\theta < 54^\circ 45'$ there will be other ones with $\theta > 54^\circ 45'$; ions of the two categories have opposite influence on the fields H_0 . It seems plausible that a small error in the crystal orientation does not seriously affect the fields H_0 . In table III we notice

TABLE III

Field values of the cross-relaxation minima in Cr-Cs alum, $H_c // [100]$ -direction						
measured		calculated from the ionic energy level diagram ($D = -0.0715 \text{ cm}^{-1}$)			ratios*)	
10% Cr-Cs alum	5½% Cr-Cs alum	$\theta = 54\frac{1}{2}^\circ$	$\theta = 50^\circ$ **)	$\theta = 60^\circ$ **)	measured in 5½% Cr-Cs alum	calculated from the ionic energy level diagram
—	227 Oe	226 Oe	215 Oe	250 Oe	0.77	0.73
300 Oe	295 Oe	309 Oe	280 Oe	360 Oe	1.00	1.00
—	355 Oe	380 Oe	358 Oe	465 Oe	1.23	1.23
505 Oe	500 Oe	515 Oe	465 Oe	630 Oe	1.69	1.67
—	≈ 700 Oe	750 Oe	600 Oe	—	≈ 2.4	2.43

*) Ratios between the fields H_0 normalised on the field where the 3-spin cross relaxation occurs. These ratios show that an error in the D -value may be the reason for the small discrepancy between measured and calculated fields.

***) Calculated to show the influence of the crystal orientation.

that, if we assume $\theta = 54^\circ 45'$ for all ions, the field values in the 5½% Cr-Cs alum are somewhat low. We calculated the ratios between the fields in both cases (column 6 and 7) taking the field for the 3-spin process around $H_c = 300$ Oe as a standard. The agreement is quite good so we suppose that the value for $|D|$, which Zimmerman¹²⁾ measured in 10% Cr-Cs alum, is somewhat too high for this sample. We suggest $D = -0.068 \text{ cm}^{-1}$ for the 5½% Cr-Cs alum.

b) Internal fields. If the spin-system is in internal equilibrium but isolated from the lattice (measuring frequencies $\nu \gg \rho_L^{-1}$), then the susceptibility has its so-called adiabatic value: χ_{ad} . The theory of Casimir and Du Pré⁴⁾ gives for χ_{ad} :

$$\frac{\chi_{ad}}{\chi_0} = \frac{1}{1 + \frac{H_c^2}{b/C}} \quad (2)$$

where C is the Curie constant and b is defined by the specific heat at constant magnetization: $c_M (= c_{H=0}) = b/T^2$.

If we plot χ_{ad}/χ_0 vs H_c the value $(b/C)^{\frac{1}{2}}$ is easily detected as the field value where $\chi_{ad}/\chi_0 = 0.5$.

If the hamiltonian of the spin-system is given by:

$$\mathcal{H} = \mathcal{H}_z + \mathcal{H}_{el} + \mathcal{H}_{dip} + \mathcal{H}_{ex},$$

the specific heat c_M can be written as:

$$c_M = \frac{b}{T^2} = \frac{b_{el}}{T^2} + \frac{b_{dip}}{T^2} + \frac{b_{ex}}{T^2}$$

which may also be written as:

$$c_M = \frac{1}{2} \frac{C}{T^2} (H_{\text{el}}^2 + H_{\text{dip}}^2 + H_{\text{ex}}^2)$$

where

$$\frac{1}{2}CH_{\text{el}}^2 = b_{\text{el}} = \frac{1}{k} \langle \mathcal{H}_{\text{el}}^2 \rangle \quad \text{etc.}$$

The exact expression for \mathcal{H} and the theoretical foundations of this approach have been given by several authors, *e.g.* Verstelle²⁾, Caspers¹³⁾¹⁴⁾. In cross-relaxation processes, small energy differences are compensated by the dipolar and exchange interactions. From our measurements it is possible to get an approximate value of the internal field $H_1 = (H_{\text{dip}}^2 + H_{\text{ex}}^2)^{\frac{1}{2}}$, as will be shown in the next subsections. It is interesting to compare these results with the values as calculated from the crystal structure (table IV).

TABLE IV

	Measured and expected values of H_1^2		
	5½% Cr-Cs alum	10% Cr-Cs alum	6% NiSiF ₆ ·6H ₂ O
H_1^2 from cross-rel. measurements	$0.46 \times 10^4 \text{ Oe}^2$	$1 \times 10^4 \text{ Oe}^2$	$2.0 \times 10^4 \text{ Oe}^2$
H_1^2 from susc. close to $H_c = 0$	$0.50 \times 10^4 \text{ Oe}^2$	$< 2 \times 10^4 \text{ Oe}^2$	$4.6 \times 10^4 \text{ Oe}^2$
$H_1^2 (= H_{\text{dip}}^2 + H_{\text{ex}}^2)$ calculated	$0.56 \times 10^4 \text{ Oe}^2$ ($= H_{\text{dip}}^2$)	$1.0 \times 10^4 \text{ Oe}^2$ ($= H_{\text{dip}}^2$)	$H_{\text{dip}}^2 = 0.73 \times 10^4 \text{ Oe}^2$ $H_{\text{ex}}^2 = 5.0 \times 10^4 \text{ Oe}^2$ $H_1^2 \approx 5.7 \times 10^4 \text{ Oe}^2$

i) Bloembergen *et al.*³⁾ calculated the part of the susceptibility which undergoes the cross relaxation for a two-spin process. From their results the following expression can be derived for $\Delta\chi'$:

$$\Delta\chi' \propto \frac{\langle \mathcal{H}_{\text{int}}^2 \rangle}{\langle \mathcal{H}_{\text{int}}^2 \rangle + \frac{1}{6}N(\Delta E)^2} \quad (3)$$

\mathcal{H}_{int} is the part of the hamiltonian of the spin-system which consists of terms describing the dipolar and exchange interactions between pairs of ions. ΔE is the energy difference which has to be compensated within the spin-system. H_0 is the field at which the cross relaxation conserves energy, so $(\Delta E)_{H=H_0} = 0$. For the cross-relaxation processes of interest in the Cr-Cs alum with $H_c \parallel [100]$ -direction we can describe ΔE in the neighbourhood of $H = H_0$ as:

$$\Delta E = ag\beta(H - H_0) \quad (4)$$

with $a = 2.4$ for the 2-spin process around $H = 500$ Oe,
 $a = 4.1$,, ,, 3- ,, ,, ,, $H = 300$ Oe,
 $a = 6.5$,, ,, 4- ,, ,, ,, $H = 225$ Oe,
and $a = 7$,, ,, 5- ,, ,, ,, $H = 350$ Oe.

In the field ranges where we observe the processes these approximations are accurate within 10%.

Substituting (4) in equation (3) leads to:

$$\Delta\chi' \propto \frac{\langle \mathcal{H}_{\text{int}}^2 \rangle}{\langle \mathcal{H}_{\text{int}}^2 \rangle + \frac{1}{6}Na^2g^2\beta^2(H - H_0)^2},$$

and thus:

$$\frac{\Delta\chi'}{\chi_0} \propto \frac{1}{1 + \frac{(H - H_0)^2}{B^2}}, \quad (5)$$

with $B^{-2} = a^2A^{-2}$, and:

$$A^{-2} = \frac{1}{6} \frac{Ng^2\beta^2}{\langle \mathcal{H}_{\text{int}}^2 \rangle}. \quad (6)$$

Caspers¹⁴) pointed out that Bloembergen *et al.* made an error in the derivation of the relaxation times. However, the form of the dispersion as a function of ΔE should remain as expressed by equation (3).

We were able to compare our dispersion measurements of 5½% Cr-Cs alum with equation (5) for the 2-spin and the 3-spin processes. The two-spin cross-relaxation process around 500 Oe can be measured easily at frequencies ν : $\rho_L^{-1} \ll \nu \ll \rho_{\text{cr}}^{-1}$. In that case the dispersion shows directly that part of the susceptibility which will undergo the cross relaxation. Our measurements agree with a curve of the form:

$$\frac{\Delta\chi'}{\chi_0} = \frac{0.2}{1 + \left(\frac{H - H_0}{55 \pm 5} \right)^2}.$$

For the 3-spin process around 300 Oe $\Delta\chi'/\chi_0$ cannot be measured directly from the susceptibility, because the 4- and 5-spin cross-relaxation processes are possible rather close in field. The cross relaxation was shown to be of a Debye shape; in that case the part of the susceptibility which undergoes the relaxation for a certain magnetic field is equal to twice the maximum contribution to χ'' at that field (Casimir and Du Pré⁴). $\Delta\chi'/\chi_0$ as given by the maximum intensity of the absorption for the processes below 400 Oe is shown in fig. 10. Now the part of the susceptibility undergoing the 3-spin

process can be described by:

$$\frac{\Delta\chi'}{\chi_0} = \frac{0.5}{1 + \left(\frac{H - H_0}{35 \pm 5}\right)^2}$$

Equation (5) gives A^{-2} for a 2-spin process. Following Bloembergen *et al.*, A^{-2} for a 3-spin process can be calculated in a similar way; as a result we find:

$$\frac{(A^2)_{3\text{-spins}}}{(A^2)_{2\text{-spins}}} = 0.89.$$

This leads to

$$\frac{(B)_{300 \text{ Oe}}}{(B)_{500 \text{ Oe}}} = 0.55.$$

From our measurements we get:

$$\frac{(B)_{300 \text{ Oe}}}{(B)_{500 \text{ Oe}}} = 0.6 \pm 0.1.$$

Applying equation (5) we are able to get from our measurements an estimate of $\langle \mathcal{H}_{\text{int}}^2 \rangle$ and find: $\langle \mathcal{H}_{\text{int}}^2 \rangle = 6.0 \times 10^{-13} \text{ erg}^2$.

If we define an internal field H_i , in analogy with Caspers¹⁴):

$$H_i^2 = \frac{2\langle \mathcal{H}_{\text{int}}^2 \rangle}{kC}$$

we get $H_i^2 = 0.46 \times 10^4 \text{ Oe}^2$.

In the 10% Cr-Cs alum we cannot accurately measure the part of the susceptibility which undergoes the cross relaxation because the spin-lattice relaxation is rather close. An estimate yields $H_i^2 = 1 \times 10^4 \text{ Oe}^2$.

Also in the 6% NiSiF₆·6H₂O we have no possibility to measure that part of the susceptibility which plays a role in the three low-field cross-relaxation processes. Only around 1300 Oe the dispersion curves (fig. 3) show for the highest measuring frequencies that the part of the susceptibility which remains in our frequency range can be given as:

$$\frac{\Delta\chi'}{\chi_0} = \frac{0.12}{1 + \left(\frac{H - H_0}{230}\right)^2}$$

Following Bloembergen's derivation for $\Delta\chi'$ of a one-spin process leads to: $\langle \mathcal{H}_{\text{int}}^2 \rangle = 1.8 \times 10^{-13} \text{ erg}^2$. With the definition of the internal field as given above this gives: $H_i^2 = 2.0 \times 10^4 \text{ Oe}^2$. The results for H_i^2 , obtained as described in this subsection, are shown in the first row of table IV.

ii) If the frequency of the alternating field increases, the spins become

isolated from each other and χ drops to the isolated susceptibility $\chi_{is} < \chi_{ad}$. χ_{is} is determined by the off-diagonal elements of the magnetic moment $M = \langle \partial \mathcal{H} / \partial H_c \rangle_T$, so χ_{is} is connected with the curvature of the ionic energy levels. In the case of Cr-Cs alum with $\theta = 54^\circ 45'$, this part χ_{is}/χ_0 has been calculated by Verstelle¹⁵); it is also drawn in fig. 7. The energy levels of the Ni ions with $\theta = 0^\circ$ are straight lines, so $\chi_{is} = 0$.

At high measuring frequencies χ'/χ_0 near zero field remains larger than χ_{is}/χ_0 . This is due to the fact that $H_1 = (H_{dip}^2 + H_{ex}^2)^{1/2}$ is still larger than H_c , so the spins in a doublet stay in local equilibrium easily while the spins separated by D in zero field are isolated already at these measuring frequencies. We expect χ'/χ_0 at high frequencies to drop down corresponding to a curve:

$$\frac{\chi'}{\chi_0} = \frac{1}{1 + \frac{H_c^2}{b_1/C}} \quad \text{with} \quad b_1 = b_{dip} + b_{ex}.$$

Using this formula we can get a value of H_1 from the susceptibility near zero field in the case of $5\frac{1}{2}\%$ Cr-Cs alum and 6% NiSiF₆.6H₂O. These results are shown in the second row of table IV. In the case of 10% Cr-Cs alum our measuring frequencies are not sufficiently high (see also fig. 5) and we can only give a maximum value for H_1 .

iii) In Cr-Cs alum exchange interaction has never been observed, so we only consider \mathcal{H}_{dip} . In the nondiluted Cr-Cs alum H_{dip}^2 can be calculated¹⁴); we get $H_{dip}^2 = 10 \times 10^4 \text{ Oe}^2$. In the expression for H_{dip}^2 we have a factor a^{-6} (a = distance between nearest neighbours). With the assumption that H_{dip}^2 is only formed by contributions of nearest neighbours and next-nearest neighbours the contribution to H_{dip}^2 per ion can be calculated within an accuracy of 10% . In the diluted sample the probability that an ion has no paramagnetic neighbours or has only one paramagnetic neighbour, etc. is known and it is possible in this way to get an idea of H_{dip}^2 in the diluted Cr-Cs alums. In table IV a comparison is made between the internal fields as they were measured (two ways) and as they were calculated for the diluted samples. The agreement between these fields in both the Cr-Cs alums is quite satisfactory.

In the NiSiF₆.6H₂O $\mathcal{H}_{ex} \neq 0$. Eggermont¹⁶) calculated the values of H_{dip}^2 and H_{ex}^2 for the concentrated salts, assuming a cubic structure. From his results we estimated H_{dip}^2 and H_{ex}^2 for the diluted salts in the way indicated above. For H_{ex}^2 only the nearest-neighbour interaction is taken into account. The results for H_1^2 as estimated from the cross-relaxation measurements do not agree very well with the calculations for $H_{dip}^2 + H_{ex}^2$. If we remember that $\chi_{is} = 0$ in this case, we expect χ'/χ_0 to be very small at approximately 900 Oe for high measuring frequencies. At our frequencies this is not true yet, so we may assume that the elevation in χ'/χ_0 around

1300 Oe at 678 kHz is still smaller than the maximum part of the susceptibility which is undergoing the cross relaxation. Roughly we would expect the value of H_i^2 , as derived from the cross-relaxation susceptibility, to increase by a factor 2. This means that the half width of the elevation in χ'/χ_0 will increase to 300 Oe (instead of 230 Oe) at frequencies above 1 MHz; considering fig. 3 we find that this is quite well possible.

iv) Finally we will discuss the b/C values. Knowing D from the cross-relaxation measurements, one can calculate b_{e1}/C (e.g. De Vrijer¹⁷) and thus derive $b/C = b_{e1}/C + b_1/C$.

For 6% NiSiF₆·6H₂O $D = -0.13 \text{ cm}^{-1}$, as derived in section 4a, leads to $b/C = 55 \times 10^4 \text{ Oe}^2$. Consequently the adiabatic susceptibility can be calculated from equation (2). In fig. 3 in which χ'/χ_0 has been plotted against H_c the calculated value of χ_{ad}/χ_0 is inserted for some external fields (symbol \circ). If the susceptibility is measured at frequencies $\nu: \rho_L^{-1} \ll \nu \ll \rho_{cr}^{-1}$ one would expect χ'/χ_0 to be equal to χ_{ad}/χ_0 . The curve of 5.3 kHz, as one can see in fig. 3, fulfils this condition for the low external fields and around $H_c = 1300 \text{ Oe}$. Near 1000 Oe and 1600 Oe $(\chi'/\chi_0)_{\nu=5.3 \text{ kHz}}$ has a value lower than χ_{ad}/χ_0 . At these external fields no simple cross relaxation is possible and obviously frequencies below 5.3 kHz are required for the study of the spin-system in complete equilibrium. Lower frequencies are not shown in fig. 3 because spin-lattice relaxation could not be neglected any more.

For 5½% Cr-Cs alum $D = -0.068 \text{ cm}^{-1}$ (subsection 5a), thus $b/C = 44 \times 10^4 \text{ Oe}^2$. In fig. 7 the calculated value of χ_{ad}/χ_0 (equation 2) is drawn for four external field values. In this sample the spin-lattice relaxation parameter ρ_L is of the order of 0.1 s at 2 K, so one expects $\chi'/\chi_0 \leq \chi_{ad}/\chi_0$ at $\nu \geq 10 \text{ Hz}$. As one can see in fig. 7, this is not confirmed at high fields, the measurements supporting a slightly higher b/C -value of about $53 \times 10^4 \text{ Oe}^2$.

A similar effect on b/C can be noticed in 10% Cr-Cs alum (fig. 5). Here the situation is more complicated because spin-lattice relaxation leads to an increase of the χ' at frequencies below 60 kHz. However, the calculated b/C -value ($47 \times 10^4 \text{ Oe}^2$) is again smaller than the b/C measured directly at high frequencies and high fields (the 480 kHz curve in fig. 5 gives $b/C = 52 \times 10^4 \text{ Oe}^2$).

In Cr-K alums Verstelle¹⁸) observed an increase of b/C in time. He attributed this effect to a slow dehydration of the crystal. Although the Cr-Cs alum is supposed to be a more stable crystal, dehydration cannot be excluded as a possible cause of the discrepancy in the b/C -values.

c) Relaxation times. *i)* For most of the cross-relaxation processes we were able to propose at least an estimate of the relaxation times at the fields H_0 . If more spins are involved in a cross-relaxation process, the transition probability becomes much smaller because higher order pertur-

bations are required in order to bring such a process about (Pershan¹⁹), Verstelle and Curtis²⁰). So if we compare results on one sample we will expect $(\rho_{cr})_{H=H_0}$ to be in general longer if the number of participating spins is larger. The measurements reported in this paper confirm this. However, in 5½% Cr-Cs alum there is one discrepancy. The 5-spin processes around 350 Oe have relaxation parameters ρ_{cr} of approximately the same order of magnitude as the 4-spin processes around 225 Oe. These processes are rather complicated and for a comparison of the relaxation times we would have to know the exact expression for the transition probabilities.

ii) According to the theoretical analysis of Grant²¹) the transition probabilities of the cross-relaxation processes do depend on the concentrations of the paramagnetic ions. For a cross-relaxation process, involving n -spin transitions and occurring in two paramagnetic samples a and b , Grant gives the following relation:

$$\frac{w_a}{w_b} = \left(\frac{c_a}{c_b} \right)^n$$

where w is the transition probability of the cross-relaxation process and c is the concentration of the paramagnetic ion.

For the Cr-Cs alum, measured in the [100]-direction, we were able to compare the relaxation times of the 3-spin process at approximately 300 Oe. The theoretical analysis gives:

$$\frac{\{\rho_{cr}\}_{10\%}}{\{\rho_{cr}\}_{5\frac{1}{2}\%}} = \frac{\{w\}_{5\frac{1}{2}\%}}{\{w\}_{10\%}} = \left(\frac{c_{5\frac{1}{2}\%}}{c_{10\%}} \right)^3,$$

while the experiments indicate:

$$\frac{\{\rho_{cr}\}_{10\%}}{\{\rho_{cr}\}_{5\frac{1}{2}\%}} = 0.14 \quad \text{and} \quad \left(\frac{c_{5\frac{1}{2}\%}}{c_{10\%}} \right)^3 = 0.17$$

$$\left[\text{cf.} \left(\frac{c_{5\frac{1}{2}\%}}{c_{10\%}} \right)^2 = 0.30 \quad \text{and} \quad \left(\frac{c_{5\frac{1}{2}\%}}{c_{10\%}} \right)^4 = 0.09 \right].$$

The values used for the concentrations are only estimates obtained by comparison of the output voltages of the bridge for different samples. Taking this into account the theoretical prediction is satisfactory.

iii) Caspers¹³) suggests that the character of the field dependence of cross-relaxation times is of the form:

$$\rho_{cr} = \rho_{cr}(H_0) \exp \frac{(H_e - H_0)^2}{\alpha H_1^2} \quad (7)$$

where α is a quantity of the order 1.

In 5½% Cr-Cs alum we were able to find ρ_{cr} vs H_e for the processes at fields less than 500 Oe. If we plot the results for ρ_{cr} on a logarithmic scale against H_e the measurements have a parabolic form (fig. 9). From this figure $d \log \rho_{cr} / dH_e$ is calculated and we see (fig. 11) that the agreement

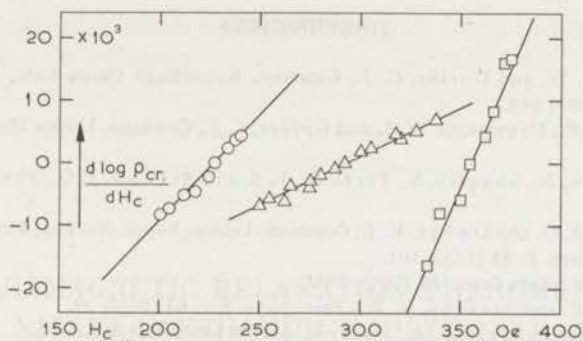


Fig. 11. $\frac{d \log \rho_{cr}}{d H_c}$ vs H_c for $5\frac{1}{2}\%$ Cr-Cs alum.

with $\log \rho_{cr} \propto \gamma(H_c - H_0)^2$ is reasonable. The coefficient γ in the exponent is different for the three processes:

$\gamma = 1.8 \cdot 10^{-4} \text{ Oe}^{-2}$ for the three-spin process around $H_0 = 300 \text{ Oe}$

$\gamma = 3.7 \cdot 10^{-4} \text{ Oe}^{-2}$ for the four-spin process around $H_0 = 225 \text{ Oe}$ and

$\gamma = 9.0 \cdot 10^{-4} \text{ Oe}^{-2}$ for the five-spin process around $H_0 = 350 \text{ Oe}$.

To compare results of the different cross-relaxation processes it seems reasonable to consider the relaxation times as functions of the energy difference between the spin jumps involved in the processes, instead of as functions of $H_c - H_0$. With the description of ΔE as given in (4) we can write eq. (7) as:

$$\rho_{cr} = \rho_{cr}(\Delta E = 0) \exp\left(\frac{\Delta E}{ag\beta\sqrt{\alpha}H_1}\right)^2 \quad (8)$$

With the value of a , as given in section 5b, we now can compare our results with formula (8). As an average for αH_1^2 in the $5\frac{1}{2}\%$ Cr-Cs alum we get: $(2.3 \pm 1.0) \times 10^4 \text{ Oe}^2$.

Caspers predicts α to be of the order of 1. However, α may vary for the different processes. Using $H_1^2 = 0.5 \times 10^4 \text{ Oe}^2$, as derived from the susceptibility (section 5b), we see that α lies between 3 and 6 for the processes observed.

REFERENCES

- 1) De Vrijer, F. W. and Gorter, C. J., Commun. Kamerlingh Onnes Lab., Leiden No. 289b; Physica **18** (1952) 549.
- 2) Verstelle, J. C., Drewes, G. W. J. and Gorter, C. J., Commun. Leiden No. 311b; Physica **24** (1958) 632.
- 3) Bloembergen, N., Shapiro, S., Pershan, P. S. and Artman, J. O., Phys. Rev. **114** (1959) 445.
- 4) Casimir, H. B. G. and Du Pré, F. J., Commun. Leiden, Suppl. No. 85a; Physica **5** (1938) 507.
- 5) Debye, P., Phys. Z. **35** (1935) 101.
- 6) Hamilton, W., Acta Cryst. **15** (1962) 353.
- 7) Penrose, R. P. and Stevens, K. W., Proc. phys. Soc. **63** (1950) 29.
- 8) Lipson, H. and Beevers, C. A., Proc. roy. Soc. **A 148** (1953) 664.
- 9) Schulz-Dubois, E. O., Bell syst. techn. journal **38** (1959) 271.
- 10) De Vries, A. J. and Livius, J. W. M., Commun. Leiden No. 349a; Appl. sci. Res. **17** (1967) 31.
- 11) Hoskins, R. H., Pastor, R. C. and Trigger, R. H., J. chem. Phys. **30** (1959) 601.
- 12) Zimmerman, N. J., Private Communication.
- 13) Caspers, W. J., Commun. Leiden, Suppl. No. 118c; Physica **26** (1960) 809.
- 14) Caspers, W. J., Commun. Leiden, Suppl. No. 118b; Physica **26** (1960) 798.
- 15) Verstelle, J. C., Private Communication.
- 16) Eggermont, J. J., Private Communication.
- 17) De Vrijer, F. W., Thesis, Leiden (1951).
- 18) Verstelle, J. C., Thesis, Leiden (1962).
- 19) Pershan, P. S., Phys. Rev. **117** (1960) 109.
- 20) Verstelle, J. C. and Curtis, D. A., Handbuch der Physik Bd **18/1** (1968).
- 21) Grant, W. J. C., Phys. Rev. **134A** (1964) 1554.

PARAMAGNETIC RELAXATION PHENOMENA IN NICKEL-LANTHANUM DOUBLE NITRATE

Synopsis

Paramagnetic relaxation phenomena in single crystals of $\text{Ni}_3\text{La}_2(\text{NO}_3)_{12} \cdot 24\text{H}_2\text{O}$ have been examined by measuring the susceptibility $\bar{\chi}$ in the frequency range from 200 Hz to 1 MHz. At helium temperatures double relaxation has been observed. One of these relaxation times is found to vary over more than three decades if the magnetic field increases from 2 kOe to 6 kOe. This time becomes short ($\tau \simeq 10^{-7}$ s at $H_e = 6$ kOe) and is hardly temperature dependent. In a magnetically diluted single crystal (7% $\text{Ni}_3\text{La}_2(\text{NO}_3)_{12} \cdot 24\text{H}_2\text{O}$) a complicated cross-relaxation behaviour has been observed. The Ni ions at crystallographic *X* sites behave as exchange coupled pairs⁶⁾ and these Ni-ion pairs cause the observed cross-relaxation processes. The fast relaxation in the concentrated samples is identified as cross relaxation also. Because of the large internal field values, the characteristic cross-relaxation behaviour of χ' vs. H_e , as observed in the 7% sample as well as in earlier experiments⁸⁾, cannot be expected in the concentrated $\text{Ni}_3\text{La}_2(\text{NO}_3)_{12} \cdot 24\text{H}_2\text{O}$ salts.

1. *Introduction.* The observation of anomalous relaxation phenomena in a Ni-La double nitrate has been the start of an extensive study on these salts. Double relaxations were observed which showed a somewhat similar behaviour to that observed in cobalt Tutton salts^{1, 2)}.

The apparatus and the measuring procedure have been described in detail by De Vries³⁾. The samples are placed in a constant magnetic field H_e on which a parallel oscillating field ($h \exp i\omega t$) is superimposed. The frequency $\nu = \omega/2\pi$ can be varied from 200 Hz to 1 MHz.

Spin-lattice relaxation in paramagnetics can be described by the thermodynamical theory of Casimir and Du Pré⁴⁾; this leads to the well-known relations for the susceptibility $\bar{\chi} = \chi' - i\chi''$:

$$\chi' = \chi_{ad} + \frac{\chi_0 - \chi_{ad}}{1 + \tau_L^2 \omega^2}$$

(1)

and

$$\chi'' = (\chi_0 - \chi_{ad}) \frac{\tau_L \omega}{1 + \tau_L^2 \omega^2},$$

τ_L being the spin-lattice relaxation time, χ_0 the static value of the susceptibility. χ_{ad} is the susceptibility measured at frequencies $\nu \gg (2\pi\tau_L)^{-1}$, this is the situation in which the spin-system (system in which the paramagnetic properties are manifested) is isolated from the lattice oscillations. For a substance obeying Curie's law one can derive:

$$\chi_{ad}/\chi_0 = \frac{b}{b + CH^2} \quad (2)$$

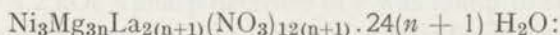
where C is the Curie constant and b is the coefficient in the specific heat of the spin system at constant magnetization: $c_M = b/T_s^2$. $\text{Ni}_3\text{La}_2(\text{NO}_3)_{12} \cdot 24\text{H}_2\text{O}$ does obey a Curie-Weiss law. In that case b/C derived from eq. (2) has to be corrected according to ref. 5): $(b/C)_{\text{corr.}} = (b/C)_{\text{meas.}} \{T/(T - \theta)\}^3$, where θ is the Curie-Weiss constant.

So far it has been assumed that the distribution of the magnetic ions over the energy states can be characterised by a so-called spin temperature T_s , which varies periodically with the frequency ω of the oscillating part of the magnetic field. These periodical variations are cancelled at low frequencies by means of spin-lattice relaxation. If the paramagnetic ions are distributed over more than two energy states ($J > \frac{1}{2}$) one cannot expect T_s to be a useful quantity under all circumstances. Then cross relaxations are possible by interactions between the spins. These relaxations will occur close to magnetic fields where neighbouring ions can make transitions in which the energy is conserved but the magnetic moment is changed. Such cross-relaxation processes lead to an increase in χ' at certain field ranges. By means of cross relaxations instantaneous equilibrium can be obtained between all magnetic ions; the corresponding value of the susceptibility will be referred to as $\chi_{ad}^{(1)}$ which then corresponds to a relatively large value of b/C : $b^{(1)}/C$. At angular frequencies far above the inverse cross-relaxation time a spin temperature for the whole system cannot be defined; then one finds another susceptibility: $\chi_{ad}^{(2)} (< \chi_{ad}^{(1)})$ corresponding to $b^{(2)}/C (< b^{(1)}/C)$. At helium temperatures the times of the cross-relaxation processes are often short compared to the spin-lattice relaxation time. In magnetically diluted substances the cross-relaxation times become longer and both relaxation processes may mix up.

2. *Samples.* $\text{Ni}_3\text{La}_2(\text{NO}_3)_{12} \cdot 24\text{H}_2\text{O}$ is one of the isomorphous series of double nitrates. The crystal structure has been described in some detail in a previous paper⁶⁾. The crystals are trigonal. All the Ni ions are surrounded by octahedra of water molecules. EPR data⁷⁾ show that two third of the Ni ions are situated at crystallographic X sites and one third at Y sites. Every X-site Ni ion has as nearest neighbours three Y-site Ni ions at 7.1 Å and one X-site Ni ion at 5.0 Å. These X-site Ni ions form exchange-coupled

pairs⁶). The c axis of the crystal coincides with the $g_{//}$ direction of both the X -site and the Y -site Ni ions.

Measurements have been performed on a nondiluted crystal, referred to as 100% $\text{Ni}_3\text{La}_2(\text{NO}_3)_{12} \cdot 24\text{H}_2\text{O}$ and on three crystals in which the Ni ions are partially replaced by nonmagnetic Mg^{2+} ions. The magnetic susceptibility of these crystals was compared with that of the nondiluted sample. This gave the following results for the concentration of the mixed crystals



I $n = 0.67$, referred to as 60% $\text{Ni}_3\text{La}_2(\text{NO}_3)_{12} \cdot 24\text{H}_2\text{O}$,

II $n = 4$, referred to as 20% $\text{Ni}_3\text{La}_2(\text{NO}_3)_{12} \cdot 24\text{H}_2\text{O}$ and

III $n = 13$, referred to as 7% $\text{Ni}_3\text{La}_2(\text{NO}_3)_{12} \cdot 24\text{H}_2\text{O}$.

3. Results. a. 100% $\text{Ni}_3\text{La}_2(\text{NO}_3)_{12} \cdot 24\text{H}_2\text{O}$, external magnetic field $H_c // c$ axis. Relaxation phenomena have been measured at temperatures below 21 K. The relaxation time τ if plotted vs. temperature shows two regions. For an external field of 2 kOe (fig. 1) down to about 6 K

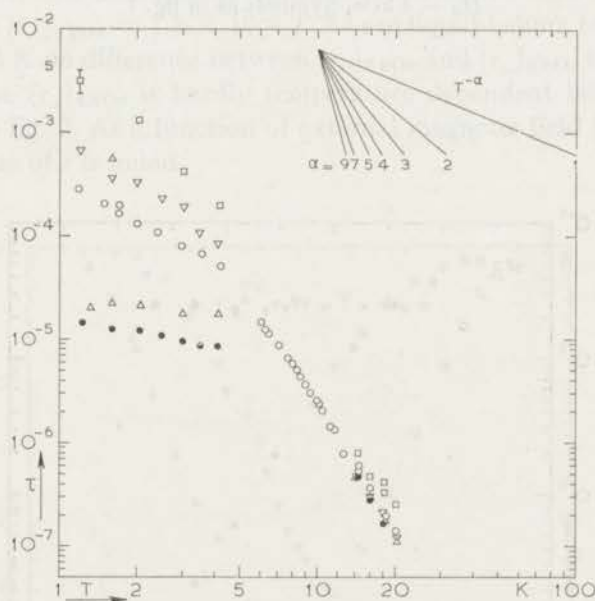


Fig. 1. Relaxation times vs. temperature for various nickel-lanthanum double nitrates. External magnetic field $H_c = 2$ kOe.

○: 100% $\text{Ni}_3\text{La}_2(\text{NO}_3)_{12} \cdot 24\text{H}_2\text{O}$; $H_c // c$ axis

●: id.; $H_c \perp c$ axis

▽: 60% $\text{Ni}_3\text{La}_2(\text{NO}_3)_{12} \cdot 24\text{H}_2\text{O}$; $H_c // c$ axis

△: id.; $H_c \perp c$ axis

□: 20% $\text{Ni}_3\text{La}_2(\text{NO}_3)_{12} \cdot 24\text{H}_2\text{O}$; $H_c // c$ axis

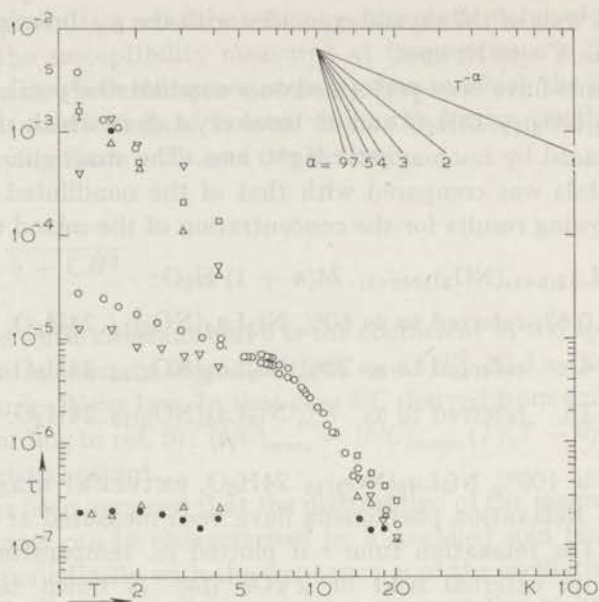


Fig. 2. Relaxation times *vs.* temperature for various nickel-lanthanum nitrates.
 $H_e = 4$ kOe. Symbols as in fig. 1.

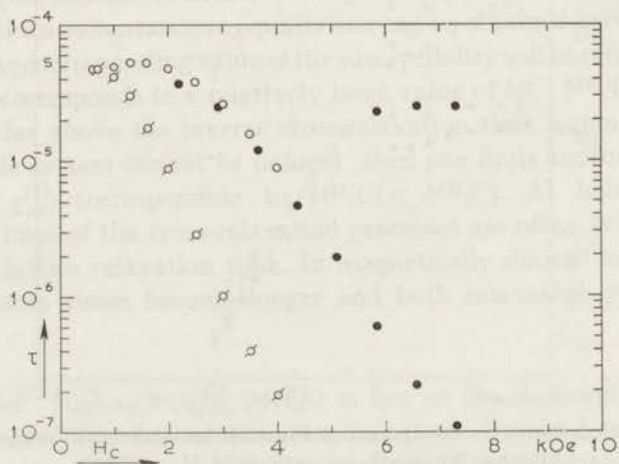


Fig. 3. Relaxation times *vs.* magnetic field for 100% $\text{Ni}_3\text{La}_2(\text{NO}_3)_{12} \cdot 24\text{H}_2\text{O}$.

○, ●: $H_e // c$ axis; $T = 4.20$ K

□: $H_e \perp c$ axis; $T = 4.10$ K

Closed symbols refer to measurements with the nitrogen-cooled magnet; for these results a five percent error in the field values is possible.

$(\tau_{//})_{2\text{kOe}} = 2.8 \times 10^{-2} T^{-4.3} \text{ s}$ while at liquid-helium temperatures $(\tau_{//})_{2\text{kOe}} = 3.4 \times 10^{-4} T^{-1.4} \text{ s}$. At higher magnetic fields (fig. 2) at low temperatures a double relaxation is observed. One of the branches lies on one line with the results above 8 K and can be described as:

$(\tau_{//})_{4\text{kOe}} = 1.1 \times 10^{-2} T^{-4.2} \text{ s}$, while the other branch shows short relaxation times: $(\tau'_{//})_{4\text{kOe}} = 3.5 \times 10^{-5} T^{-1.0} \text{ s}$.

Using the standard measuring procedure with external magnetic fields up to 4.2 kOe a sharp decrease of τ was found to start near 2 kOe. A study of the relaxation times at higher magnetic fields was desirable. The nitrogen-cooled pulse magnet could not be applied since τ' varies too rapidly as a function of external magnetic field. For this reason a provisory arrangement was made to use this magnet with slowly varying fields. It was possible in this way to reach 8 kOe.

As can be seen in fig. 3, τ' decreases more than three decades as a function of the external magnetic field. At high magnetic fields, however, the double relaxation mentioned above was found. This double relaxation process is more pronounced at lower temperatures.

b. 100% $\text{Ni}_3\text{La}_2(\text{NO}_3)_{12} \cdot 24\text{H}_2\text{O}$, external magnetic field $H_c \perp c$ axis. In this direction also rather short relaxation times have been found. From fig. 1 one finds $(\tau_{\perp})_{2\text{kOe}} = 1.5 \times 10^{-5} T^{-0.5} \text{ s}$ at liquid-helium temperatures, while above 14 K no difference between $(\tau_{//})_{2\text{kOe}}$ and $(\tau_{\perp})_{2\text{kOe}}$ is noted. The relaxation time $(\tau_{\perp})_{4\text{kOe}}$ is hardly temperature dependent below 21 K as can be seen in fig. 2. As a function of external magnetic field (fig. 3) again a rapid decrease of τ is found.

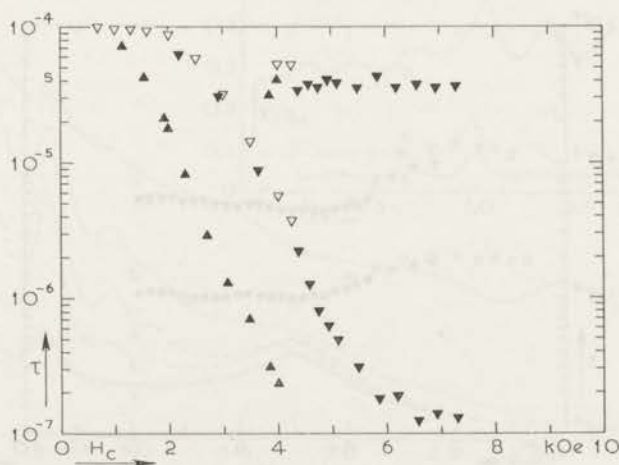


Fig. 4. Relaxation times vs. magnetic field for 60% $\text{Ni}_3\text{La}_2(\text{NO}_3)_{12} \cdot 24\text{H}_2\text{O}$.

$\nabla, \blacktriangledown$: $H_c // c$ axis; $T = 4.15 \text{ K}$

\blacktriangle : $H_c \perp c$ axis; $T = 4.15 \text{ K}$

Closed symbols as in fig. 3.

Especially the fast relaxations have been the subject of the further studies on $\text{Ni}_3\text{La}_2(\text{NO}_3)_{12}\cdot 24\text{H}_2\text{O}$ salts. Obviously 8 kOe was not enough to find "the end" of the fast relaxation process and in view of this a study of a series of magnetically diluted samples was started.

c. 60% $\text{Ni}_3\text{La}_2(\text{NO}_3)_{12}\cdot 24\text{H}_2\text{O}$, $H_c \parallel c$ axis. The relaxation times showed generally the same behaviour as in the concentrated salt. Above 14 K even no difference with the results of 100% $\text{Ni}_3\text{La}_2(\text{NO}_3)_{12}\cdot 24\text{H}_2\text{O}$ could be observed. Below 4.2 K the following temperature dependences are found: $(\tau_{\parallel})_{2\text{kOe}} = 1.1 \times 10^{-3} T^{-1.5}$ s and $(\tau'_{\parallel})_{4\text{kOe}} = 1.6 \times 10^{-5} T^{-0.6}$ s for the fast relaxation process. At $H_c = 4$ kOe the other relaxation times lie again on one line with the results at hydrogen temperatures (fig. 2).

The relaxation times as a function of external magnetic field (in fig. 4 plotted for $T = 4.10$ K) show again the steep fall above about 2 kOe, and the double relaxation at high magnetic fields is observed.

With the external magnetic field $H_c \perp c$ axis no new phenomena are observed. Both $(\tau_{\perp})_{2\text{kOe}}$ and $(\tau_{\perp})_{4\text{kOe}}$ show the fast relaxation process which hardly varies with temperature.

d. 20% $\text{Ni}_3\text{La}_2(\text{NO}_3)_{12}\cdot 24\text{H}_2\text{O}$, $H_c \parallel c$ axis. This sample does not show a fast relaxation process at helium temperatures and also τ hardly decreases as a function of external magnetic field (fig. 5). From the τ vs. temperature curves one derives at hydrogen temperatures: $(\tau_{\parallel})_{2\text{kOe}} = 7.0 \times 10^{-3} T^{-2.7}$ s and $(\tau_{\parallel})_{4\text{kOe}} = 1.1 \times 10^{-3} T^{-2.3}$ s, while at temperatures of liquid helium: $(\tau_{\parallel})_{2\text{kOe}} = 1.1 \times 10^{-3} T^{-2.0}$ s and $(\tau_{\parallel})_{4\text{kOe}} = 2.0 \times 10^{-3} T^{-1.7}$ s.

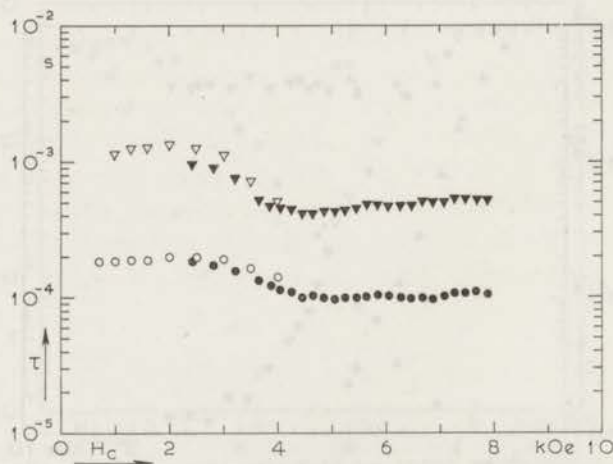


Fig. 5. Relaxation times vs. magnetic field for 20% $\text{Ni}_3\text{La}_2(\text{NO}_3)_{12}\cdot 24\text{H}_2\text{O}$.

○, ●: $H_c \parallel c$ axis; $T = 4.18$ K

▽, ▼: $H_c \parallel c$ axis; $T = 3.05$ K

Closed symbols as in fig. 3.

In the description of the results we have not yet mentioned that in both the 100% and the 60% salt small maxima were observed in the χ' vs. H_c curves. Measurements on 20% $\text{Ni}_3\text{La}_2(\text{NO}_3)_{12} \cdot 24\text{H}_2\text{O}$ showed an increase in number and in intensity of these elevations as well as corresponding effects in the χ'' vs. H_c curves.

As is known from the cross-relaxation measurements on $\text{NiSiF}_6 \cdot 6\text{H}_2\text{O}$ ⁸) maxima and minima in χ' vs. H_c and χ'' vs. H_c curves correspond to locally fast relaxation processes. To verify the occurrence of cross-relaxation processes in $\text{Ni}_3\text{La}_2(\text{NO}_3)_{12} \cdot 24\text{H}_2\text{O}$ another more diluted sample was chosen to be studied in detail.

e. 7% $\text{Ni}_3\text{La}_2(\text{NO}_3)_{12} \cdot 24\text{H}_2\text{O}$, $H_c // c$ axis. In fig. 6 some of the observed χ'/χ_0 vs. H_c curves are shown. It is clear that fast relaxation processes occur at a remarkable number of external magnetic fields (see also table II). In the discussion we will see that this unexpectedly large number of processes at high as well as at low magnetic fields can be interpreted by cross relaxations not between single Ni ions but between pairs of them.

At high magnetic fields the cross-relaxation times lie close to the spin-lattice relaxation time. Precise values for the cross-relaxation times cannot be given but one may roughly say $\tau_{cr} \approx 10^{-4}$ s at magnetic fields above 4 kOe. In low magnetic fields differences between the values of the spin-lattice and the cross-relaxation time are more pronounced. At the minima of the cross-relaxation times $\tau_{cr} < 10^{-7}$ s. Between the minima τ_{cr}

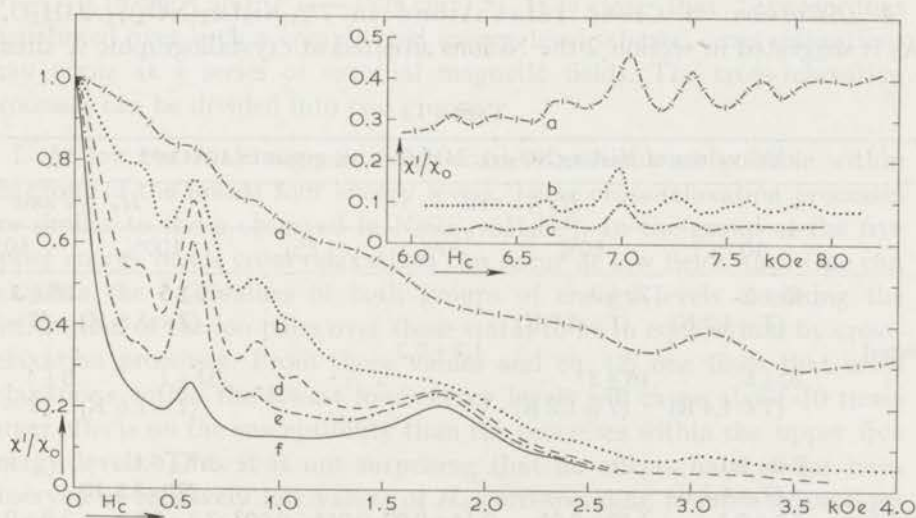


Fig. 6. χ'/χ_0 vs. H_c for 7% $\text{Ni}_3\text{La}_2(\text{NO}_3)_{12} \cdot 24\text{H}_2\text{O}$
 $H_c // c$ axis; $T = 4.13$ K.

curve a: $\nu = 0.94$ kHz; b: $\nu = 3.75$ kHz; c: $\nu = 7.5$ kHz;
d: $\nu = 10.6$ kHz; e: $\nu = 30$ kHz; f: $\nu = 480$ kHz.

becomes as long as 10^{-5} s. These values give only the orders of magnitude of τ_{er} at 4.2 K; obviously the processes are too complicated to be described by a pure Casimir-Du Pré behaviour of χ' and χ'' according to eq. (1).

At higher concentrations the cross-relaxation times become shorter. In the 20% sample τ_{er} was estimated to be approximately 10^{-8} s at low external magnetic fields. In the more concentrated salts these processes will fall beyond the frequency range of our equipment. At high magnetic fields the observed relaxation times are about 10^3 times longer so these cross relaxations might still be measurable in the most concentrated salts.

The spin-lattice relaxation times of 7% $\text{Ni}_3\text{La}_2(\text{NO}_3)_{12}\cdot 24\text{H}_2\text{O}$ could not be measured accurately by means of our present equipment, τ being larger than 0.3×10^{-3} s at helium temperatures.

f. b/C values. At frequencies $\nu \gg 2\pi\tau^{-1}$ one usually measures the so-called adiabatic value of the susceptibility from which according to eq. (2) a value for b/C can be derived. If two relaxation processes occur with relaxation times τ and τ' : $\tau \gg \tau'$, one may introduce two adiabatic susceptibilities $\chi_{ad}^{(1)}$ and $\chi_{ad}^{(2)}$. $\chi_{ad}^{(2)}$ is observed at $\nu > 2\pi(\tau')^{-1}$ and $\chi_{ad}^{(1)}$ at $2\pi\tau^{-1} < \nu < 2\pi(\tau')^{-1}$. This yields two results for the b/C of 100%, 60% and 20% $\text{Ni}_3\text{La}_2(\text{NO}_3)_{12}\cdot 24\text{H}_2\text{O}$. In the case of 7% $\text{Ni}_3\text{La}_2(\text{NO}_3)_{12}\cdot 24\text{H}_2\text{O}$ it is difficult to present a value for $\chi_{ad}^{(1)}$ since τ and τ' ($=\tau_{er}$) do not differ very much. The b/C values as calculated from our measurements are listed in table I, they will be discussed in section 4.

4. Discussion. *a. Cross relaxations in 7% $\text{Ni}_3\text{La}_2(\text{NO}_3)_{12}\cdot 24\text{H}_2\text{O}$.* As is suggested in section 2 the Ni ions situated at crystallographic X sites

TABLE I

b/C values of $\text{Ni}_3\text{La}_2(\text{NO}_3)_{12}\cdot 24\text{H}_2\text{O}$ salts, given in 10^6Oe^2*						
	$H_c // c$ axis				$H_c \perp c$ axis	
	100%	60%	20%	7%	100%	60%
$b^{(1)}/C$ uncorrected	45 ± 5 ($T=4.2 \text{ K}$)	20 ± 3 ($T=3.0 \text{ K}$)			80 ± 5 ($T=3.5 \text{ K}$)	28 ± 3 ($T=4.2 \text{ K}$)
	20 ± 5 ($T=1.4 \text{ K}$)	10 ± 3 ($T=1.2 \text{ K}$)	1.2 ± 0.3	—	31 ± 1 ($T=1.6 \text{ K}$)	8 ± 1 ($T=1.3 \text{ K}$)
$b^{(2)}/C$ corrected for deviations from Curie's law.	2.0 ± 0.1 ($T=4.2 \text{ K}$)				3.7 ± 0.1 ($T=3.5 \text{ K}$)	
	2.5 ± 0.1 ($T=1.2 \text{ K}$)	1.85 ± 0.05	0.14 ± 0.02	0.014 ± 0.003	2.3 ± 0.1 ($T=1.6 \text{ K}$)	3.8 ± 0.5 (uncorrected)

* If a temperature-dependent result was obtained, two values are given.

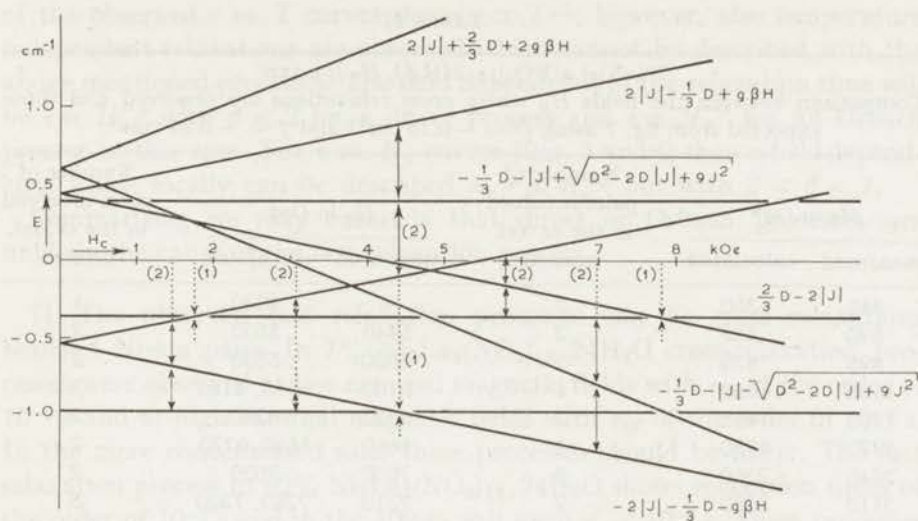


Fig. 7. Energy level scheme for the Ni-ion pairs in nickel-lanthanum double nitrate; $H_c \parallel c$ axis; $D = -0.18 \text{ cm}^{-1}$ and $J = -0.24 \text{ cm}^{-1}$ (6). The arrows indicate a few possibilities for cross-relaxation processes; within brackets the number of spins involved in the process.

form exchange-coupled pairs. The ground state of these pairs ($S = 2$) has a ninefold spin-degeneracy. In fig. 7 these energy levels are drawn for $D = -0.18 \text{ cm}^{-1}$ and $J = -0.24 \text{ cm}^{-1}$ (6). It is clear that between ions distributed over such a complicated energy level scheme, cross relaxations may occur at a series of external magnetic fields. The cross-relaxation processes can be divided into two groups:

I. At low external magnetic fields cross relaxations are possible within the group of the lowest four energy levels. These cross-relaxation processes are similar to those observed in $\text{NiSiF}_6 \cdot 6\text{H}_2\text{O}$ (8). In the group of the five upper energy levels cross relaxations can occur at low fields also. One can calculate the b/C values of both groups of energy levels assuming the distribution of the ion pairs over these states to be in equilibrium by cross-relaxation processes. From those values and eq. (2) one finds that cross relaxations within the lowest four energy levels will cause about 10 times larger effects on the susceptibility than the processes within the upper five energy levels. Thus it is not surprising that no effects have so far been observed at relatively low values of H_c corresponding to cross relaxations within the five upper energy levels.

II. Above 4 kOe cross relaxations are possible between all Ni-ion pairs. A few of the simple possibilities for cross-relaxation processes are indicated

TABLE II

7% Ni₃La(NO₃)₁₂·24H₂O, $H_c // c$ axis.
 Comparison between the fields H_0 where cross relaxations are observed and those expected from fig. 7 using $D = -0.18 \text{ cm}^{-1}$ and $J = -0.24 \text{ cm}^{-1}$.

H_0 in Oe*		Number of pairs involved in the cr.-rel. process	H_0 in Oe†		Number of pairs involved in the cr.-rel. process
measured	calculated		measured	calculated	
345	350	3	—	4830	1
590	582	2	5440	5530	2
895	875	3	5820	5830	2
1105	1050	4	6150	6150, 6180	3
1480	1465	2	6350	6340	2
1770	1750	1	6660	6680, 6770	2
2440	2360	3	7000	7030	2
3110	3080	2	7310	7280, 7300	3
4530	4420	1	7630	7530	3
			7860	7830	1
			8210	8370	2

* Cross relaxations between ion pairs situated in the four lowest energy levels.

† id. between all ion pairs.

in fig. 7. In table II a comparison is made between the field values where cross relaxations are observed in 7% Ni₃La₂(NO₃)₁₂·24H₂O and the values obtained with the help of the energy levels of fig. 7. For high magnetic fields only the simplest possible processes are calculated. At one magnetic field where cross-relaxation is expected no effect on $\bar{\chi}$ is observed. The agreement at the other 19 field values is quite satisfactory. In fact these results strongly support the idea that X-site Ni ions occur in exchange-coupled pairs⁶).

b. Fast relaxation processes in 100% and 60% Ni₃La₂(NO₃)₁₂·24 H₂O. The observed times of the field-dependent relaxation process are much faster than the usual spin-lattice relaxation times at helium temperatures. One might think of two possibilities to describe these fast relaxations.

I. Direct processes or Orbach processes of Ni-ion pairs⁹). These processes can be much faster than the relaxation of single Ni ions. For a direct process τ varies inversely with temperature, Orbach processes in a Ni-ion pair will have an exponential temperature dependence. Because the splittings in the energy level scheme of the Ni-ion pairs are of the order of kT , these exponentials do not differ much from $\tau \propto T^{-1}$ at helium temperatures. Part

of the observed τ vs. T curves shows $\tau \propto T^{-1}$; however, also temperature independent relaxations are observed which cannot be described with the above mentioned processes. The field dependence of the relaxation time will be $\tau \propto H_c^{-\beta}$ with $\beta \leq 2$ for a direct process and $\tau \propto H_c^{-3}$ for an Orbach process in this case. The τ vs. H_c curves (figs. 3 and 4) show a field dependence which locally can be described as $\tau \propto H_c^{-\beta}$ but with $3 < \beta < 7$.

Summarizing we may conclude that direct or Orbach processes are unlikely the cause of the fast relaxation process.

II. The observed fast relaxation processes can be cross relaxations between Ni-ion pairs. In 7% $\text{Ni}_3\text{La}_2(\text{NO}_3)_{12} \cdot 24\text{H}_2\text{O}$ cross-relaxation processes were observed at low external magnetic fields with τ_{cr} of the order of 10^{-6} s and at high external magnetic fields with τ_{cr} of the order of 10^{-4} s. In the more concentrated salts these processes should be faster. The fast relaxation process in 60% $\text{Ni}_3\text{La}_2(\text{NO}_3)_{12} \cdot 24\text{H}_2\text{O}$ shows relaxation times of the order of 10^{-7} s and in the 100% salt even $\tau' < 10^{-7}$ s. These processes can quite well be the same high-field cross relaxations as observed in the 7% $\text{Ni}_3\text{La}_2(\text{NO}_3)_{12} \cdot 24\text{H}_2\text{O}$ salt. The cross relaxations occurring at low external magnetic fields may be expected to be faster too and thus be beyond the range of our measuring equipment. However, these low field cross-relaxation processes cannot maintain equilibrium between all Ni-ion pairs, and thus a partial equilibrium can be reached. This means that at low magnetic fields one observes spin-lattice relaxation with values of $\chi_{\text{ad}}^{(2)}$ corresponding to a low b/C : $b^{(2)}/C$, indicating a system with isolated or partially isolated Ni-ion pairs. At high external magnetic fields (above 4 kOe) cross relaxations are able to establish equilibrium within the whole system of Ni-ion pairs. At these magnetic fields spin-lattice relaxation can be observed with a $\chi_{\text{ad}}^{(1)}$ which corresponds to a large internal field. This large value of $b^{(1)}/C$ is mainly due to the zero-field energy level splittings of

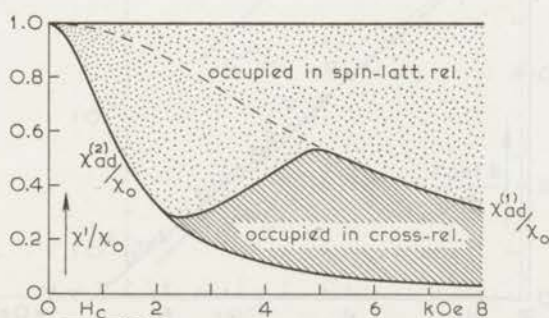


Fig. 8. Schematic view of $\chi_{\text{ad}}^{(1)}/\chi_0$ and $\chi_{\text{ad}}^{(2)}/\chi_0$ as a function of external field.

$$\chi_{\text{ad}}^{(1)} \text{ is observed at } 2\pi\tau_{\text{L}}^{-1} < \nu < 2\pi\tau_{\text{cr}}^{-1},$$

$$\chi_{\text{ad}}^{(2)} \text{ is observed at } \nu > 2\pi\tau_{\text{cr}}^{-1}.$$

the Ni-ion pairs. Cross relaxation will decrease the susceptibility from the value $\chi_{ad}^{(1)}$ to $\chi_{ad}^{(2)}$. The parts of the susceptibility participating in spin-lattice relaxation and in cross relaxation are sketched in fig. 8 where two curves $\chi_{ad}^{(1)}$ and $\chi_{ad}^{(2)}$ are drawn as a function of external magnetic field.

If H_0 is the magnetic field at which energy-conserving spin jumps between neighbouring ion pairs may occur, the relaxation times at fields H_e not far from H_0 might be given by:

$$\tau_{er} = (\tau_{er})_0 \exp\{\alpha(H_e - H_0)^2\} \quad (3)$$

where α^{-1} is of the order of the b/C of the system if the Ni-ion pairs are isolated from each other¹⁰). In $\text{Ni}_3\text{La}_2(\text{NO}_3)_{12} \cdot 24\text{H}_2\text{O}$ a whole series of cross relaxations is possible at magnetic fields H_{0i} : $(H_{0i} - H_0) < \alpha^{-1}$ (see also table II). In that case one cannot expect to observe the different cross-relaxation processes separately. Only the cross relaxation at the lowest magnetic field may show an area where the relaxation time varies according to eq. (3). This can be verified in fig. 9 where $(d \log \tau' / dH_e)$ vs. H_e is plotted for the fast relaxation process in 60% $\text{Ni}_3\text{La}_2(\text{NO}_3)_{12} \cdot 24\text{H}_2\text{O}$. This graph shows a straight line so eq. (3) is obeyed. From the observed slope one derives $\alpha^{-1} = 2.5 \times 10^6 \text{ Oe}^2$ while $b/C = 1.8 \times 10^6 \text{ Oe}^2$. Cross-relaxation processes are usually temperature independent. This is indeed the case for the fast relaxation processes at the high magnetic fields. The relaxation times halfway the curve corresponding to eq. (3), however, do show some temperature dependence: $\tau \propto T^{-\beta}$ with $\beta \leq 1$ (e.g. $(\tau')_{4\text{kOe}}$) but in that field range the influence of the spin-lattice relaxation time may already become important.

The results with $H_e \perp c$ axis show the fast relaxation process at lower external magnetic fields in analogy to the case with $H_e \parallel c$ axis. We did

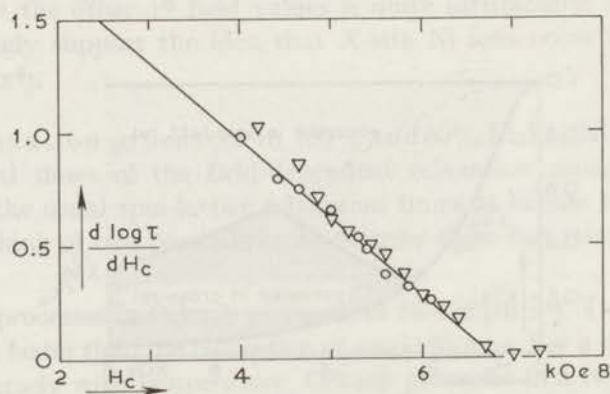


Fig. 9. $\frac{d \log \tau'}{d H_e}$ vs. H_e for the cross relaxations in 60% $\text{Ni}_3\text{La}_2(\text{NO}_3)_{12} \cdot 24\text{H}_2\text{O}$.

○: $T = 3.05 \text{ K}$; △: $T = 4.15 \text{ K}$.

not try to estimate the energy levels of the Ni-ion pairs with $H_c \perp c$ axis. It is quite well possible that in this direction cross relaxation between all Ni-ion pairs is already possible at lower fields than with $H_c \parallel c$ axis. This effect and the larger internal field value (table I) might cause the difference between the results in both crystal directions.

c. b/C values. In 100% $\text{Ni}_3\text{La}_2(\text{NO}_3)_{12} \cdot 24\text{H}_2\text{O}$ the b/C of the isolated system derived from the adiabatic susceptibility differs 30% from the result of $3.6 \times 10^6 \text{ Oe}^2$ estimated from the specific-heat data below 1 K⁶). One can calculate the contribution to the specific heat due to the zero-field energy level splittings of the Ni-ion pairs. If T is much larger than the energy splittings divided by k , $b/C = 22 \times 10^6 \text{ Oe}^2$. This assumption is not fulfilled at helium temperatures, which will cause a decrease of the b/C values observed. However, deviation from Curie's law will again increase the values for b/C . An explicit calculation has not been performed but the observed values of $b^{(1)}/C$ (table I) are of the right order of magnitude.

Lowering the concentration of the Ni ions will give a decrease of the magnetic specific heat. The measurements show $b^{(1)}/C \propto c^2$ (fig. 10) as can be expected because the number of pairs decreases with c^2 , while the main contribution to $b^{(1)}/C$ comes from the pair energy level splittings.

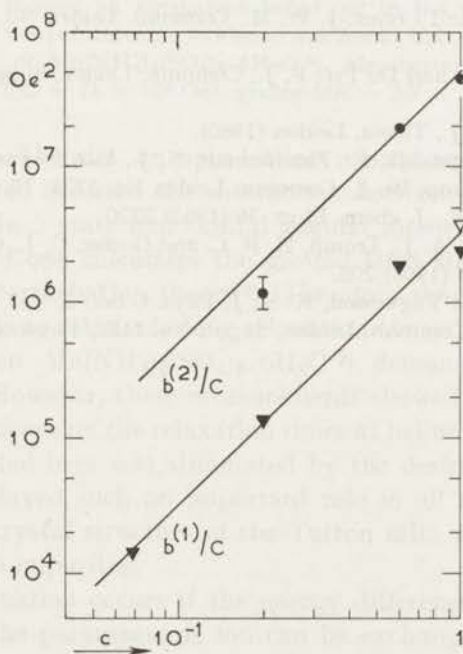


Fig. 10. $b^{(1)}/C$ (symbol \blacktriangledown) and $b^{(2)}/C$ (symbol \bullet) as a function of the Ni-ion concentration.

∇ is the result obtained from specific-heat measurements⁶).

The value of $b^{(2)}/C$ decreases proportionally to c^2 also. The main contribution to $b^{(2)}/C$ is due to the exchange coupling between the X-site ions⁶⁾ so $b^{(2)}/C$ will also depend on the number of pairs.

5. *Conclusion.* The cross-relaxation processes in $\text{Ni}_3\text{La}_2(\text{NO}_3)_{12}\cdot 24\text{H}_2\text{O}$ occur between pairs of exchange coupled X-site Ni ions. In the diluted crystals these cross relaxations have been observed as separate processes at definite external magnetic field values. The results are in some respects similar to those obtained on diluted $\text{NiSiF}_6\cdot 6\text{H}_2\text{O}$ and $\text{CrCs}(\text{SO}_4)_2\cdot 12\text{H}_2\text{O}$ crystals. In the 100% and 60% salts at high magnetic fields the cross relaxations dominate over the spin-lattice relaxation processes. However, the value of α^{-1} in eq. (3) becoming relatively large, the different cross-relaxation processes overlap. As a result a fast relaxation which occurs in a whole range of the external magnetic field is observed.

REFERENCES

- 1) Van den Broek, J., Van der Marel, L. C. and Gorter, C. J., Commun. Kamerlingh Onnes Lab., Leiden No. 314c; *Physica* **25** (1959) 371.
- 2) De Vries, A. J., Thesis, Leiden (1965).
- 3) De Vries, A. J. and Livius, J. W. M., Commun. Leiden No. 349a; *Appl. sci. Res.* **17** (1967) 31.
- 4) Casimir, H. B. G. and Du Pré, F. J., Commun. Leiden, Suppl. No. 85a; *Physica* **5** (1938) 507.
- 5) Van den Broek, J., Thesis, Leiden (1960).
- 6) Mess, K. W., Lagendijk, E., Zimmerman, N. J., Van Duyneveldt, A. J., Giessen, J. J. and Huiskamp, W. J., Commun. Leiden No. 372a; *Physica* **43** (1969) 165.
- 7) Culvahouse, J. W., *J. chem. Phys.* **36** (1962) 2720.
- 8) Van Duyneveldt, A. J., Tromp, H. R. C. and Gorter, C. J., Commun. Leiden No. 361c; *Physica* **38** (1968) 205.
- 9) Harris, E. A. and Yngvesson, K. S., *J. Phys. C Ser. 2*, Vol. 1 (1968) 1011.
- 10) Caspers, W. J., Commun. Leiden, Suppl. No. 118c; *Physica* **26** (1960) 809.

SPIN-LATTICE RELAXATION IN MANGANESE FLUOSILICATE

Synopsis

Spin-lattice relaxation times of $\text{MnSiF}_6 \cdot 6\text{H}_2\text{O}$ are reported. Non-diluted samples showed a Raman relaxation with $\tau_L \propto T^{-5}$ above 10 K, while at helium temperatures $\tau_L \propto T^{-\beta}$ with $1 < \beta < 2$ for single crystals and $\beta = 1.0$ for a powdered specimen. These results indicate that a direct relaxation process is dominating in the powder, while in the single crystals the relaxation is modified by phonon-bottleneck processes. The observed temperature dependences in the liquid helium range could be described with the assumption that $\tau_L = \tau_{ph}$ at $T = 3.5$ K. The relaxation times observed in the diluted samples showed an anomalous behaviour in the region of the Raman processes. At helium temperatures no evidence was found that impurities play a rôle such as in the case of $\text{Mn}(\text{NH}_4)_2(\text{SO}_4)_2 \cdot 6\text{H}_2\text{O}$ ³). Measurements of the adiabatic susceptibility reveal $b/C = 71 \times 10^4 \text{ Oe}^2$, giving $b/R = 3.7 \times 10^{-2} \text{ K}^2$.

1. *Introduction.* Theories on spin-lattice relaxation require spin-orbit coupling in order to describe the interaction between the spins and the phonon modes¹). In *S*-state ions orbital angular momentum is mixed into the ground state if one calculates the ground level state functions using several orders of perturbation theory²). Therefore the spin-orbit coupling is weak which leads to relatively long relaxation times.

Measurements on $\text{Mn}(\text{NH}_4)_2(\text{SO}_4)_2 \cdot 6\text{H}_2\text{O}$ ³) demonstrated these long relaxation times. However, these measurements showed impurities to have a considerable influence on the relaxation times at helium temperatures.

The work reported here was stimulated by the desire to know whether these impurities played such an important role in all manganese salts or whether it is the crystal structure of the Tutton salts which sensitizes the relaxation times to impurities.

Spin-lattice relaxation occurs if the energy difference ΔE between two ground states of the paramagnetic ion can be exchanged with the lattice waves by processes involving one phonon with angular frequency ω : $\Delta E = \hbar\omega$ or by processes involving two phonons, ω_1 and ω_2 : $\Delta E = \hbar\omega_1 - \hbar\omega_2$. The former give rise to 'direct relaxation' which in the case of a Kramers

doublet leads to an inverse relaxation time $\tau_L^{-1} \propto TH_c^4$, where T is the temperature and H_c the external magnetic field. The latter cause the so-called 'quasi Raman relaxation', normally characterized by τ_L^{-1} proportional to T^7 or T^9 .

Orbach and Blume⁴⁾ pointed out that the phonons taking part in the Raman relaxation processes which possess energies higher than the separation Δ between the ground states and the next Kramers doublets ($\Delta \ll kT$), lead to inverse relaxation times:

$$\tau_L^{-1} \propto T^5 J_4(\theta_D) \quad (1)$$

where

$$J_4(\theta_D) = \int_0^{x_m} \frac{x^4 e^x}{(e^x - 1)^2} dx, \quad x = \omega/kT, \quad x_m = \theta_D/T,$$

θ_D being the Debye temperature which is related to the cutoff frequency ω_m of the phonon spectrum by $k\theta_D = \hbar\omega_m$.

This expression simplifies to $\tau_L^{-1} \propto T^2$ if $T \gg \theta_D$ and to $\tau_L^{-1} \propto T^5$ at temperatures $T \ll \theta_D$. Brons and Van Vleck⁵⁾ made the early suggestion that the field dependence of the relaxation time for the Raman processes can be expressed by:

$$\tau_L = \tau_0(b + CH_c^2)/(b + pCH_c^2) \quad (2)$$

where b is the coefficient of the magnetic specific heat $c_M = b/T^2$ and C is Curie's constant. The parameter p usually does not differ much from 0.5.

2. Experimental methods, samples. The equipment has been described in detail by De Vries and Livius⁶⁾. The samples are placed in a constant magnetic field H_c on which a small oscillating field h is superimposed. In the paramagnetic substance a varying magnetization m is induced. The complex susceptibility $\bar{\chi} = m/h$ can be derived from the output voltage of a Wheatstone bridge with four inductors, one with the sample inserted. The relaxation times τ_L were obtained by using two methods:

a. The dispersion-absorption technique. In the frequency range of the bridge (200 Hz to 1 MHz) both the components of the susceptibility χ' and χ'' are measured. Using the formalism as derived by Casimir and Du Pré⁷⁾ one finds:

$$\chi' = \chi_{ad} + (\chi_0 - \chi_{ad})/(1 + \tau_L^2 \omega^2) \quad (3)$$

and

$$\chi'' = (\chi_0 - \chi_{ad}) \tau_L \omega / (1 + \tau_L^2 \omega^2).$$

χ_0 is the static value of the susceptibility. This method allows us to evaluate

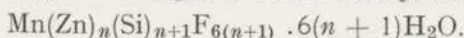
the spin-lattice relaxation time τ_L as a function of temperature and external magnetic field if its value lies between 0.3×10^{-3} s and 10^{-7} s. If the measuring frequency is high compared with the inverse relaxation time one obtains for the susceptibility a frequency independent value, χ_{ad} , which has to be interpreted as the susceptibility of the paramagnetic spin-system isolated from the lattice. If the paramagnetic substance obeys Curie's law: $\chi_{ad}/\chi_0 = b/(b + CH_c^2) = (1 + H_c^2/(b/C))^{-1}$. Thus measuring χ_{ad} as a function of H_c yields b/C .

b. Field-step method. If the spin-lattice relaxation process becomes slow it is possible to measure τ_L by monitoring the output of the bridge after a sudden change in the external magnetic field. A detailed calculation of the observed susceptibility in this case can be found in ref. 8. This method merely leads to a plain result if one deals with a relaxation process with a single relaxation time. Another disadvantage is that this method is restricted to external magnetic fields of the order of the value $\sqrt{(b/C)}$. At much higher fields χ_{ad} hardly changes as a function of field so the sensitivity of the step-field method decreases. With the present equipment it is possible in this way to derive the relaxation times if $\tau_L > 0.02$ s.

The fluosilicates ($X^{2+}SiF_6 \cdot 6H_2O$) form a group of crystals with a hexagonal structure⁹). The unit cell contains one bivalent ion surrounded by six water molecules only. The crystalline field at the bivalent ions is nearly cubic with a small trigonal distortion which coincides with the c axis of the crystal.

The manganese ions have S -state ground levels ($L = 0$) with a spin of $5/2$. The zero-field energy level splittings of $MnSiF_6 \cdot 6H_2O$ are of the order of 0.02 cm^{-1} at the lowest temperatures¹⁰).

For the experiments a series of diluted and nondiluted crystals have been used. The diluted crystals were grown from a solution of $MnSiF_6$ and $ZnSiF_6$ and they are thought to be mixed crystals:



The values of n are estimated from the magnetic susceptibilities. The following samples have been used: $n = 1$ (50% $MnSiF_6 \cdot 6H_2O$), $n = 7.3$ (12%), $n = 19$ (5%), $n = 24$ (4%), $n = 66$ (1.5%), $n = 125$ (0.8%) and $n = 330$ (0.3%). In this paper the samples will be referred to as 0.3% $MnSiF_6 \cdot 6H_2O$, etc.

3. *Experimental results.* *a. Nondiluted samples.* Above 14 K the spin-lattice relaxation time was measured using the dispersion-absorption technique. The results obtained on two crystals, one orientated with the external magnetic field $H_c // c$ axis and one with $H_c \perp c$ axis, were identical. As can be seen in fig. 1 the τ_L vs. T curve above 14 K can be described by:

$$(\tau_L)_{1 \text{ KOe}}^{-1} = 1.2 \times 10^{-4} T^5 J_4(\theta_D = 140 \text{ K}) \text{ s}^{-1}.$$

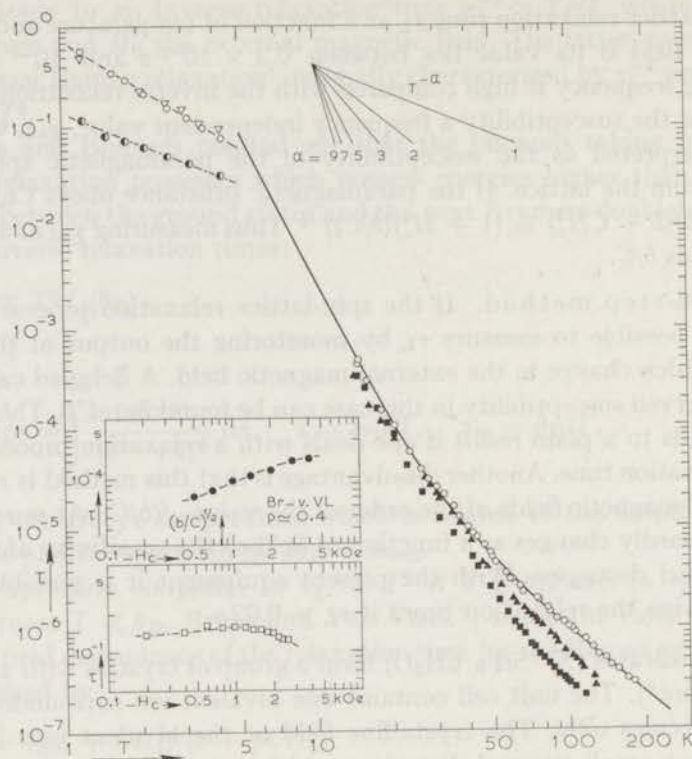


Fig. 1. Relaxation time τ vs. temperature for manganese fluosilicate.

- 100% $\text{MnSiF}_6 \cdot 6\text{H}_2\text{O}$; $H_c \parallel c$ axis; $H_c = 1$ kOe
- ▽ 100% $\text{MnSiF}_6 \cdot 6\text{H}_2\text{O}$; $H_c \perp c$ axis; $H_c = 1$ kOe
- 100% $\text{MnSiF}_6 \cdot 6\text{H}_2\text{O}$; powder
- 12% $\text{MnSiF}_6 \cdot 6\text{H}_2\text{O}$; $H_c \parallel c$ axis; $H_c = 0.5$ kOe
- ▲ 5% $\text{MnSiF}_6 \cdot 6\text{H}_2\text{O}$; $H_c \parallel c$ axis; $H_c = 0.5$ kOe
- : $\tau^{-1} = 1.2 \times 10^{-4} T^5 J_4$ ($\theta_D = 140$ K) s^{-1}
- inset: τ vs. external magnetic field for 100% $\text{MnSiF}_6 \cdot 6\text{H}_2\text{O}$ with $H_c \parallel c$ axis; ● $T = 20.3$ K; □ $T = 2.62$ K.

In this temperature range the dependence of τ_L on magnetic field (inset fig. 1) can be described by a Brons–Van Vleck formula with $p = 0.4$.

At helium temperatures the relaxation times fall in the range covered by the step-field method. The signals showed good c-curves indicating a relaxation process with one single relaxation time. In the τ_L vs. T graph some difference is seen between the two crystal orientations. For the sample with $H_c \parallel c$ axis: $(\tau_L)_{1\text{kOe}} = 0.78 \times T^{-1.6}$ s (crystal *a*) and for the sample with $H_c \perp c$ axis $(\tau_L)_{1\text{kOe}} = 0.60 \times T^{-1.3}$ s. These two exponents do not agree with the above mentioned theoretical temperature dependences. Experiments on several other salts at helium temperatures often show similar discrepancies from theory. In order to interpret these deviations one may think of: i) impurities causing fast relaxation centres in the crystal³,

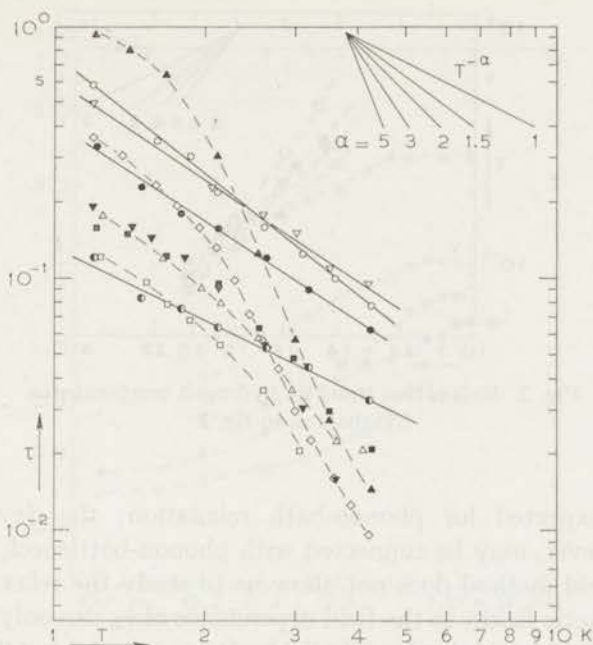


Fig. 2. Relaxation times at helium temperatures for various manganese fluosilicates.

- 100% $\text{MnSiF}_6 \cdot 6\text{H}_2\text{O}$ with $H_c // c$ axis, sample *a*; $H_c = 1$ kOe
- 100% $\text{MnSiF}_6 \cdot 6\text{H}_2\text{O}$ with $H_c // c$ axis, sample *b*; $H_c = 1$ kOe
- ▽ 100% $\text{MnSiF}_6 \cdot 6\text{H}_2\text{O}$; $H_c \perp c$ axis; $H_c = 1$ kOe
- 100% $\text{MnSiF}_6 \cdot 6\text{H}_2\text{O}$, powder
- 12% $\text{MnSiF}_6 \cdot 6\text{H}_2\text{O}$
- ▲ 5% $\text{MnSiF}_6 \cdot 6\text{H}_2\text{O}$
- ◇ 4% $\text{MnSiF}_6 \cdot 6\text{H}_2\text{O}$
- △ 2% $\text{MnSiF}_6 \cdot 6\text{H}_2\text{O}$
- ▼ 0.8% $\text{MnSiF}_6 \cdot 6\text{H}_2\text{O}$

The relaxation times for the diluted samples are given for an external field of 0.5 kOe orientated parallel to the *c* axis.

ii) phonon-bottleneck processes¹¹). Both possibilities have been examined, the latter will be described here, the former will be mentioned in the next subsection.

The phonon bottleneck was considered as the cause of the observed temperature dependence. This was confirmed by taking another single crystal (crystal *b* in figure 2) and comparing the results with those of a powder grown from the same solution. As may be seen in fig. 2 there is a noticeable difference between the relaxation times in the two samples. Those of the powder can be described by $(\tau_L)_{1\text{kOe}} = 0.14 \times T^{-1.0}$ s while crystal *b* obeys $(\tau_L)_{1\text{kOe}} = 0.42 \times T^{-1.35}$ s.

The results indicate a direct relaxation process to be dominant in the powder. The measurements on single crystals do not obey the $\tau \propto T^{-2}$

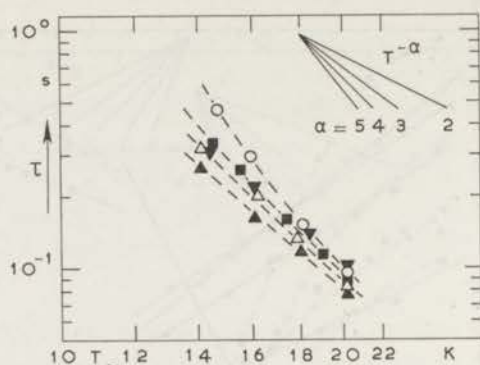


Fig. 3. Relaxation times at hydrogen temperatures. Symbols as in fig. 2.

dependence expected for phonon-bath relaxation; the deviations from $\tau \propto T^{-1}$, however, may be connected with phonon-bottleneck effects.

The step-field method does not allow us to study the relaxation in high external magnetic fields, so the field dependence of τ_L can only be measured at relatively low external magnetic fields. It is noticed (inset fig. 1) that τ_L starts to decrease as a function of H_c as is to be expected for direct relaxation and for phonon-bath relaxation.

b. Diluted samples. These were studied to examine the influence of impurities on the observed relaxation times. The results above 14 K show that the diluted $\text{MnSiF}_6 \cdot 6\text{H}_2\text{O}$ samples have shorter relaxation times than

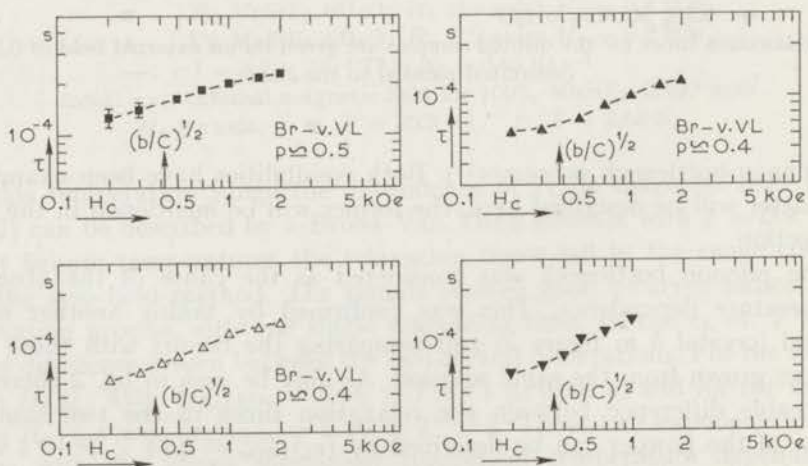


Fig. 4a. $\tau(H_c)$ at hydrogen temperatures for diluted manganese fluosilicates.
 ■ 12% $\text{MnSiF}_6 \cdot 6\text{H}_2\text{O}$; $T = 17.4$ K; ▲ 5% $\text{MnSiF}_6 \cdot 6\text{H}_2\text{O}$; $T = 20.2$ K
 Δ 2% $\text{MnSiF}_6 \cdot 6\text{H}_2\text{O}$; $T = 20.4$ K; ▼ 0.8% $\text{MnSiF}_6 \cdot 6\text{H}_2\text{O}$; $T = 20.4$ K

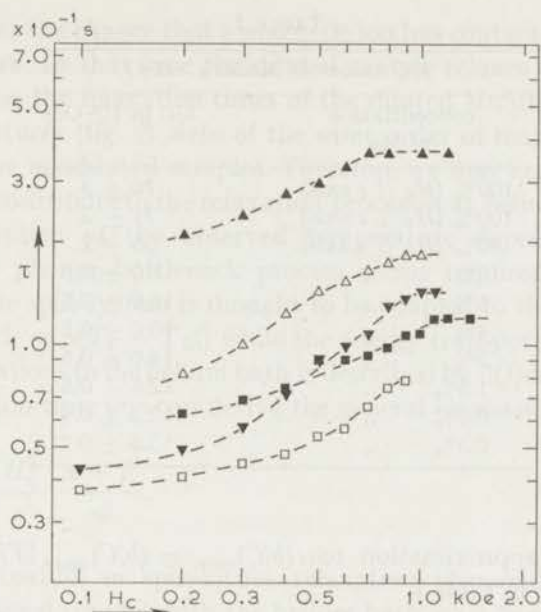


Fig. 4b. $\tau(H_c)$ at helium temperatures for diluted manganese fluosilicates.

- 12% $\text{MnSiF}_6 \cdot 6\text{H}_2\text{O}$; $T = 2.12$ K
- ▲ 5% $\text{MnSiF}_6 \cdot 6\text{H}_2\text{O}$; $T = 2.12$ K
- △ 2% $\text{MnSiF}_6 \cdot 6\text{H}_2\text{O}$; $T = 1.70$ K
- ▼ 0.8% $\text{MnSiF}_6 \cdot 6\text{H}_2\text{O}$; $T = 2.12$ K
- 0.3% $\text{MnSiF}_6 \cdot 6\text{H}_2\text{O}$; $T = 2.12$ K

the nondiluted samples. Because of the lack of sensitivity only the 12% and the 5% $\text{MnSiF}_6 \cdot 6\text{H}_2\text{O}$ have been studied up to 200 K (fig. 1). These curves do not comply with eq. (1). The more diluted samples have only been measured between 14 K and 20.3 K (fig. 3). The slope of the τ_L vs. T curves in this temperature range decreases when the manganese concentration decreases.

The Brons-Van Vleck formula for the dependence of the relaxation time on the external magnetic field (eq. (2)) applies for all measurements in the Raman relaxation region, see also fig. 4a.

At helium temperatures the relaxation times of the various diluted samples are shown in fig. 2 as functions of T and in fig. 4b as functions of H_c . All results were obtained on single crystals with the external magnetic field $H_c \parallel c$ axis, using the field-step method. In general not much difference with the results on concentrated salts has been observed.

c. b/C values have been measured for a series of concentrations of Mn ions in $(\text{Mn}, \text{Zn})\text{SiF}_6 \cdot 6\text{H}_2\text{O}$. For the highest Mn concentrations a correction is applied for deviations from Curie's law, which according to Van den Broek¹²⁾

TABLE I

<i>b/C</i> values of MnSiF ₆ ·6H ₂ O	
concentration of Mn	<i>b/C</i> in 10 ⁴ Oe ²
100% (<i>H_e</i> // <i>c</i> axis)	70 ± 3
100% (<i>H_e</i> ⊥ <i>c</i> axis)	71 ± 2
50% (<i>H_e</i> // <i>c</i> axis)	35 ± 2
12% ..	18.0 ± 0.5
5% ..	15.0 ± 0.5
4% ..	15.0 ± 0.5
2% ..	14.0 ± 0.5
1.5% ..	12.5 ± 0.5
0.8% ..	12.2 ± 0.4
0.3% ..	13.5 ± 0.7

lead in a first approximation to: $(b/C)_{\text{corr.}} = (b/C)_{\text{meas.}}\{T/(T - \theta)\}^3$. The results are given in table I.

4. *Discussion.* Raman relaxation region: Above 10 K the relaxation times of the nondiluted crystals clearly followed the predicted temperature dependence (section 3). Unfortunately we were not able to find in the literature a value for θ_D but according to the results for the Tutton salts¹³⁾ 140 K seems acceptable.

A description of the Raman relaxation in the diluted samples cannot be given yet. The Debye distribution of the phonons may be disturbed in the mixed crystals. Such an effect would lead to a temperature dependence deviating from eq. (1). Detailed measurements on highly diluted crystals are required to confirm this. The sensitivity of our equipment does not allow us to carry out such experiments. Measurements on diluted nickel and copper fluosilicates¹⁴⁾ also show anomalous behaviour in the Raman relaxation region while this effect has never been observed in the diluted Tutton salts. A better knowledge of both the chemical and physical properties of these mixed crystals may be required to solve this problem.

Direct relaxation region: In fig. 2 it is seen that the powdered 100% MnSiF₆·6H₂O sample shows a direct relaxation process with $\tau \propto T^{-1.0}$. The single crystals have temperature dependences which show neither the first power of a direct process nor the second power as expected for phonon-bottleneck processes.

Experiments on manganese Tutton salts indicated that the presence of non-magnetic impurity ions may shorten the spin-lattice relaxation times and also changes its temperature and field dependence³⁾. Replacing some of the Mn ions by non-magnetic ions does not affect the impurities, but

generally reduces the chance that a magnetic ion has contact with such a fast relaxation centre. In that case the diluted sample relaxes 10 or 100 times slower. However, the relaxation times of the diluted $\text{MnSiF}_6 \cdot 6\text{H}_2\text{O}$ salts at helium temperatures (fig. 2) were of the same order of magnitude as those measured for the nondiluted samples. Therefore we may conclude that impurities hardly contribute to the relaxation processes at helium temperature.

For a description of the observed temperature dependences a close analysis of the phonon-bottleneck process seems required. According to Van Vleck¹⁵) the spin-system is thought to be coupled to the low frequency oscillations $dQ/dt = \alpha(T_s - T_L)$ while the energy transport from these low frequency oscillations to the helium bath is described by $dQ/dt = \beta(T_L - T_B)$. For the relaxation time one can derive the general expression:

$$\tau = \frac{b + CH_c^2}{T^2} \frac{\alpha + \beta}{\alpha\beta}. \quad (4)$$

The usual situation in spin-lattice relaxation phenomena is that the phonons are in good contact with the helium bath, so $\beta \gg \alpha$. This gives the relation: $\tau_L = (b + CH_c^2)/T^2\alpha$ which with $\alpha \propto T^{-1}$ yields $\tau_L \propto T^{-1}$.

If the contact between the phonon-system and the helium bath is bad ($\alpha \gg \beta$) one finds the so-called phonon-bottleneck relaxation time:

$\tau_{\text{ph}} = (b + CH_c^2)/T^2\beta$ and because β is temperature independent $\tau_{\text{ph}} \propto T^{-2}$.

In the case of a single crystal of $\text{MnSiF}_6 \cdot 6\text{H}_2\text{O}$ neither of these two cases applies. The spin-lattice relaxation times measured for the powdered sample are of the same order of magnitude as the bottlenecked relaxation processes in the single crystals. If we assume $\alpha = \beta_{\text{s.c.}}$ for a certain temperature T_1 , then the relaxation time of the single crystal at that temperature will be $\tau = 2(b + CH_c^2)/T_1^2\alpha$. The powder, having a good contact with the helium bath ($\beta_{\text{powd.}} \gg \alpha$), will show a relaxation time $\tau = (b + CH_c^2)/T_1^2\alpha$ so one may expect a factor two difference in the relaxation times at the temperature T_1 where $\alpha = \beta_{\text{s.c.}}$.

In fig. 2 the relaxation times of the powdered sample and those of the single crystal that was taken from the same growing solution (sample *b*) do differ by a factor of two at $T = 3.5$ K. Now one can calculate following eq. (4) the temperature dependence of the single crystal relaxation time. One expects a curve which varies from $\tau \propto T^{-1}$ at temperatures $T \gg 3.5$ K to $\tau \propto T^{-2}$ at $T \ll 3.5$ K. However, in the temperature range where our measurements have been performed (1.2 K to 4.2 K) the curve as derived from eq. (4) hardly deviates from $\tau \propto T^{-1.5}$. In fact the experimental error of the measurements in the helium temperature range makes it impossible to notice a difference between eq. (4) and a simple curve $\tau \propto T^{-\gamma}$ with $1 < \gamma < 2$. The value of γ varies if the temperature T_1 where $\alpha = \beta_{\text{s.c.}}$ varies. $\beta_{\text{s.c.}}$ depends on the crystal dimensions, the cracks in the crystal *etc.*

Giordmaine *et al.*¹⁶⁾ estimated the order of magnitude of the phonon-bottleneck relaxation time, for a spherical sample (radius R). They give:

$$\tau_{\text{ph}} = \frac{2R^2 \hbar^2 N_0 v}{9(kT)^2} \quad (5)$$

where N_0 is the number of spins per unit volume and v is the velocity of sound. Crystal b was a parallelepiped, but we calculated eq. (5) for a sphere of roughly the same volume, taking $N_0 = 10^{19} \text{ cm}^{-3}$ and $v = 2 \times 10^5 \text{ cm/s}$ we get $\tau_{\text{ph}} = 10^{-1} \text{ s}$. This value is indeed of the order of magnitude of the relaxation time of the direct process. The assumption that $\alpha \simeq \beta_{\text{s.c.}}$ in the helium temperature range is obviously correct.

The Raman relaxation is effective for most diluted salts down to approximately 2 K, while in the concentrated salts direct processes or phonon-bottleneck processes are important over the whole helium temperature range. This effect can be expected because, as mentioned above, the Raman relaxation times in the diluted samples become shorter and less temperature dependent, which means that this relaxation can stay effective even below 4 K.

Below 2 K the relaxation times measured on the most diluted crystals come close to those of the powdered 100% $\text{MnSiF}_6 \cdot 6\text{H}_2\text{O}$. In highly diluted samples phonon-bottleneck effects will become less important¹⁶⁾ so one expects to measure $\tau \propto T^{-1}$ as in the powder. Measurements below 1.2 K are required to confirm the T^{-1} dependence in the diluted salts.

It is peculiar that the 4% and the 5% $\text{MnSiF}_6 \cdot 6\text{H}_2\text{O}$ crystals relax more slowly at the lowest temperatures than expected compared to other concentrations. These crystals were of extremely good quality, without cracks and transparent, while all other crystals had small cracks and were not completely transparent. A 'perfect' crystal will have longer phonon-bottleneck relaxation times¹⁶⁾. The results on 4% and 5% $\text{MnSiF}_6 \cdot 6\text{H}_2\text{O}$ confirm this; thus again supporting the idea that phonon-bottleneck effects are essential.

b/C values: For the nondiluted $\text{MnSiF}_6 \cdot 6\text{H}_2\text{O}$ the measurements of the adiabatic susceptibility reveal $b/C = 71 \times 10^4 \text{ Oe}^2$, giving $b/R = 3.7 \times 10^{-2} \text{ K}^2$. Ohtsubo¹⁷⁾ derived $b/R = 5.0 \times 10^{-2} \text{ K}^2$ from the tail of his specific-heat measurements. However, plotting $c_M/R = b/RT^2 = 3.7 \times 10^{-2}/T^2$ in his graph of c_M/R vs. T also gives a good fit to his experimental results.

Extrapolating the b/C values, as given in table I, to 0% Mn yields a value for $b_{\text{el}}/C + b_{\text{hfs}}/C = 12.5 \times 10^4 \text{ Oe}^2$, which is in fair agreement with the value calculated by Ohtsubo: $b_{\text{el}}/C + b_{\text{hfs}}/C = 12 \times 10^4 \text{ Oe}^2$. One can also calculate $b_{\text{dip}}/C = 36 \times 10^4 \text{ Oe}^2$. Subtracting these values from the b/C of the concentrated salt gives a result for the exchange contribution: $b_{\text{ex}}/C = 23 \times 10^4 \text{ Oe}^2$ or $b_{\text{ex}}/R = 1.2 \times 10^{-2} \text{ K}^2$; Ohtsubo quotes $b_{\text{ex}}/R =$

$= 2.5 \times 10^{-2} \text{ K}^2$. Thus the observed difference in the magnetic specific heat of $\text{MnSiF}_6 \cdot 6\text{H}_2\text{O}$ leads to a factor of two difference in the exchange part of the magnetic specific heat.

5. *Conclusions.* Simple theoretical predictions describe the spin-lattice relaxation times observed in $\text{MnSiF}_6 \cdot 6\text{H}_2\text{O}$ quite well. In the Raman relaxation region the predicted T^5 dependence is observed. At helium temperatures the relaxation times can be interpreted as a mixture of direct processes and phonon-bottleneck processes. There were no indications that impurities played an important role in the relaxation mechanisms, as is the case in manganese Tutton salts.

The reported value for b/C supports a contribution to the specific heat due to exchange interaction which is smaller than that derived from specific heat measurements.

REFERENCES

- 1) Orbach, R., Proc. Roy. Soc. A **264** (1961) 458.
- 2) Verstelle, J. C. and Curtis, D. A., Handbuch der Physik Bd **18/1** (1968).
- 3) De Vries, A. J., Livius, J. W. M., Curtis, D. A., Van Duyneveldt, A. J. and Gorter, C. J., Commun. Kamerlingh Onnes Lab., Leiden No. 356a; Physica **36** (1967) 65.
- 4) Orbach, R. and Blume, M., Phys. Rev. Letters **8** (1962) 478.
- 5) Brons, F., Thesis, Groningen (1938).
Van Vleck, J. H., Phys. Rev. **57** (1940) 426.
- 6) De Vries, A. J. and Livius, J. W. M., Commun. Leiden No. 349a; Appl. sci. Res. **17** (1967) 31.
- 7) Casimir, H. B. G. and Du Pré, F. J., Commun. Leiden, Suppl. No. 85a; Physica **5** (1938) 507.
- 8) De Vries, A. J., Thesis, Leiden (1965).
- 9) Pauling, L., Z. Krist. **72** (1930) 482.
Hamilton, W., Acta Cryst. **15** (1962) 353.
- 10) Bleaney, B. and Ingram, D. J. E., Proc. Roy. Soc. A **205** (1951) 336.
- 11) Scott, P. L. and Jeffries, C. D., Phys. Rev. **127** (1962) 51.
- 12) Van den Broek, J., Thesis, Leiden (1960).
- 13) De Vries, A. J., Curtis, D. A., Livius, J. W. M., Van Duyneveldt, A. J. and Gorter, C. J., Commun. Leiden No. 356b; Physica **36** (1967) 91.
- 14) Van Duyneveldt, A. J., Physica to be published.
- 15) Van Vleck, J. H., Phys. Rev. **59** (1941) 724.
- 16) Giordmaine, J. A., Alsop, A. L. E., Nash, F. R. and Townes, C. H., Phys. Rev. **109** (1958) 302.
- 17) Ohtsubo, A., J. Phys. Soc. Japan **20** (1965) 82.

SPIN-LATTICE RELAXATION IN ERBIUM ETHYLSULPHATE

Synopsis

Data are presented on the paramagnetic spin-lattice relaxation times in concentrated erbium ethylsulphate. The results, above 4 K, can be described by means of an Orbach process: $(\tau_L)_{H_c=0.5 \text{ kOe}} = 1.55 \times 10^{-10} \exp(54/T)$ s. In a single crystal with $H_c \perp c$ axis double relaxation processes have been observed at the temperature of liquid helium at external magnetic fields above 3 kOe. This behaviour is studied extensively on several samples. It is noticed that the double relaxations become less pronounced if the crystal size decreases and this suggests the double relaxation behaviour is related to phonon bottleneck effects. The relaxation time in the powdered sample, at low temperatures and high external magnetic fields, is found to be proportional to $T^{-1.8} H_c^{-1.8}$; this may indicate that relaxation dependences have been observed intermediate between that of an Orbach process and that of a direct process. The b/C value is found to be $9.7 \times 10^4 \text{ Oe}^2$ if $H_c \perp c$ axis and $1.5 \times 10^6 \text{ Oe}^2$ if $H_c \parallel c$ axis.

1. *Introduction.* Van den Broek *et al.*¹⁾ investigated the relaxation behaviour of a series of rare earth ethylsulphates, but erbium ethylsulphate was omitted. Some preliminary measurements performed on erbium ethylsulphate by Toet *et al.*²⁾ indicated the existence of double relaxation phenomena at the temperatures of liquid helium. With the present equipment relaxation times down to 10^{-7} s can be measured in external magnetic fields up to 8 kOe; thus we expected to be able to determine the relaxation mechanisms in erbium ethylsulphate in greater detail.

Erbium ethylsulphate, $\text{Er}(\text{C}_2\text{H}_5\text{SO}_4)_3 \cdot 9\text{H}_2\text{O}$, forms, as all ethylsulphates a hexagonal crystal of the spacegroup C_{3h}^3 . Per unit cell there are two magnetically equivalent erbium ions, each in an electric field of trigonal symmetry with the trigonal axis parallel to the c axis of the crystal. Er^{3+} has an odd number of electrons in the $4f$ shell, causing the magnetic properties. Therefore the energy level scheme consists of Kramers doublets. Elliott and Stevens⁴⁾ have described the influence of the electric fields on the energy level scheme. In the lowest energy states the Er^{3+} ion can be described with an effective spin $S' = \frac{1}{2}$ with different Landé splitting factors if the applied

magnetic field is orientated parallel or perpendicular to the c axis. E.S.R. measurements by Cooke⁵) yield $g_{\perp} = 8.78$ and $g_{\parallel} = 1.51$ for a 1:200 diluted crystal.

The paramagnetic relaxation behaviour was studied by observing the complex susceptibility $\bar{\chi} = \chi' - i\chi''$ with the apparatus designed by De Vries⁶). The sample is placed in a magnetic field H consisting of a constant part H_c and a parallel oscillating component: $h \exp(i\omega t)$. Casimir and Du Pré's elementary thermodynamical description supposes the paramagnetic salt to consist of two systems: the spin system determining all the paramagnetic properties of the sample and the lattice system describing the remaining properties (*e.g.* lattice vibrations). Assuming internal equilibrium in both systems and the energy transfer between the spin system and the lattice to be proportional to the small temperature difference between these systems, one obtains for the frequency dependence of $\bar{\chi}$ ⁷):

$$\begin{aligned}\chi' &= \chi_{ad} + (\chi_0 - \chi_{ad}) / (1 + \tau_L^2 \omega^2), \\ \chi'' &= (\chi_0 - \chi_{ad}) \tau_L \omega / (1 + \tau_L^2 \omega^2),\end{aligned}\quad (1)$$

where τ_L is the spin-lattice relaxation time, χ_0 is the static susceptibility and χ_{ad} the value of $\bar{\chi}$, measured at frequencies $\omega \gg \tau_L^{-1}$ where the spin system follows the field variation without exchanging energy with the lattice. If a description of the magnetic properties with a simple spin system is not adequate, more spin systems can be introduced, each with its own energy exchange mechanism to the lattice. In that case eqs. (1) become a sum over the relaxation mechanisms involved⁸):

$$\chi'(H_c) / \chi_0(H_c = 0) = 1 - \sum_i F_i + \sum_i F_i / (1 + \tau_i^2 \omega^2)$$

and

$$\chi''(H_c) / \chi_0(H_c = 0) = \sum_i F_i \tau_i \omega / (1 + \tau_i^2 \omega^2), \quad (2)$$

where $\sum_i F_i = (\chi_0(H_c) - \chi_{ad}(H_c)) / \chi_0(H_c = 0)$. Our equipment permits us to observe the susceptibility as a function of frequency. If there is a considerable difference between $\chi_0(H_c)$ and $\chi_{ad}(H_c)$ the relaxation times in the interval between 10^{-2} and 10^{-7} s can be derived from eqs. (1) or (2). When the bridge is balanced at a frequency $\omega \gg \tau_L^{-1}$ and the magnetic field then changed abruptly, the response of the output voltage shows an exponential variation of χ_{ad} . This so-called field-step method allows us to measure relaxation times longer than 5×10^{-2} s. If one deals with multiple relaxation processes the field-step method cannot be applied.

2. *Experimental results.* Measurements above 4.2 K are carried out after the liquid helium is evaporated. As a consequence of the heat influx in the cryostat the sample will warm up slowly. During this warming-up period

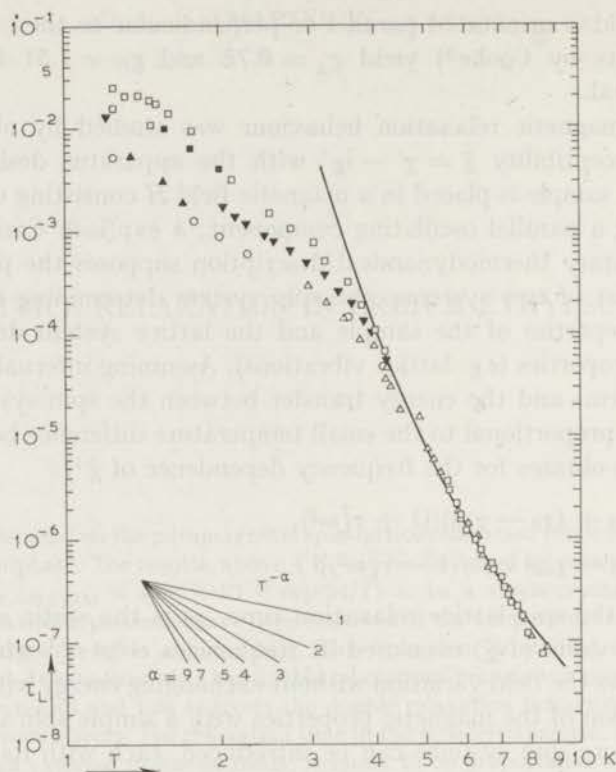


Fig. 1. Relaxation time τ_L vs. temperature for erbium ethylsulphate at an external magnetic field $H_e = 0.5$ kOe.

- : single crystal, $H_e \perp c$ axis
- : single crystal, $H_e \perp c$ axis, Toet, *et al.*²⁾
- ▼: 'crystallites'
- : 'powder'
- △: single crystal, $H_e // c$ axis
- ▲: single crystal, $H_e // c$ axis; Toet, *et al.*²⁾
- $\tau_L = 1.55 \times 10^{-10} \exp(54/T)$ s

τ_L can be derived from susceptibility measurements performed at suitable frequencies. If the zero field susceptibility in the interval between 4.2 K and 14 K is known this may be used to determine the temperature. In the case of rare earth ethylsulphate the temperature-independent part of the susceptibility due to the higher energy levels⁹⁾ cannot be neglected, thus $\chi_0 = C/T + \alpha$. No experimental values of the ratio α/χ_0 for erbium ethylsulphate was found in the literature. We estimated α by comparing the static susceptibilities at several standard temperatures. With these values of α , temperatures during the warming-up period are derived. Because of the experimental error in α the accuracy of T will decrease with increasing temperature.

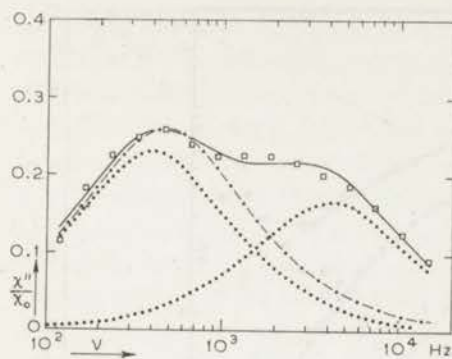


Fig. 2a

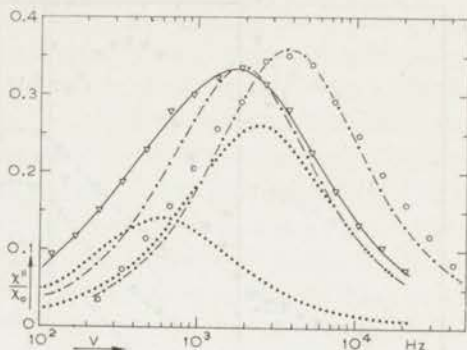


Fig. 2b

Fig. 2. Absorption against frequency at an external field of 6 kOe.

- a. \square : χ''/χ_0 for the single crystal, $H_e \perp c$ axis, at $T = 4.23$ K
 —: description of χ''/χ_0 vs. ν according to eq. (2) as a sum of two standard curves (dotted lines)
 - - -: description of χ''/χ_0 vs. ν according to eq. (1)
- b. ∇ : χ''/χ_0 for the "crystallites" at $T = 4.16$ K
 \circ : χ''/χ_0 for the "powder" at $T = 4.16$ K
 —, and - - - as in fig. 2a.

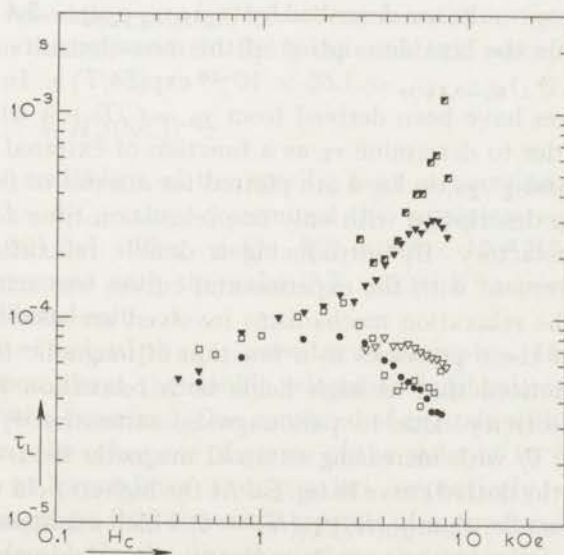


Fig. 3. Relaxation times vs. external magnetic field at approximately 4.2 K.

- \square , \blacksquare : single crystal, $H_e \perp c$ axis
 ∇ , \blacktriangledown : 'crystallites'
 \bullet : 'powder'

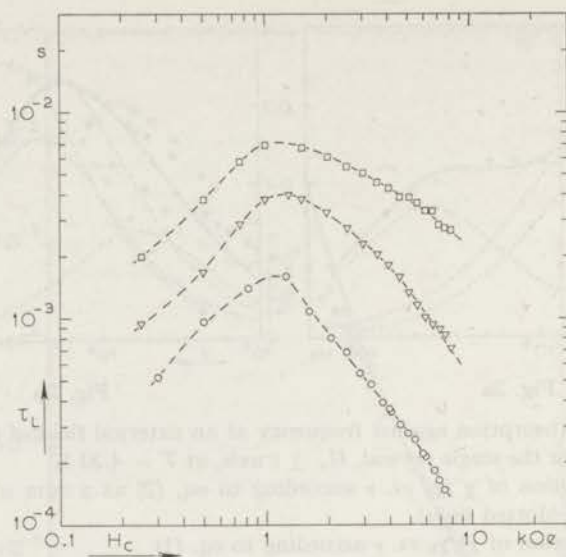


Fig. 4. Relaxation times *vs.* external magnetic field at $T = 2.0$ K.

- : single crystal, $H_c \perp c$ axis
- ▽: 'crystallites'
- : 'powder'

a. Erbium ethylsulphate; $H_c \perp c$ axis. The spin-lattice relaxation times as a function of temperature are given in fig. 1 for an external field of 0.5 kOe. These results are described by $(\tau_{\perp})_{H_c=0.5 \text{ kOe}} = 5.4 \times 10^{-2} T^{-3.8}$ s below 3 K, while the best description of the measurements above 4.2 K is obtained with $(\tau_{\perp})_{H_c=0.5 \text{ kOe}} = 1.55 \times 10^{-10} \exp(54/T)$ s. In this last case the temperatures have been derived from $\chi_0 = C/T + \alpha$ with $\alpha/\chi_0 = 0.14$ at 4.2 K. In order to determine τ_L as a function of external magnetic field χ'/χ_0 *vs.* $\log \nu$ and χ''/χ_0 *vs.* $\log \nu$ are plotted for a series of fields at 4.23 K. At high fields a description with only one relaxation time according to eq. (1) is less satisfactory. By introducing a double relaxation mechanism reasonable agreement with the experimental curves was achieved (fig. 2a). The times of the relaxation mechanisms involved are shown in fig. 3. The effectivity F of these processes as a function of magnetic field is given in fig. 5a; it is noticed that at high fields both relaxation processes occur with equal effectivity. Due to paramagnetic saturation¹⁰) a decrease of $\chi_0(H_c)/\chi_0(H_c = 0)$ with increasing external magnetic field will occur as is indicated with the dotted curve in fig. 5a. At the highest field values $F_1 + F_2$ is remarkably smaller than $\chi_0(H_c)/\chi_0(H_c = 0)$ which might suggest multiple-relaxation processes at the very low frequencies. Measurements at 2.0 K have been performed using a new equipment with frequencies down to 10 Hz. The experimental accuracy did not allow us to distinguish whether the χ'/χ_0 and χ''/χ_0 *vs.* frequency curves are to be described using one or

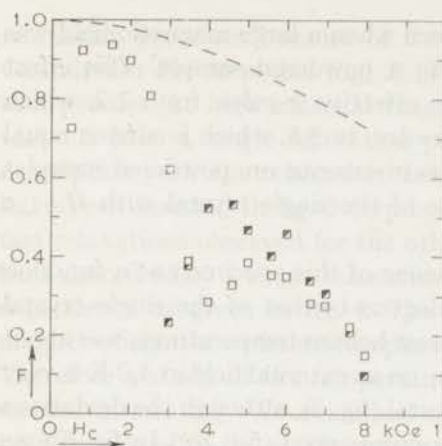


Fig. 5a

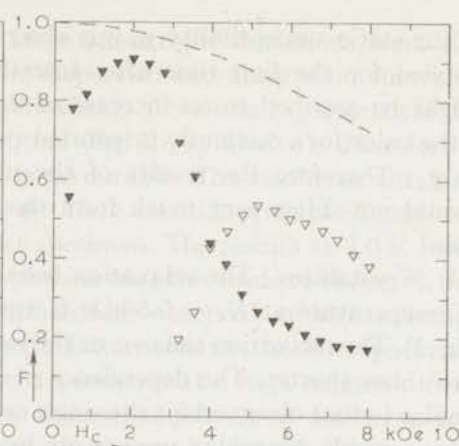


Fig. 5b

Effectivity F vs. external magnetic field.

Fig. 5a. Single crystal with $H_c \perp c$ axis; $T = 4.23$ K.

□, ■: effectivity of the fast and slow relaxation process, respectively (cf. fig. 3).
 ---: $\chi_0(H_c)/\chi_0(H_c = 0)$ according to paramagnetic saturation¹⁰.

Fig. 5b. 'Crystallites'; $T = 4.16$ K.

▽, ▼: effectivity of the fast and slow relaxation process, respectively (cf. fig. 3).
 ---: as in fig. 5a.

using more relaxation mechanisms. The results for τ_L vs. H_c at 2.0 K, assuming one relaxation process, have been inserted in fig. 4.

According to Casimir and Du Pré⁷) the adiabatic susceptibility is given by:

$$\chi_{ad}/\chi_0 = (1 + H_c^2/(b/C))^{-1}, \quad (3)$$

where b is the coefficient of the specific heat at constant magnetization: $c_M = b/T^2$. The b/C value determined by applying eq. (3) amounts $(9.7 \pm 0.2) \times 10^4$ Oe². This yields $b/R = 8.5 \times 10^{-3}$ K², which is in reasonable agreement with the value 7.7×10^{-3} K² reported by Cooke⁵) for a 1 : 200 diluted salt.

b. Erbium ethylsulphate; powdered samples. In order to obtain more information about the double relaxation mechanisms two powdered samples have been examined. One consisted of crystals with a diameter of a few millimeters, the other one of grains of the order of 10^{-2} mm. They will be referred to as 'crystallites' and 'powder', respectively.

In a large magnetic field the small crystals of a powdered sample will be orientated preferably in the direction where the potential energy $-M \cdot H$ has its minimum value. In not too high fields the magnetization M is proportional to g^2 and $g_{\perp} > g_{\parallel}$, so an orientation with the c axis perpendicular to the magnetic field is to be expected. Experimentally a considerable increase

of the static susceptibility χ_0 was observed when a large magnetic field was applied for the first time after inserting a powdered sample. This effect might be ascribed to an increase of the effective g value from 7.2, which is the value for a randomly orientated powder, to 8.5, which is almost equal to g_L . Therefore the results of the measurements on powdered samples should not differ very much from those of the single crystal with $H_e \perp c$ axis.

i) 'Crystallites'. The relaxation behaviour of this specimen as a function of temperature at $H_e = 0.5$ kOe is analogous to that of the single crystal (fig. 1). The relaxation time τ_L , at the lowest helium temperatures, was about two times shorter. The dependence of τ_L on an external field at 4.2 K is very similar to that observed for the single crystal (fig. 3), although the deviations from a single relaxation process are less pronounced (fig. 2b). In fig. 5b we noticed a decrease of the effectivity of the process connected with the slow relaxation at high external magnetic fields. The value of $F_1 + F_2$ stays below $\chi_0(H_e)/\chi_0(H_e = 0)$ but the difference is smaller than in the single crystal. At 2 K deviations from single relaxation processes have been observed too. However, the results were not consistent with a description with two relaxation processes. The τ_L vs. H_e dependence obtained at 2.0 K is displayed in fig. 4.

ii) 'Powder'. The relaxation times observed for an external magnetic field of 0.5 kOe were slightly shorter than in the case of 'crystallites', however, the temperature dependences are similar (fig. 1). The susceptibility vs. frequency curves of the above mentioned samples, at 4.2 K and at high external magnetic fields, have been described with two simultaneous

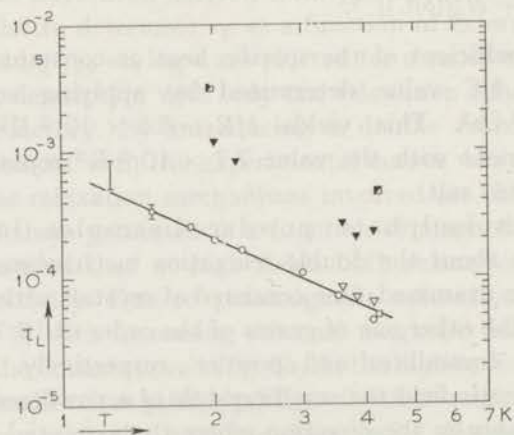


Fig. 6. Relaxation times vs. temperature at an external magnetic field of 6 kOe.

- , ■: single crystal, $H_e \perp c$ axis
- ▽, ▼: 'crystallites'
- : 'powder'

relaxation processes because of the large anisotropic deviations from the Casimir-Du Pré formulae (fig. 2). The dispersion and absorption curves of the 'powder' at high external magnetic fields show small symmetrical deviations from a single relaxation process (fig. 2b, symbol \circ). Therefore a description with one relaxation time is favourable. The results so obtained have been inserted in fig. 3 (symbol \bullet). They coincide with the branch of fast relaxations observed for the other specimen. The results at 2.0 K have been described by a single relaxation process too; this leads to the τ_L vs. H_e dependence as given in fig. 4. The relaxations observed at high external magnetic fields showed a less complicated behaviour than in the other specimen. Therefore a study of the temperature dependence at a high magnetic field seemed interesting. We examined the relaxation process at 6 kOe, as has been displayed in fig. 6. The relaxation times may be described by:

$$(\tau_L)_{H_e=6\text{kOe}} = 0.7 \times 10^{-3} T^{-1.8} \text{ s.}$$

c. Erbium ethylsulphate; $H_e // c$ axis. The spin-lattice relaxation times at an external field of 0.5 kOe have been presented in fig. 1. Below 4.2 K: $(\tau_{//})_{H_e=0.5\text{kOe}} = 1.7 \times 10^{-2} T^{-3.8} \text{ s.}$ From $\chi_0 = C/T + \alpha$, with $\alpha/\chi_0 = 0.21$ at 4.2 K, temperatures during the warming up period have been calculated. The results obtained in this way coincide with those in the other crystal direction, thus $(\tau_{//})_{H_e=0.5\text{kOe}} = 1.55 \times 10^{-10} \exp(54/T) \text{ s.}$ A detailed study of the field dependence of τ_L in this direction has not been performed. Because of the large b/C value magnetic fields up to 30 kOe are required to reach effectively the same maximum field as in the direction $H_e \perp c$ axis. From the adiabatic susceptibility one derives $b/C = (1.5 \pm 0.2) \times 10^6 \text{ Oe}^2$, while from direct specific-heat measurements⁵⁾ $3.3 \times 10^6 \text{ Oe}^2$ is to be expected. The disagreement might be ascribed to a slight misorientation of the c axis of the crystal with respect to the external magnetic field. Because of the large anisotropy in the g values a misorientation of half a degree will induce a resulting magnetization which makes an angle of approximately 10° with the c axis, so the b/C value will be a factor 2 smaller. With our present equipment it is hardly possible to orientate a crystal with an accuracy of one degree.

3. *Discussion.* The inverse of the spin-lattice relaxation time for the Er^{3+} ion with an excited state $|c\rangle$ at an energy distance Δ above the groundstate can be expressed by¹¹⁾:

$$\tau_L^{-1} = \underbrace{ATH_c^4}_{\text{direct process}} + \underbrace{B_1T^9 + B_2T^7H_c^2}_{\text{Raman processes}} + \underbrace{C \exp(-\Delta/kT)}_{\text{Orbach process}}.$$

The first excited energy state of the erbium ion in ethylsulphate is found at $\Delta/k = 63 \text{ K}$ ¹²⁾. The Debye temperature θ_D is of the order of 300 K, therefore the so-called Orbach process must be expected to occur. The wave

functions of the Er^{3+} ion are given by Larson and Jeffries¹⁴). One can substitute these values in the explicit expression for the Orbach relaxation time¹³) to derive C . As a result one then obtains: $\tau_L = 2.82 \times 10^{-10} \times \exp(63/T)$ s.

The relaxation times at an external field of 0.5 kOe, above 4.2 K, were described well by $\tau_L = 1.55 \times 10^{-10} \exp(54/T)$ s for both crystal directions. The agreement with the theoretical expression is reasonable; the exponent of 54 K seems somewhat too low. The value of Δ is influenced by the temperature determination after the liquid helium is evaporated. Measurements of the adiabatic susceptibility indicate the temperature-independent part of the susceptibility, α , might be smaller than the value extrapolated from the static susceptibility in zero field. A decrease of α/χ_0 would lead to a decrease of the temperatures calculated for the warming-up period and consequently Δ might increase. In spite of the temperature inaccuracy the relaxation times above 4 K cannot be fitted to a curve $\tau \propto T^{-9}$, so a Raman process has to be excluded in this temperature range.

The relaxation times at helium temperatures do not show the dominance of the direct process. The $(\tau_L)_{H_c=6\text{kOe}}$ vs. T curve obtained might indicate that one has to go to lower temperatures to observe a direct process. Our results tend to $\tau_L \propto T^{-2} H_c^{-2}$ at high external magnetic fields at low temperatures. If the observed relaxations fall in a range intermediate between that of an Orbach process ($\tau_L \propto H_c^0 \exp(\Delta/kT)$) and that of a Direct process with $\tau_L \propto T^{-1} H_c^{-4}$ then consequently the $T^{-2} H_c^{-2}$ dependence can reasonably be expected. Due to the paramagnetic saturation it is doubtful whether below 1.2 K the relaxation time at high magnetic fields can be measured with a reasonable accuracy. The branch of slow relaxations observed at 4.2 K disappears if the size of the crystals decreases. At 2.0 K there is less evidence for the occurrence of a second relaxation process. Therefore it seems plausible to ascribe the slow relaxations at 4.2 K to the poor heat contact between the lattice and the helium bath. In fig. 4 an influence of the crystal size on the observed relaxation time at 2.0 K is noticed. Thus the contact mechanism between the lattice and the helium bath is still related to the observed relaxation times. The phonon-bottleneck relaxation time, which is usually involved in these processes, is calculated to be of the order of 10^{-1} s in the single crystal at 2.0 K¹⁵), a value which seems rather large compared to the observed relaxation times. A satisfactory explanation for the influence of the crystal size cannot be given yet.

4. *Conclusion.* The spin-lattice relaxations in erbium ethylsulphate as a function of temperature showed two distinct regions. Above 4 K the τ_L vs. T curves could be described by means of an Orbach process; below 4 K the observed relaxation times are probably related to the direct process, but influences of the poor heat contact of the sample with the liquid helium

could not be excluded. It seems interesting to study diluted specimens at low frequencies and high external magnetic fields.

REFERENCES

- 1) Van den Broek, J. and Van der Marel, L. C., *Physica* **29** (1963) 948 and **30** (1964) 565; (Commun. Kamerlingh Onnes Lab., Leiden No. 335c and 337b).
- 2) Toet, D. Z. and Van Duyneveldt, A. J., Private communication.
- 3) Ketelaar, J. J. A., *Physica* **4** (1937) 619.
- 4) Elliott, R. J. and Stevens, K. W. H., *Proc. Roy. Soc. A* **215** (1952) 437.
- 5) Cooke, A. H., *Conf. de Phys. basses Temp.*, Paris (1955) 178.
- 6) De Vries, A. J. and Livius, J. W. M., *Appl. sci. Res.* **17** (1967) 31; (Commun. Leiden No. 349a).
- 7) Casimir, H. B. G. and Du Pré, F. J., *Physica* **5** (1938) 507; (Commun. Leiden, Suppl. No. 85a).
- 8) Van den Broek, J., Thesis, Leiden (1960).
- 9) Van Vleck, J. H., *Electric and Magnetic Susceptibilities* (Oxford 1932).
- 10) Van den Broek, J., van der Marel, L. C. and Gorter, C. J., *Physica* **27** (1961) 661; (Commun. Leiden No. 327a).
- 11) Orbach, R., *Fluctuation Relaxation and Resonance in magnetic Systems*, Scottish Universities' Summer School, Edinburgh (1961) 219.
- 12) Erath, E. H., *J. chem. Phys.* **34** (1961) 1985.
- 13) Orbach, R., *Proc. Roy. Soc. A* **264** (1961) 458.
- 14) Larson, G. H. and Jeffries, C. D., *Phys. Rev.* **141** (1966) 461.
- 15) Giordmaine, J. A., Alon, A. L. E., Nash, F. R. and Townes, C. H., *Phys. Rev.* **109** (1958) 302.

THE INFLUENCE OF NONMAGNETIC IMPURITIES ON THE
PARAMAGNETIC SPIN-LATTICE RELAXATION IN
COPPER TUTTON SALTS**Synopsis**

Measurements are reported on various copper Tutton salts. The introduction of nonmagnetic impurities on the place of the monovalent cation leads to faster relaxation processes. These faster relaxations are similar to those observed earlier in manganese ammonium Tutton salt when potassium or rubidium was added in the crystal. A satisfactory description of the τ_L vs. T , H_c curves was given by De Vries *et al.*¹⁾ on the basis of a model with two magnetic spin systems. In the 'impurified' copper Tutton salts such a model may also be used; the fast relaxation processes ascribed to the second spin-systems obey an Orbach type of temperature dependence of the relaxation time: $\tau_L \propto (\exp(\Delta/kT) - 1)$ with $3\text{K} \leq \Delta/k \leq 7\text{K}$. It is suggested that the occurrence of the fast relaxation processes is related to irregularities in the orientation (α , ψ) of the tetragonal symmetry axis in the mixed crystals and to the difference in crystal ionic radii between impurity ions and replaced monovalent cations.

1. *Introduction.* In manganese ammonium Tutton salts the influence of nonmagnetic impurities on the observed spin-lattice relaxation times has been examined in some detail by De Vries *et al.*¹⁾. The coupling of an S-state ion to the lattice waves usually leads to rather long spin-lattice relaxation times. For this reason the effect of impurities, causing fast relaxation centres, will be noticed quite easily in salts with S-state ions such as the manganese salts. The data on the temperature dependence and external magnetic field dependence of the relaxation times in the manganese ammonium Tutton salts have been described qualitatively on the basis of a model with two magnetic spin-systems. One of those systems is formed by the 'normal' Mn^{2+} ions, the second one consists of faster relaxing Mn ions. The identification of this second spin-system, however, was difficult. De Vries *et al.*¹⁾ tried several possibilities and ended with the conclusion that the nature of the second spin-system might be connected with the

radioactive properties of K and Rb introduced at some of the sites normally occupied by NH_4 in the manganese ammonium Tutton salt.

The experiments reported now have been started because the radioactive elements ^{40}K and ^{87}Rb occur in such small amounts that it is doubtful that these natural radioactivities might have such an enormous influence on the spin-lattice relaxation times.

Measurements on $\text{Cu}(\text{NH}_4)_2(\text{SO}_4)_2 \cdot 6\text{H}_2\text{O}$ showed that K impurities have an effect on the spin-lattice relaxation times of these salts also²⁾. The manganese Tutton salts are stable with ammonium as the monovalent cation, but not with other alkalis. However, with copper a whole series of Tutton salts can easily be grown. A close analysis of the effects of mixing different alkalis in the crystals of copper Tutton salts is able to shine some light on the nature of the second spin system.

The Tutton salts form a group of isomorphous monoclinic crystals with a tetragonal symmetry at the site of the divalent metal ion. There are two molecules per unit cell. The orientation of the axis of the tetragonal symmetry (= z axis) for each magnetic complex is determined by the angles α and ψ . α is the angle of inclination of the z axis to the ac plane of the crystal. The projection of z on the ac plane makes the angle ψ with the c axis.

TABLE I

	α^*	ψ^*	r^{**}	$b_{\text{ex}}/C^3)$
Copper ammonium Tutton	39°	65°	1.42 Å	$10.5 \times 10^4 \text{ Oe}^2$
Copper potassium Tutton	42°	105°	1.33 Å	$6.2 \times 10^4 \text{ Oe}^2$
Copper rubidium Tutton	40°	105°	1.48 Å	$1.15 \times 10^4 \text{ Oe}^2$
Copper cesium Tutton	40°	114°	1.69 Å	$0.37 \times 10^4 \text{ Oe}^2$

* Values derived from resonance data at 90 K⁴⁾.

** r is the crystal ionic radius of the monovalent cation³⁾.

The values of α and ψ , derived from resonance data³⁾ are given in table I. In this table we also quote the ionic radii r of the monovalent cations as given by Pauling⁴⁾ and the exchange contribution to the specific heat according to the measurements of Benzie *et al.*⁵⁾.

The behaviour of τ_L on the crystal orientation was not the subject of the present research, all measurements have been performed on powdered samples which consisted of about 1 g of small crystallites. These crystallites were grown from a mixed solution of coppersulphate and an alkali-sulphate in water. Impurities on the place of the monovalent cation were introduced by mixing the different alkalisulphates. The obtained crystals did contain the alkalis in roughly the same concentration as was the case in the growing solution. Professor J. B. Schute of the pharmaceutical laboratory was so kind to verify this. Therefore the samples will be referred

to as e.g. 10% K in $\text{Cu}(\text{NH}_4)_2(\text{SO}_4)_2 \cdot 6\text{H}_2\text{O}$, which means that in the growing solution 10% of the $(\text{NH}_4)_2\text{SO}_4$ was replaced by K_2SO_4 .

To study the paramagnetic relaxation behaviour, the samples are placed in a magnetic field H_c on which an oscillating part $h \exp(i\omega t)$ is superimposed. Both components of the complex susceptibility $\bar{\chi} = \chi' - i\chi''$ are measured as a function of frequency. The spin-lattice relaxation times have been derived by means of the well-known dispersion-absorption relations for a single relaxation process as given by Casimir and Du Pré⁶). For two samples a distribution of relaxation processes was observed, in

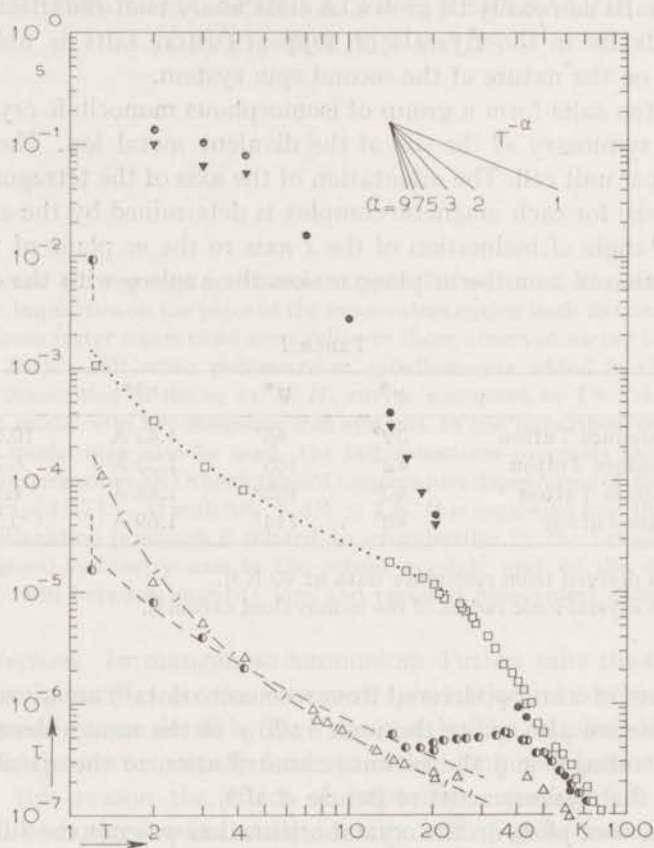


Fig. 1. Relaxation time τ_L vs. temperature for copper ammonium Tutton salts with different nonmagnetic impurities added;

- : pure $\text{Cu}(\text{NH}_4)_2(\text{SO}_4)_2 \cdot 6\text{H}_2\text{O}$, $H_c = 750$ Oe
- △: $\text{Cu}(\text{NH}_4)_2(\text{SO}_4)_2 \cdot 6\text{H}_2\text{O} + 10\%$ K, $H_c = 700$ Oe;
- ▼: $\text{Cu}(\text{NH}_4)_2(\text{SO}_4)_2 \cdot 6\text{H}_2\text{O} + 10\%$ Rb, $H_c = 700$ Oe;
- : $\text{Cu}(\text{NH}_4)_2(\text{SO}_4)_2 \cdot 6\text{H}_2\text{O} + 50\%$ Rb, $H_c = 700$ Oe;
- : $\text{Cu}(\text{NH}_4)_2(\text{SO}_4)_2 \cdot 6\text{H}_2\text{O} + 40\%$ Cs, $H_c = 700$ Oe;
- $\tau_L \propto \exp(3/T) - 1$; $\tau_L \propto \exp(4/T) - 1$;
- |-|- $\tau_L \propto \exp(7/T) - 1$.

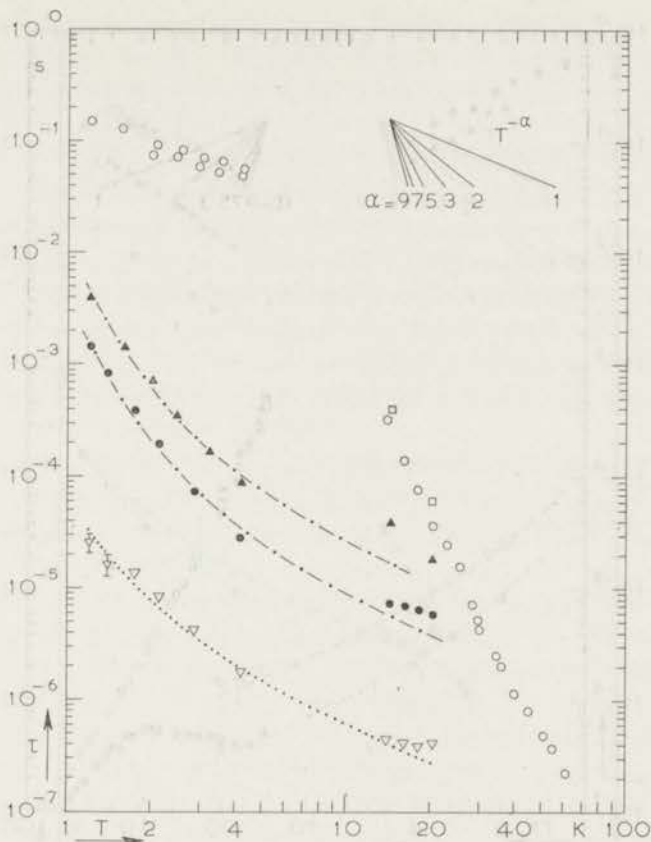


Fig. 2. Relaxation time τ_L vs. temperature for copper potassium Tutton salts with different nonmagnetic impurities added.

- : pure $\text{CuK}_2(\text{SO}_4)_2 \cdot 6\text{H}_2\text{O}$, $H_c = 300$ Oe;
- : $\text{CuK}_2(\text{SO}_4)_2 \cdot 6\text{H}_2\text{O} + 10\% \text{NH}_4$, $H_c = 700$ Oe;
- ▽: $\text{CuK}_2(\text{SO}_4)_2 \cdot 6\text{H}_2\text{O} + 40\% \text{NH}_4$, $H_c = 700$ Oe;
- ▲: $\text{CuK}_2(\text{SO}_4)_2 \cdot 6\text{H}_2\text{O} + 40\% \text{Cs}$, $H_c = 700$ Oe;
- : $\text{CuK}_2(\text{SO}_4)_2 \cdot 6\text{H}_2\text{O} + 40\% \text{Rb}$, $H_c = 700$ Oe;
- $\tau_L \propto \exp(4/T) - 1$; - · - · $\tau_L \propto \exp(6/T) - 1$.

these cases only the times of the shortest relaxations could be estimated. The apparatus and the measuring procedure has been described in detail by De Vries⁷).

2. *Experimental results.* In this section the spin-lattice relaxation times τ_L measured will be presented. The τ_L vs. temperature dependences for the four copper Tutton salts of interest are displayed in figs. 1 to 4. In each figure the relaxation times of a 'pure' copper Tutton salt are given, plus a series of results obtained on specimens with impurities. We will not discuss

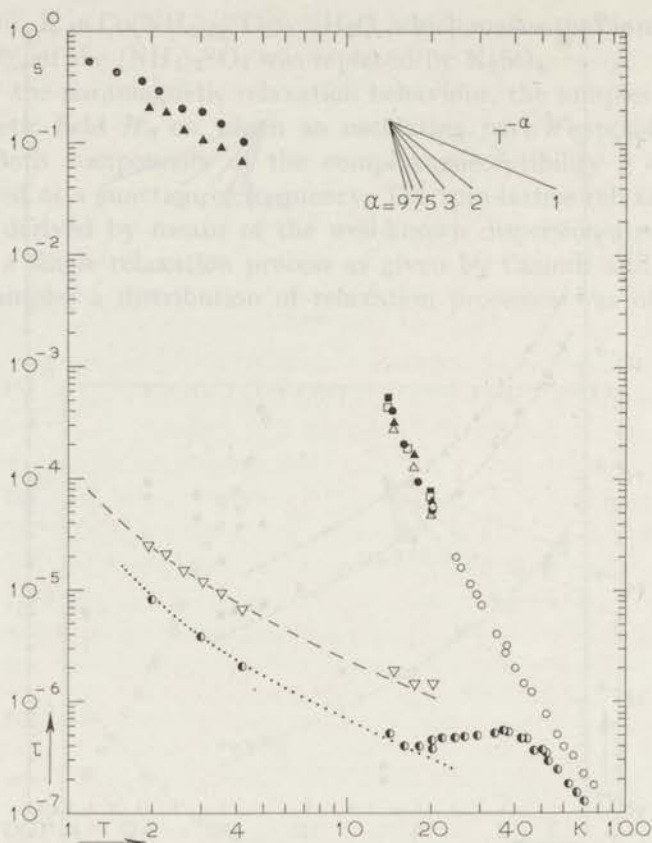


Fig. 3. Relaxation time τ_L vs. temperature for copper rubidium Tutton salts with different nonmagnetic impurities added.

- : pure $\text{CuRb}_2(\text{SO}_4)_2 \cdot 6\text{H}_2\text{O}$, $H_e = 300$ Oe;
 - : pure $\text{CuRb}_2(\text{SO}_4)_2 \cdot 6\text{H}_2\text{O}$, $H_e = 300$ Oe; single crystal $H_e // K_1$ axis;
 - △: $\text{CuRb}_2(\text{SO}_4)_2 \cdot 6\text{H}_2\text{O} + 10\% \text{NH}_4$, $H_e = 300$ Oe;
 - ▲: $\text{CuRb}_2(\text{SO}_4)_2 \cdot 6\text{H}_2\text{O} + 10\% \text{NH}_4$, $H_e = 700$ Oe;
 - ▽: $\text{CuRb}_2(\text{SO}_4)_2 \cdot 6\text{H}_2\text{O} + 40\% \text{NH}_4$, $H_e = 700$ Oe;
 - ◐: $\text{CuRb}_2(\text{SO}_4)_2 \cdot 6\text{H}_2\text{O} + 50\% \text{NH}_4$, $H_e = 700$ Oe;
 - : $\text{CuRb}_2(\text{SO}_4)_2 \cdot 6\text{H}_2\text{O} + 40\% \text{K}$, $H_e = 700$ Oe;
 - : $\text{CuRb}_2(\text{SO}_4)_2 \cdot 6\text{H}_2\text{O} + 40\% \text{Cs}$, $H_e = 700$ Oe;
- curves as in fig. 1.

the four types of Tutton salts separately, but rather follow the experiments in their chronological order.

In manganese ammonium Tutton salt potassium and rubidium impurities cause large effects on τ_L ¹). We introduced potassium in several copper Tutton salts and observed the relaxation times between 1.2 K and 80 K. The following results were obtained:

a) 10% K in $\text{Cu}(\text{NH}_4)_2(\text{SO}_4)_2 \cdot 6\text{H}_2\text{O}$: τ_L much shorter, as was already ob-

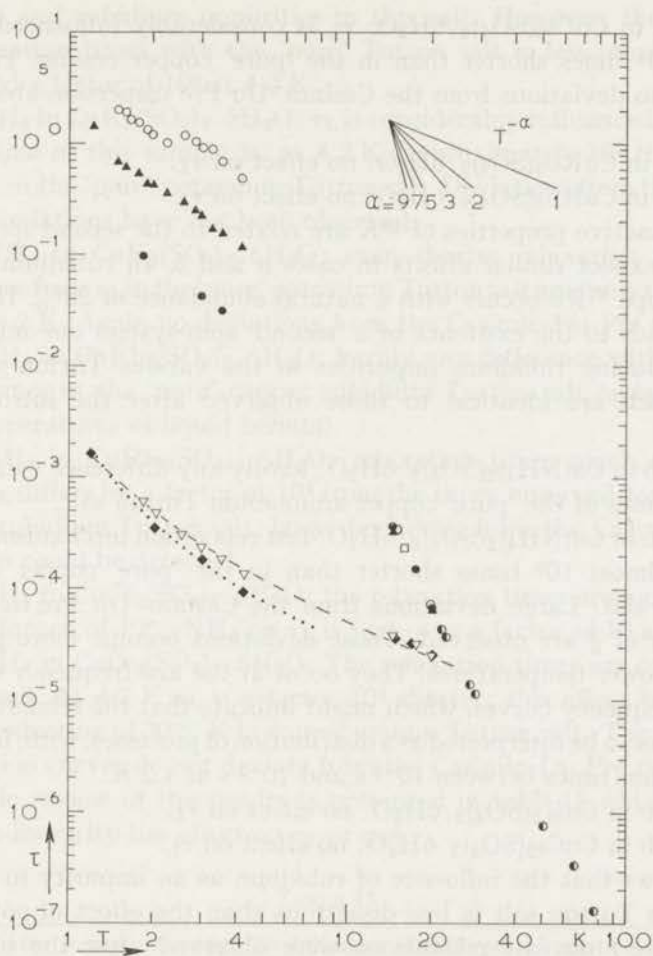


Fig. 4. Relaxation time τ_L vs. temperature for copper cesium tutton salts with different nonmagnetic impurities added.

- : pure $\text{CuCs}_2(\text{SO}_4)_2 \cdot 6\text{H}_2\text{O}$, $H_c = 300$ Oe;
 - : pure $\text{CuCs}_2(\text{SO}_4)_2 \cdot 6\text{H}_2\text{O}$, $H_c = 1250$ Oe; single crystal $H_c \parallel K_1$ axis;
 - : $\text{CuCs}_2(\text{SO}_4)_2 \cdot 6\text{H}_2\text{O} + 10\% \text{NH}_4$, $H_c = 700$ Oe;
 - ▽: $\text{CuCs}_2(\text{SO}_4)_2 \cdot 6\text{H}_2\text{O} + 40\% \text{NH}_4$, $H_c = 700$ Oe;
 - ▲: $\text{CuCs}_2(\text{SO}_4)_2 \cdot 6\text{H}_2\text{O} + 10\% \text{K}$, $H_c = 300$ Oe;
 - ◆: $\text{CuCs}_2(\text{SO}_4)_2 \cdot 6\text{H}_2\text{O} + 30\% \text{K}$, $H_c = 700$ Oe;
 - : $\text{CuCs}_2(\text{SO}_4)_2 \cdot 6\text{H}_2\text{O} + 40\% \text{Rb}$, $H_c = 700$ Oe;
- curves as in fig. 1.

served earlier²); at 4.2 K the relaxation process is almost 10^5 times faster than in the 'pure' copper ammonium tutton salt. The susceptibility shows the Casimir-Du Pré dispersion-absorption behaviour over the whole temperature range.

- b) 10% K in $\text{CuCs}_2(\text{SO}_4)_2 \cdot 6\text{H}_2\text{O}$: the relaxation processes are slightly faster (less than a factor 10) at the temperatures of liquid helium.

30% K in $\text{CuCs}_2(\text{SO}_4)_2 \cdot 6\text{H}_2\text{O}$: τ_L is considerably influenced; at 4.2 K τ_L is 10^4 times shorter than in the 'pure' copper cesium Tutton salt. Again no deviations from the Casimir-Du Pré dispersion-absorption relations.

- c) 10% K in $\text{CuRb}_2(\text{SO}_4)_2 \cdot 6\text{H}_2\text{O}$: no effect on τ_L .
40% K in $\text{CuRb}_2(\text{SO}_4)_2 \cdot 6\text{H}_2\text{O}$: no effect on τ_L .

If the radioactive properties of ^{40}K are related to the second spin system¹⁾ one would expect similar effects in cases *a* and *b*. In rubidium the radioactive isotope ^{87}Rb occurs with a natural abundance of 28%. If the radioactivity leads to the existence of a 'second' spin-system one might expect that introducing rubidium impurities in the various Tutton salts causes effects which are identical to those observed after the introduction of potassium.

- d) 10% Rb in $\text{Cu}(\text{NH}_4)_2(\text{SO}_4)_2 \cdot 6\text{H}_2\text{O}$: hardly any difference with the relaxation times of the 'pure' copper ammonium Tutton salt.
50% Rb in $\text{Cu}(\text{NH}_4)_2(\text{SO}_4)_2 \cdot 6\text{H}_2\text{O}$: fast relaxation mechanisms. At 4.2 K τ_L is almost 10^5 times shorter than in the 'pure' copper ammonium Tutton salt. Large deviations from the Casimir-Du Pré frequency behaviour of $\bar{\chi}$ are observed. These deviations become more pronounced at the lower temperatures. They occur at the low frequency sides of the $\bar{\chi}$ vs. frequency curves, which might indicate that the relaxation mechanism has to be interpreted as a distribution of processes, with, for example, relaxation times between 10^{-5} s and 10^{-2} s at 1.2 K.

- e) 40% Rb in $\text{CuK}_2(\text{SO}_4)_2 \cdot 6\text{H}_2\text{O}$: no effect on τ_L .
f) 40% Rb in $\text{CuCs}_2(\text{SO}_4)_2 \cdot 6\text{H}_2\text{O}$: no effect on τ_L .

Case *d* shows that the influence of rubidium as an impurity in the copper ammonium Tutton salt is less disastrous than the effect of potassium. In fact, in case *f* no fast relaxations were observed after the introduction of rubidium. Natural rubidium contains more radioactive atoms than potassium, but causes less or even no effect on τ_L in situations where potassium has a large influence on the relaxation times. We may conclude that in these cases no relation between the occurrence of radioactive isotopes and the 'second' spin-system exists. Excluding radioactivity as the cause of the fast relaxation mechanism, however, did not procure more information about the nature of the 'second' spin-system. The experiments were continued by mixing cesium and ammonium as impurities in the copper Tutton salts. This led to the following results:

- g) 40% Cs in $\text{CuK}_2(\text{SO}_4)_2 \cdot 6\text{H}_2\text{O}$: fast relaxation times. At 4.2 K τ_L is 10^3 times shorter than in the 'pure' copper potassium Tutton salt. The susceptibility does not deviate from the Casimir-Du Pré frequency behaviour.
h) 40% Cs in $\text{CuRb}_2(\text{SO}_4)_2 \cdot 6\text{H}_2\text{O}$: no effect on τ_L .
i) 40% Cs in $\text{Cu}(\text{NH}_4)_2(\text{SO}_4)_2 \cdot 6\text{H}_2\text{O}$: similar effect as that due to po-

tassium and rubidium impurities in this salt. However, the difference in relaxation times with the 'pure' Tutton salt is less pronounced; we observed a factor of 10^3 at 4.2 K.

f) 10% NH_4 in $\text{CuK}_2(\text{SO}_4)_2 \cdot 6\text{H}_2\text{O}$: τ_L is considerably influenced. The relaxation time of this sample is, at 4.2 K, approximately 10^3 times shorter than τ_L in the 'pure' potassium Tutton salt. Deviations from the Casimir-Du Pré relations have not been observed.

40% NH_4 in $\text{CuK}_2(\text{SO}_4)_2 \cdot 6\text{H}_2\text{O}$: even shorter relaxation times. The difference from τ_L in the 'pure' potassium Tutton salt amounts to a factor of 10^5 at 4.2 K. Again no deviations from the Casimir-Du Pré relations.

g) 10% NH_4 in $\text{CuRb}_2(\text{SO}_4)_2 \cdot 6\text{H}_2\text{O}$: hardly any difference with the relaxation times in the 'pure' copper rubidium Tutton salt (a factor two at the temperatures of liquid helium).

40% NH_4 in $\text{CuRb}_2(\text{SO}_4)_2 \cdot 6\text{H}_2\text{O}$: relaxation times much shorter. At 4.2 K τ_L differs by a factor of 10^4 from the times observed for the 'pure' copper rubidium Tutton salt; large deviations from the Casimir-Du Pré relations could be detected.

h) 10% NH_4 in $\text{CuCs}_2(\text{SO}_4)_2 \cdot 6\text{H}_2\text{O}$: the relaxation times are again shorter. The influence of 10% NH_4 on τ_L is just over a factor of 10 at 4.2 K.

40% NH_4 in $\text{CuCs}_2(\text{SO}_4)_2 \cdot 6\text{H}_2\text{O}$: The relaxation times are considerably influenced. At 4.2 K τ_L is a factor 10^4 shorter; this effect is similar to the introduction of 30% K in copper cesium Tutton salt. The dispersion-absorption curves do not deviate from the Casimir-Du Pré relations.

A schematic review of the results is presented in table II which indicates whether an impurity has effect on τ_L or not.

TABLE II

Schematic review showing the influence of different impurities on the observed spin-lattice relaxation times

	Added as impurities			
	NH_4	K	Rb	Cs
Copper ammonium Tutton	—	yes	yes	yes
Copper potassium Tutton	yes	—	no	yes
Copper rubidium Tutton	yes	no	—	no
Copper cesium Tutton	yes	yes	no	—

The field dependences of the relaxation times have not been described so far. The τ_L vs. H_c graphs are similar in all cases where impurities played an important role. In a 'pure' copper Tutton salt the field dependence of the relaxation time in the Raman relaxation region can be represented by a Brons-Van Vleck⁸⁾ formula with p in the range $0.4 < p < 0.5$. This dependence is shown in fig. 5*b* (symbol ●). In cases where fast relaxation

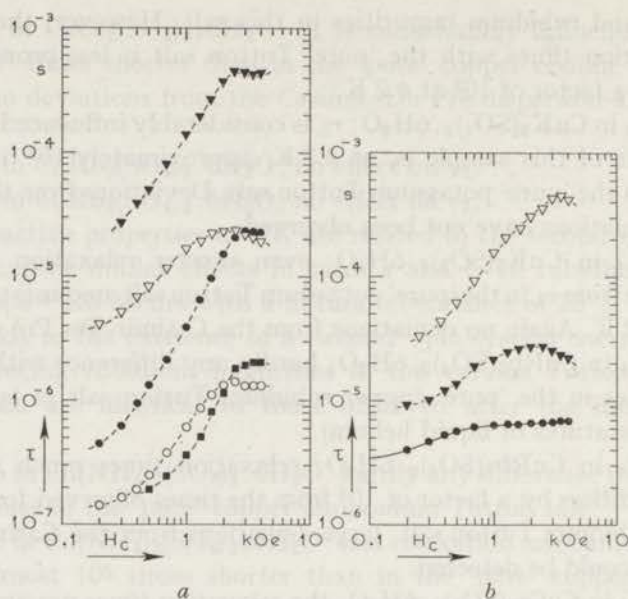


Fig. 5.

Relaxation time τ_L vs. external magnetic field H_c for various 'impurified' copper Tutton salts.

- a) $\text{Cu}(\text{NH}_4)_2(\text{SO}_4)_2 \cdot 6\text{H}_2\text{O} + 10\% \text{ K}$: \blacksquare ($T = 20.2 \text{ K}$);
 $\text{Cu}(\text{NH}_4)_2(\text{SO}_4)_2 \cdot 6\text{H}_2\text{O} + 40\% \text{ Cs}$: ∇ ($T = 20.3 \text{ K}$) and \blacktriangledown ($T = 4.1 \text{ K}$);
 $\text{Cu}(\text{NH}_4)_2(\text{SO}_4)_2 \cdot 6\text{H}_2\text{O} + 50\% \text{ Rb}$: \circ ($T = 20.4 \text{ K}$) and \bullet ($T = 4.2 \text{ K}$);
- b) $\text{CuK}_2(\text{SO}_4)_2 \cdot 6\text{H}_2\text{O} + 40\% \text{ Cs}$: \blacktriangledown ($T = 20.4 \text{ K}$) and ∇ ($T = 4.2 \text{ K}$);
 $\text{CuK}_2(\text{SO}_4)_2 \cdot 6\text{H}_2\text{O} + 40\% \text{ Rb}$: \bullet ($T = 20.4 \text{ K}$), this sample does not show fast relaxation processes.

— Brons-Van Vleck relation: $\tau_L \propto (b + CH_c^2)/(b + \frac{1}{2}CH_c^2)$.

processes are important a Brons-Van Vleck formula cannot describe the results, not even at the highest hydrogen temperatures. The fast relaxation processes show relaxation times which become considerably slower upon increasing the magnetic field as can be seen in figs. 5 and 6. This effect indicates that the influence of the impurities decreases at higher external magnetic fields.

3. *Discussion.* A detailed description of the character of the obtained τ_L vs. T , H_c curves can be found in ref. 1. In the present paper we shall restrict ourselves to a discussion of the fast relaxations and the origin of the 'second' spin-system.

It has been noticed earlier¹⁾ that the fast spin-lattice relaxation processes in the impure Tutton salts can be expressed in terms of an Orbach-type process. In these processes low-energy phonons are participating.

The spin-lattice relaxation times at defect sites has been discussed in some detail by Castle *et al.*⁹⁾ These authors describe a crystal with local phonon modes of frequency ω_2 which is much lower than the maximum

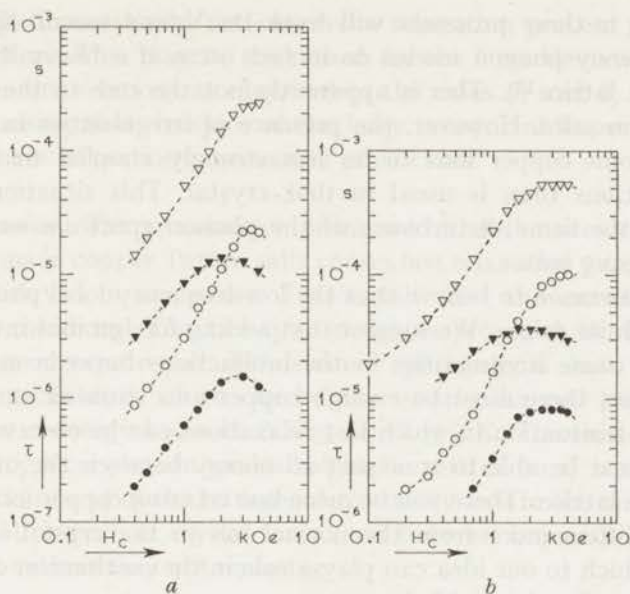


Fig. 6. Relaxation time τ_L vs. external magnetic field H_c for copper Tutton salts with ammonium impurities.

- a) $\text{CuK}_2(\text{SO}_4)_2 \cdot 6\text{H}_2\text{O} + 10\% \text{NH}_4$: \blacktriangledown ($T = 20.5 \text{ K}$) and \triangledown ($T = 4.2 \text{ K}$);
 $\text{CuK}_2(\text{SO}_4)_2 \cdot 6\text{H}_2\text{O} + 40\% \text{NH}_4$: \bullet ($T = 20.5 \text{ K}$) and \circ ($T = 4.2 \text{ K}$);
 b) $\text{CuCs}_2(\text{SO}_4)_2 \cdot 6\text{H}_2\text{O} + 40\% \text{NH}_4$: \blacktriangledown ($T = 20.1 \text{ K}$) and \triangledown ($T = 4.3 \text{ K}$);
 $\text{CuRb}_2(\text{SO}_4)_2 \cdot 6\text{H}_2\text{O} + 40\% \text{NH}_4$: \bullet ($T = 14.8 \text{ K}$) and \circ ($T = 4.2 \text{ K}$).

frequency ω_m of the Debye phonon spectrum. In the case of a Kramers salt they suggest a T^{-5} dependence for the spin-lattice relaxation time at temperatures above $\hbar\omega_\lambda/k$, changing into a T^{-13} dependence at $T \ll \hbar\omega_\lambda/k$. These temperature dependences have not been observed in the impure Tutton salts. However, if one combines the derivation given by Castle *et al.* with a different assumption for the perturbation hamiltonian as a function of the phonon frequency, an exponential temperature dependence of the relaxation time might occur also. Such an exponential temperature dependence is similar to that proposed by Feldman *et al.*¹⁰) in the case of high frequency local phonon modes.

In the figs. 1 to 4 the fast relaxation processes have been described by an exponential temperature dependence: $\tau_L \propto (\exp(\Delta/kT) - 1)$. The agreement is reasonable if for Δ/k values between 3 K and 7 K are taken. In some cases the relaxation times become temperature independent. De Vries¹⁾ interpreted this part of the τ_L vs. T curve as a cross-relaxation mechanism between the two spin-systems.

One may conclude that nonmagnetic impurities cause defects which enhance the influence of phonons around a frequency ω_λ . These low-frequency phonon modes can give rise to the observed fast relaxations; the copper ions

participating in these processes will form De Vries's second spin-system.

Low-frequency phonon modes do in fact occur if a heavy ion is introduced into a lattice¹¹). This is apparently not the case in the impurified copper Tutton salts. However, the presence of irregularities in the crystal may cause some copper ions to be less strongly coupled to their equilibrium positions than is usual in that crystal. This situation leads effectively to the same disturbance of the phonon spectrum as the introduction of heavy ions.

There is no reason to believe that the low-frequency local phonon modes have one definite origin. We suggest that adding foreign ions into a crystal may always cause irregularities in the interactions between neighbouring ions. However, there must be enough copper ions situated at a distorted site to reach a situation in which fast relaxations can be observed, because these ions must be able to transport all energy between the other copper ions and the lattice. There will be more fast relaxing copper ions if the impurity ion differs more from the normal ion in the crystal lattice. The properties which to our idea can play a role in the mechanism causing fast relaxations are listed in table I.

Let us first discuss the exchange interaction (fourth row of table I). Potassium, rubidium and cesium in copper ammonium Tutton salt have a decreasing influence on τ_L while the difference in b_{ex}/C (defined as $(b_{ex}/C)_{\text{copper ammonium Tutton}} - (b_{ex}/C)_{\text{copper potassium Tutton, etc.}}$) increases. In case *e*) (40% Rb in $\text{CuK}_2(\text{SO}_4)_2 \cdot 6\text{H}_2\text{O}$), where no fast relaxations have been observed, the difference in b_{ex}/C is larger than in case *a*) (10% K in $\text{Cu}(\text{NH}_4)_2(\text{SO}_4)_2 \cdot 6\text{H}_2\text{O}$) where extremely short relaxation times have been measured. Therefore we conclude that the exchange interaction is not related to the occurrence of fastly relaxing copper ions.

Now consider in table I the figures for the orientation of the tetragonal symmetry axis (α, ψ) and the crystal ionic radii (r). The variation in α is less than 10% and will be neglected. The value of ψ in copper ammonium Tutton salt differs by approximately 40% from those observed in the other copper Tutton salts. Thus the introduction of alkali impurities in copper ammonium Tutton salt or ammonium impurities in any other Tutton salt may cause considerable irregularities in ψ . These cases coincide with the first row and the first column in table II, all showing fast relaxations. Two more cases with fast relaxations have been observed: the mixtures of potassium and cesium Tutton salts. These are just the combinations where the difference in crystal ionic radii is large (appr. 25%). Therefore one may conclude that irregularities in ψ and r are related to an enhanced influence of low-frequency phonons which cause the fast relaxation processes.

In the description of the relaxation behaviour of a paramagnet with two spin-systems as given by De Vries¹), the assumption is made that the specific heat of the second spin-system can be neglected. If this condition

is not fulfilled one should not observe a relaxation process with a single relaxation time. This may be the reason for the large deviations from the Casimir-Du Pré relations as observed in the cases *d*) and *k*). In fact it is rather surprising that, in spite of the large amount of impurity ions, one observes single relaxation processes in most cases.

4. *Conclusion.* The introduction of impurities at the sites of the monovalent cations in copper Tutton salts causes fast relaxation processes, similar to those observed in manganese Tutton salt after the introduction of potassium or rubidium. The two-spin model as proposed by De Vries describes the results quite well. The 'second' spin-systems show Orbach type relaxation mechanisms which can be due to an enhanced local strain for the phonons of energy $\hbar\omega_\lambda$ with $3 \text{ K} \leq \hbar\omega_\lambda/k \leq 7 \text{ K}$. The existence of these low-frequency local phonon modes might be related to *i*) irregularities in the orientation (α, ψ) of the tetragonal symmetry axis in the mixed crystals, and *ii*) the difference in crystal ionic radii between impurity ions and the monovalent cations they are replacing.

REFERENCES

- 1) De Vries, A. J., Livius, J. W. M., Curtis, D. A., Van Duyneveldt, A. J. and Gorter, C. J., Commun. Kamerlingh Onnes Lab., Leiden No. 356*a*; Physica 36 (1967) 65.
- 2) De Vries, A. J., Curtis, D. A., Livius, J. W. M., Van Duyneveldt, A. J. and Gorter, C. J., Commun. Leiden No. 356*b*; Physica 36 (1967) 91.
- 3) Bleaney, B., Penrose, R. P. and Plumpton, B. I., Proc. Roy. Soc. A198 (1949) 406.
- 4) Pauling, L., Nature of the chemical bond, Cornell University Press, (New York, 1945).
- 5) Benzie, R. J., Cooke, A. H. and Whitley, S., Proc. Roy. Soc. A232 (1955) 277.
- 6) Casimir, H. B. G. and Du Pré, F. J., Commun. Leiden, Suppl. No. 85*a*; Physica 5 (1938) 507.
- 7) De Vries, A. J. and Livius, J. W. M., Commun. Leiden No. 349*a*; Appl. sci. Res. 17 (1967) 31.
- 8) Brons, F., Thesis Groningen (1938).
- 9) Castle, J. G., Feldman, D. W., Klemens, P. G. and Weeks, R. A., Phys. Rev. 130 (1963) 577.
- 10) Feldman, D. W., Castle, J. G. and Murphy, J., Phys. Rev. 138 (1965) A1208.
- 11) Brout, R. and Visscher, W., Phys. Rev. Letters 9 (1962) 54.

RELAXATION MEASUREMENTS ON MnCl₂.4H₂O AND MnBr₂.4H₂O

Synopsis

Magnetic relaxation has been studied on MnCl₂.4H₂O and MnBr₂.4H₂O in the antiferromagnetic as well as in the paramagnetic state. The observed relaxation phenomena in the antiferromagnetic state cannot be described by a single relaxation time. In agreement with the relation $\tau = c_H/\alpha$ - the specific heat c_H has a sharp maximum at the magnetic phase transition - a narrow maximum of the relaxation time at the transition temperature has been found. Attempts were made to reproduce the 'second' relaxation observed by Lasheen and Van den Broek⁷) in a powdered sample of MnCl₂.4H₂O but without success. Measurements of χ_{ad} at high magnetic pulse fields confirm the existence of the so-called *b* phase in MnCl₂.4H₂O below 1.20 K.

1. *Introduction.* Investigations on these salts have been resumed to examine relaxation phenomena in both the paramagnetic and the antiferromagnetic state.

Assuming (i) that the spin-system is in internal thermal equilibrium at a spin temperature T_s , (ii) that the energy transfer per second between this spin-system and the lattice can be written as $dQ/dt = \alpha(T_s - T_{lattice})$, α being the heat transfer coefficient, and (iii) that the variations of the magnetic field are so small and so slow that non-linearities are avoided, the differential susceptibility $\bar{\chi} = \chi' - i\chi''$ in the case of spin-lattice relaxation is given by the following relations¹):

$$\begin{aligned}\chi' &= \chi_{ad} + (\chi_0 - \chi_{ad})/(1 + \omega^2\tau^2), \\ \chi'' &= (\chi_0 - \chi_{ad}) \omega\tau/(1 + \omega^2\tau^2),\end{aligned}\tag{1}$$

where:

ω is the angular frequency of the oscillating part of the external magnetic field,

χ_0 is the susceptibility at zero field,

$\bar{\chi}$ measured at frequencies $\omega \gg \tau^{-1}$ approaches the adiabatic susceptibility χ_{ad} , which is equal to $(c_M/c_H) \chi_0$; c_M and c_H being the specific heats of the spin-system at constant magnetization and constant external magnetic field respectively,

and τ is the spin-lattice relaxation time, equal to c_H/α .

The variations of χ'/χ_0 and χ''/χ_0 with frequency are called dispersion and absorption respectively.

2. The field-step method and the character of the results to be expected.

Relaxation times above about 10^{-2} s can be determined by observing the exponential recovery of χ_{ad} as a function of time after a small step change of the external magnetic field²). At the moment $t_0 + \Delta t$, immediately after the step change at t_0 with $\Delta t \ll \tau$ - no energy being transferred between spin-system and lattice - the spin temperature T_s has changed by:

$$\Delta T_s = - \frac{T_s}{c_H} \left(\frac{\partial M}{\partial T_s} \right)_{H_e} \Delta H_e.$$

At the same moment χ_{ad} has varied by:

$$\Delta \chi_{ad} = \left(\frac{\partial \chi_{ad}}{\partial H_e} \right)_{T_s} \Delta H_e + \left(\frac{\partial \chi_{ad}}{\partial T_s} \right)_{H_e} \Delta T_s.$$

For $t > t_0 + \Delta t$ the spin temperature relaxes towards the original value $T_s(t < t_0) = T_0$ with a time constant τ , the spin-lattice relaxation time. For χ_{ad} as a function of time one finds:

$$\Delta \chi_{ad}(t) = \left(\frac{\partial \chi_{ad}}{\partial H_e} \right)_{T_s} \Delta H_e - \frac{T_s}{c_H} \left(\frac{\partial M}{\partial T_s} \right)_{H_e} \left(\frac{\partial \chi_{ad}}{\partial T_s} \right)_{H_e} \Delta H_e e^{-(t-t_0)/\tau}, \quad (2)$$

thus

$$\Delta \chi_{ad}(t = \infty) = \left(\frac{\partial \chi_{ad}}{\partial H_e} \right)_{T_s} \Delta H_e. \quad (3)$$

In order to describe qualitatively the observed behaviour of χ_{ad} after a step change of the magnetic field H_e for the paramagnetic and the antiferromagnetic state, we shall consider the signs of the derivatives in eq. (2). $\text{MnCl}_2 \cdot 4\text{H}_2\text{O}$ and $\text{MnBr}_2 \cdot 4\text{H}_2\text{O}$ approximately obey a Curie-Weiss law above the Néel-temperature T_N . In that case $(\partial M/\partial T_s)_{H_e}$ has a negative value. Assuming the Curie-Weiss law to be valid and applying the Casimir-Du Pré formalism¹) one can derive:

$$\chi_{ad}(T_s, H_e) = C \left[(T_e - \theta) \left\{ 1 + H_e^2 \frac{b}{C} \left(\frac{T_s}{T_s - \theta} \right)^{-3} \right\} \right]^{-1} \quad (4)$$

where C is Curie's constant, b is given by $c_M = b/T_s^2$ and $(b/C)(T_s/(T_s - \theta))^{-3}$

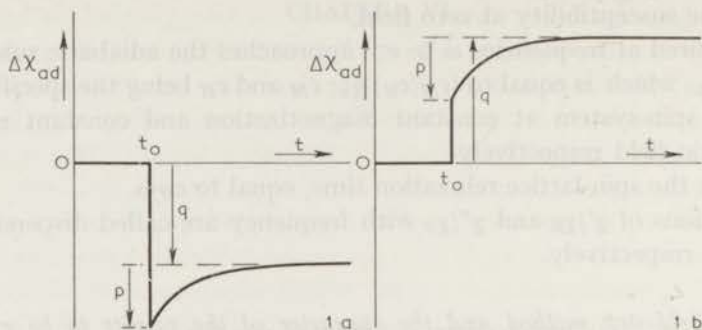


Fig. 1. Schematic view of the variation of $\Delta\chi_{ad}$ after a step ΔH in field.

1a: paramagnetic state 1b: antiferromagnetic state

$$q: \left(\frac{\partial \chi_{ad}}{\partial H_c} \right)_{T_s} \Delta H$$

$$p: \left(\frac{\partial \chi_{ad}}{\partial T_s} \right)_{H_c} \Delta T_s$$

is the measured value of b/C , uncorrected for deviations from Curie's law³). Differentiating eq. (4) shows that both $(\partial \chi_{ad} / \partial T_s)_{H_c}$ and $(\partial \chi_{ad} / \partial H_c)_{T_s}$ have a negative value. The derivatives in eq. (2) have been determined experimentally in the antiferromagnetic state with the external field along the preferred axis. Measurements of χ_0 and χ_{ad} as a function of the magnetic field yield positive values for $(\partial M / \partial T_s)_{H_c}$, $(\partial \chi_{ad} / \partial T_s)_{H_c}$ and $(\partial \chi_{ad} / \partial H_c)_{T_s}$. From these results the signs of the terms in eq. (2) can be determined. For the paramagnetic state both terms of $\Delta\chi_{ad}(t)$ have a negative value so we obtain a curve of $\Delta\chi_{ad}$ vs. time as sketched in fig. 1a. For the antiferromagnetic state $(\partial \chi_{ad} / \partial H_c)_{T_s} \Delta H_c$ has a positive value but the second term is negative so we get a behaviour of $\Delta\chi_{ad}$ as indicated in fig. 1b.

3. *Experimental results.* 3.1. Relaxation measurements. The following specimens have been examined:

- MnCl₂·4H₂O single crystal with the external magnetic field $H_c // c$ axis,
- MnCl₂·4H₂O powder,
- MnBr₂·4H₂O single crystal with $H_c // c$ axis.

Specific-heat measurements by Friedberg and Wasscher⁴) and magnetization measurements by Henry⁵) and Gijnsman⁶) showed the antiferromagnetic behaviour of these salts with the c axis as the magnetically preferred axis.

Relaxation times longer than 10^{-2} s have been determined by means of the field-step method, shorter relaxation times have been derived by using the dispersion-absorption method²). Measurements have been performed at the temperatures of liquid helium, hydrogen and nitrogen and between those temperatures by means of the 'running method'²), *i.e.* by slowly warming up the sample from a low temperature.

We could reach fields just above 20 kOe by using a liquid nitrogen cooled

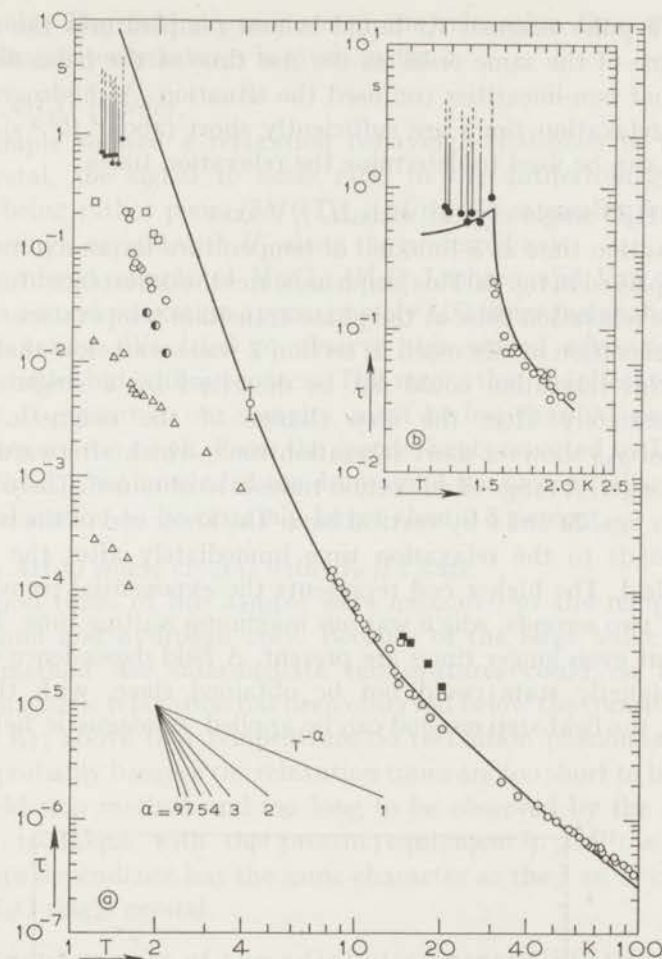


Fig. 2a. Relaxation time vs. temperature for various $\text{MnCl}_2 \cdot 4\text{H}_2\text{O}$ and $\text{MnBr}_2 \cdot 4\text{H}_2\text{O}$ samples.

- paramagnetic relaxation time of $\text{MnCl}_2 \cdot 4\text{H}_2\text{O}$; $H_c \parallel c$ axis; $H_c = 4$ kOe.
 - | antiferromagnetic relaxation time of $\text{MnCl}_2 \cdot 4\text{H}_2\text{O}$; $H_c \parallel c$ axis; $H_c = 4$ kOe;
 - a detailed explanation is given in section 3.
 - $\text{MnCl}_2 \cdot 4\text{H}_2\text{O}$; $H_c \parallel c$ axis; $H_c = 4.5$ kOe; results of Lasheen and Van den Broek⁸).
 - △ $\text{MnCl}_2 \cdot 4\text{H}_2\text{O}$; powder; $H_c = 4.5$ kOe; results of Lasheen and Van den Broek⁷)
 - $\text{MnBr}_2 \cdot 4\text{H}_2\text{O}$; $H_c \parallel c$ axis; $H_c = 4$ kOe.
 - id.; $H_c = 8.2$ kOe.
- $\tau^{-1} = 0.12 \times T^7 J_6(45/T) \text{ s}^{-1}$.

Fig. 2b. $\text{MnCl}_2 \cdot 4\text{H}_2\text{O}$; $H_c \parallel c$ axis; $H_c = 4$ kOe.

Relaxation times at helium temperatures, results from figure 2a on a larger temperature scale.

— curve $\propto cH/\alpha$.

magnet as a pulse magnet. At liquid helium temperatures the relaxation times become of the same order as the rise time of the pulse field (about 0.5 s), so that non-linearities confused the situation. At hydrogen temperatures the relaxation times are sufficiently short (about 10^{-5} s), thus the pulse fields can be used to determine the relaxation times.

a) $\text{MnCl}_2 \cdot 4\text{H}_2\text{O}$ single crystal with $H_c \parallel c$ axis.

The relaxation time as a function of temperature for an external field of 4 kOe is displayed in fig. 2a. This graph indicates the occurrence of a maximum value of the relaxation time at the phase-transition temperature. Antiferromagnetic relaxation as discussed in section 2 was seen below that temperature, but this relaxation could not be described by a single relaxation time. Immediately after the step change of the magnetic field the behaviour of χ_{ad} shows a short relaxation time, which afterwards becomes gradually longer. A range of relaxation times is so obtained. These results are indicated in figs. 2a and b by vertical bars. The lower end of the bar (symbol ●) corresponds to the relaxation time immediately after the change in magnetic field. The higher end represents the exponential recovery of χ_{ad} after about two seconds, which was our maximum waiting time. The results indicate that even longer times are present. A field dependence of τ in the antiferromagnetic state could not be obtained since, with the present equipment, the field-step method can be applied at magnetic fields around

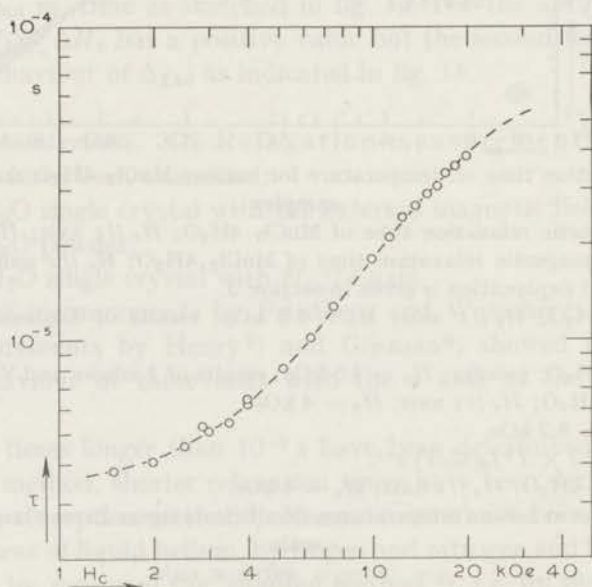


Fig. 3. Relaxation time vs. external magnetic field for $\text{MnCl}_2 \cdot 4\text{H}_2\text{O}$ at $T = 20.2$ K; $H_c \parallel c$ axis. --- curve $\propto \{(b/C)' + H_c^2\} / \{(b/C)' + 0.05 H_c^2\}$.

4.2 kOe only. The field dependence of the relaxation time measured at liquid-hydrogen temperatures is given in fig. 3.

b) $\text{MnCl}_2 \cdot 4\text{H}_2\text{O}$ powder.

This sample showed a relaxation behaviour analogous to that of the single crystal, the signal to noise ratio in the antiferromagnetic state, however, being rather poor. $(\partial M/\partial T_s)_{H_c}$ of eq. (2) is smaller for a powder than for a single crystal with H_c along the preferred axis.

In a powdered sample of $\text{MnCl}_2 \cdot 4\text{H}_2\text{O}$ Lasheen and Van den Broek⁷) observed a second relaxation approximately 100 times faster than the spin-lattice relaxation. We tried to observe this second relaxation in both chloride samples but without success. This means that the effect of the second relaxation, if present in our samples, must be less than 0.5 percent of χ_0 , the accuracy we can reach. From the specific heats reported by Lasheen and Van den Broek⁷) we concluded the decrease of the susceptibility due to this 'second' relaxation to be certainly larger than 0.5 percent.

c) $\text{MnBr}_2 \cdot 4\text{H}_2\text{O}$ single crystal with $H_c // c$ axis.

Relaxation times of this sample were measured at the temperatures of liquid helium and hydrogen only. Because of the large value of b/C the 'running method' for intermediate temperatures could not be applied. Antiferromagnetic relaxation has been observed below the transition temperature (2.0 K); above that temperature no relaxation phenomena could be detected, probably because the relaxation times are too short to be measured by the field-step method and too long to be observed by the absorption-dispersion technique with the present equipment²). On the whole the temperature dependence has the same character as the τ vs. T curve of the $\text{MnCl}_2 \cdot 4\text{H}_2\text{O}$ single crystal.

3.2. Measurements of the adiabatic susceptibility χ_{ad} . According to eq. (4), measurements on the field dependence of χ_{ad} yield values of b/C for paramagnetics following a Curie-Weiss law. The results thus obtained are given in table I. Lasheen and Van den Broek⁷) found a b/C value

TABLE I

b/C values of $\text{MnCl}_2 \cdot 4\text{H}_2\text{O}$ and $\text{MnBr}_2 \cdot 4\text{H}_2\text{O}$			
samples	T	measured value $(b/C)' = (b/C) \cdot \{(T - \theta)/T\}^3$	corrected value b/C
$\text{MnCl}_2 \cdot 4\text{H}_2\text{O}$	20.2 K	$18.8 \times 10^6 \text{ Oe}^2$	$15.1 \times 10^6 \text{ Oe}^2$
single crystal; $H_c // c$ axis	4.25 K	$41.5 \times 10^6 \text{ Oe}^2$	$14.5 \times 10^6 \text{ Oe}^2$
$\text{MnCl}_2 \cdot 4\text{H}_2\text{O}$			
powder	4.17 K	$54 \times 10^6 \text{ Oe}^2$	$18.5 \times 10^6 \text{ Oe}^2$
$\text{MnBr}_2 \cdot 4\text{H}_2\text{O}$	20.2 K	$62 \times 10^6 \text{ Oe}^2$	$44 \times 10^6 \text{ Oe}^2$
single crystal; $H_c // c$ axis	4.24 K	$170 \times 10^6 \text{ Oe}^2$	$43 \times 10^6 \text{ Oe}^2$

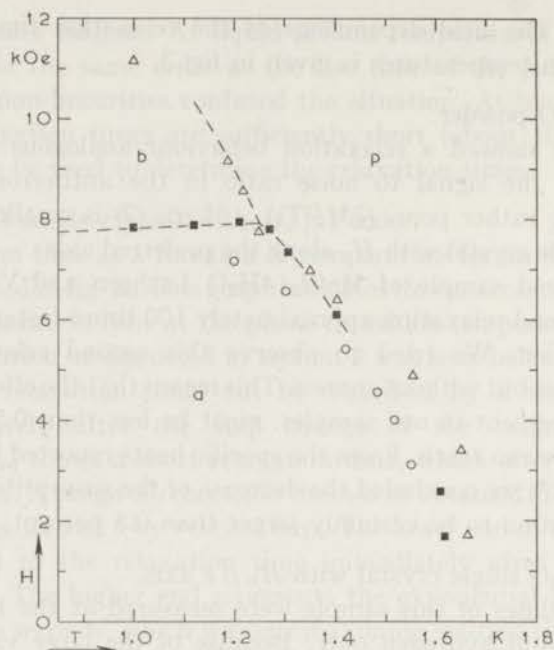


Fig. 4. Phase diagram of $\text{MnCl}_2 \cdot 4\text{H}_2\text{O}$; $H_c // c$ axis,

○ derived from χ_{ad}

■ results from E.S.R. measurements of Poulis⁶⁾

△ results from static measurements of Gijsman⁶⁾

p: paramagnetic state; *a*: antiferromagnetic state;

b: antiferromagnetic *b* phase.

of $19.5 \times 10^6 \text{ Oe}^2$ for $\text{MnCl}_2 \cdot 4\text{H}_2\text{O}$ powder. The small difference from our results may be related to the presence of the 'second' relaxation in their sample.

Measurements of χ_{ad} as a function of the external magnetic field below the Néel temperature show a maximum. Assuming that these maxima are due to the phase transition, we were able to make a phase diagram for the $\text{MnCl}_2 \cdot 4\text{H}_2\text{O}$ single crystal with $H_c // c$ axis (fig. 4). The transition line obtained in this way is found to differ notably from the conclusions drawn from the static measurements of Gijsman and the E.S.R. measurements of Poulis⁶⁾.

The results on χ_{ad} obtained with the pulse magnet at helium temperatures are influenced by heating or cooling of the spin-system, as already has been mentioned. In fig. 5 measurements of χ_{ad} at a temperature of the bath of 1.20 K show a second maximum in the χ_{ad} vs. H curve. This second maximum of χ_{ad} confirms the transition to the so-called *b* phase⁹⁾ below 1.20 K, between the antiferromagnetic and the paramagnetic phase, where the spins are orientated nearly perpendicular to the preferred axis. During the begin of the increasing pulse field the sample is antiferromagnetic, and we may

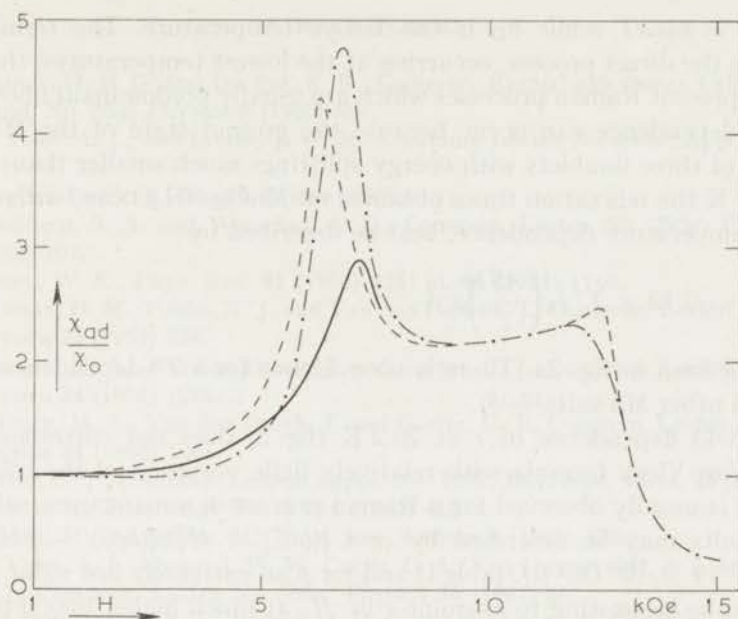


Fig. 5. χ_{ad}/χ_0 vs. external magnetic field for $\text{MnCl}_2 \cdot 4\text{H}_2\text{O}$ at 1.20 K.

- · — increasing pulse field
- decreasing pulse field
- quasistatic field

expect the spin temperature to become lower than 1.20 K, *cf.* eq. (2). At the highest fields, however, the sample is paramagnetic, and thus the decreasing pulse field will initially cool the spin-system again. The adiabatic susceptibility at 4.2 K reveals the cooling of the spin-system during the decreasing pulse field to be approximately 1.5 K. From this result, the specific heat¹⁴⁾ and measurements of M vs. T ⁶⁾, one can estimate the cooling to be 0.15 K at a bath temperature of 1.2 K. Our measurements showed the transition from the b phase to the paramagnetic state to occur at 12 kOe. According to Gijsman⁶⁾ this field is to be expected for a temperature of *appr.* 1.0 K, a value which might occur indeed in the undercooled spin-system.

4. *Discussion of the relaxation measurements.* For a Mn^{2+} -salt one expects, since it is a Kramers-salt and the Mn^{2+} -ion is an S-state ion, the spin-lattice relaxation time at high external magnetic fields to be¹⁰⁾:

$$\tau^{-1} = aH^4T + bT^5J_4(\theta_D/T) + cH^2T^7J_6(\theta_D/T) \quad (5)$$

with:

$$J_n(\theta_D/T) = \int_0^{\theta_D/T} \frac{x^n e^x}{(e^x - 1)^2} dx,$$

where $x = \hbar\omega/kT$ while θ_D is the Debye temperature. The term aH^4T indicates the direct process, occurring at the lowest temperatures, the other terms represent Raman processes which are usually predominant above 4 K. The T^5 -dependence can occur because the ground state of the Mn^{2+} -ion consists of three doublets with energy splittings much smaller than kT (11). Above 4 K the relaxation times obtained on $MnCl_2 \cdot 4H_2O$ can, with respect to the temperature dependence, best be described by:

$$\tau^{-1} = 0.12 \times T^7 J_6 \left(\frac{45}{T} \right) s^{-1}$$

as can be seen in fig. 2a. There is no evidence for a T^5 -dependence as was found in other Mn-salts^{12,13}).

The field dependence of τ at 20.2 K (fig. 3) does not correspond to a Brons-Van Vleck formula with relatively little variation of the relaxation time, as is usually observed for a Raman process in a manganese salt^{12,13}). The results may be described by: $\tau \propto \{(b/C)' + H_c^2\} / \{(b/C)' + p H_c^2\}$ with $(b/C)' = 19 \times 10^6 \text{ Oe}^2$ (cf. table I) and for p an extremely low value of 0.05. It would be interesting to examine τ vs. H_c at much higher magnetic fields to check whether the $\tau \propto H_c^{-2}$ dependence (eq. (5)) is fulfilled.

Below the phase-transition temperature the observed relaxation behaviour of χ_{ad} : immediately after the field step a short relaxation time which gradually becomes longer, might indicate that the contact mechanism with the helium bath is not identical for all Mn^{2+} -ions.

The relaxation time τ is usually identified with c_H/α (1). We shall use this relation in order to estimate the temperature dependence of the relaxation time around the transition temperature. In the paramagnetic region above 1.6 K $\tau \propto T^{-3.5}$, which implies that α is proportional to $T^{+1.5}$. At the transition temperature c_H shows a sharp maximum. For $MnCl_2 \cdot 4H_2O$ c_H at an external field of 3.84 kOe is known from the experiments of Miss Voorhoeve¹⁴). If the heat transfer coefficient α has the same temperature dependence in paramagnetic and antiferromagnetic state and does not show a singularity at the phase transition, we can derive the temperature dependence of τ . The curve so obtained has been inserted in fig. 2b; the agreement with the experimental results is quite reasonable, especially if below 1.53 K the shortest relaxation times are taken into account. More knowledge of the relaxation behaviour below the Néel temperature is required to explain the observed times in more detail. This might be obtained from investigations on specimens with higher Néel temperatures, which allow the study of antiferromagnetic relaxation over a wider range of temperatures.

REFERENCES

- 1) Casimir, H. B. G. and Du Pré, F. K., Commun. Kamerlingh Onnes Lab., Leiden, Suppl. No. 85a; Physica 5 (1938) 507.
- 2) De Vries, A. J., and Livius, J. W. M., Commun. Leiden No. 349a; Appl. sci. Res. 17 (1967) 31.
- 3) Van den Broek, J., Thesis, Leiden (1960).
- 4) Friedberg, S. A. and Wasscher, J. D., Commun. Leiden No. 293c; Physica 19 (1953) 1072.
- 5) Henry, W. E., Phys. Rev. 91 (1953) 435; id. 94 (1954) 1146.
- 6) Gijsman, H. M., Poulis, N. J. and Van den Handel, J., Commun. Leiden No. 317b; Physica 25 (1959) 954.
- 7) Lasheen, M. A., Van den Broek, J. and Gorter, C. J., Commun. Leiden No. 312c; Physica 24 (1958) 1076.
- 8) Lasheen, M. A., Van den Broek, J. and Gorter, C. J., Commun. Leiden No. 312b; Physica 24 (1958) 1061.
- 9) Gorter, C. J., Commun. Leiden, Suppl. No. 107b; Rev. mod. Phys. 25 (1953) 277.
- 10) Orbach, R., Proc. Roy. Soc. A 264 (1961) 458.
- 11) Orbach, R. and Blume, M., Phys. Rev. Letters 8 (1962) 478.
- 12) De Vries, A. J., Livius, J. W. M., Curtis, D. A., Van Duyneveldt, A. J. and Gorter, C. J., Commun. Leiden No. 356a; Physica 36 (1967) 65.
- 13) Van Duyneveldt, A. J., Tromp, H. R. C. and Gorter, C. J., Commun. Leiden No. 374b; Physica 45 (1969) 272.
- 14) Voorhoeve, Miss W. H. M. and Dokoupil, Z., Commun. Leiden No. 328b; Physica 27 (1961) 777.

SAMENVATTING

In dit proefschrift worden resultaten besproken, die verkregen zijn met de door A. J. de Vries ontworpen brug voor het meten van paramagnetische relaxatie met karakteristieke tijden tussen 10^{-3} s en 10^{-7} s. De onderzochte relaxatieverschijnselen kunnen in twee groepen worden ingedeeld: 1) Spin-rooster relaxatie, waarbij de paramagnetische ionen energie uitwisselen met het kristalrooster, en 2) 'Cross relaxatie', waarbij energie-uitwisseling tussen paramagnetische ionen optreedt als het uitwendig magneetveld geschikte waarden heeft.

In de hoofdstukken I en II worden 'cross relaxaties' in verdunde nikkel- en chroomzouten besproken. De maxima in de waargenomen krommen van de susceptibiliteit tegen het uitwendig magneetveld kunnen met behulp van de energie schema's worden toegeschreven aan 'cross relaxaties'. De exponentiële veldafhankelijkheid van de 'cross-relaxatietijd' wordt bevestigd. In $\text{Ni}_3\text{La}_2(\text{NO}_3)_{12} \cdot 24\text{H}_2\text{O}$ (hoofdstuk II) treedt 'cross relaxatie' op tussen paren nikkel ionen. In dit zout zijn bij grote nikkel concentratie de 'cross relaxaties' niet meer onderling gescheiden waar te nemen.

In de hoofdstukken III tot en met VI worden verschillende aspecten van spin-rooster relaxatie behandeld. De spin-rooster relaxatie van $\text{MnSiF}_6 \cdot 6\text{H}_2\text{O}$ (hoofdstuk III) kan bij de temperaturen van vloeibaar helium beschreven worden door een 'direct' proces met een relaxatietijd, die omgekeerd evenredig is met de temperatuur. Bij hogere temperaturen wordt een 'Raman' relaxatieproces waargenomen, waarbij de relaxatietijd τ verandert met de temperatuur tot de min-vijfde macht. De resultaten van metingen aan erbium-ethylsulfaat (hoofdstuk IV) kunnen boven 4 K het best beschreven worden met een 'Orbach' relaxatieproces. Het 'directe' proces is in dit zout bij lage temperaturen tot nu toe niet waargenomen. In beide hierboven genoemde zouten worden, bij helium temperaturen, aan éénkristallen langere relaxatietijden gemeten dan aan poedervormige preparaten; een verschil, dat veroorzaakt wordt door een gebrekkig warmtecontact tussen het kristalrooster en de koelvloeistof.

De invloed, die niet-magnetische verontreinigingen hebben op de spin-rooster-relaxatietijd, wordt voor een reeks koper Tuttonzouten besproken in hoofdstuk V. In vele sterk verontreinigde zouten treden snelle relaxatie-

processen op, die een exponentieel van de temperatuur afhankelijke relaxatietijd vertonen. De snelle relaxatieprocessen blijken verband te houden met onregelmatigheden in de oriëntatie van de tetragonale symmetrie-as in de verontreinigde kristallen en met het verschil in grootte tussen de onzuiverheden en de ionen waarvan zij de plaats innemen.

In hoofdstuk VI, tenslotte, worden enkele spin-rooster-relaxatietijden in de antiferromagnetische toestand vermeld. Het was mogelijk om τ van een mangaanchloride-kristal te meten in een temperatuurgebied rondom de overgang van de paramagnetische naar de antiferromagnetische toestand. De zo verkregen kromme van τ tegen de temperatuur heeft een relatief maximum, dat analoog aan het maximum in de soortelijke warmte verloopt. De relaxatie bij hogere temperaturen kan goed worden beschreven met een 'Raman' proces, waarbij de relaxatietijd verandert met de temperatuur tot de min-zevende macht.

Op verzoek van de faculteit der Wiskunde en Natuurwetenschappen volgt hier een overzicht van mijn studie.

Na het behalen van het einddiploma H.B.S.-B aan het Dalton lyceum te 's-Gravenhage in 1959 begon ik aan mijn studie aan de Rijksuniversiteit te Leiden. In april 1963 legde ik het kandidaatsexamen af in de Natuur- en Wiskunde met bijvak Sterrekunde.

Sinds die tijd ben ik werkzaam op het Kamerlingh Onnes Laboratorium in de werkgroep 'paramagnetische relaxatie' onder de leiding van Prof. Dr. C. J. Gorter. Aanvankelijk assisteerde ik bij metingen met de Hartshornbrug, later leerde ik omgaan met de meetopstelling van Dr. Ir. A. J. de Vries. Alle metingen die in dit proefschrift worden beschreven zijn met deze apparatuur uitgevoerd. Door de samenwerking met Dr. Ir. A. J. de Vries heb ik de charme van de experimentele Natuurkunde leren kennen.

Vanaf januari 1964 assisteerde ik op het natuurkunde practicum voor prekandidaten.

Eind 1965 begon ik het onderzoek naar 'cross-relaxatie' verschijnselen in verdunde éénkristallen. Na mijn doctoraalexamen in maart 1966 is daarnaast het onderzoek op het gebied van de paramagnetische spin-rooster relaxatie voortgezet.

Na het vertrek van Dr. Ir. A. J. de Vries in oktober 1965 heb ik veel steun gehad aan de samenwerking met Dr. D. A. Curtis; de discussies met Dr. J. C. Verstelle en Dr. W. J. Huiskamp stelde ik altijd zeer op prijs. De metingen werden verricht met assistentie van drs. J. Soeteman en drs. H. R. C. Tromp en later van de heren H. M. C. Eijkelhof en C. L. M. Pouw. Drs. J. J. Lodder besteedde veel tijd en zorg aan de uitwerking van een computerprogramma om meervoudige relaxatie-processen te analyseren. Het cryogene gedeelte van de experimenten werd verzorgd door de heren D. de Jong en W. Elbers. Alle preparaten zijn vervaardigd door mevr. J. C. Burger-Bronkhorst en mevr. M. A. Otten-Scholten. De heer W. F. Tegelaar zorgde voor de tekeningen van het proefschrift en mej. S. M. J. Ginjaar voor het manuscript. De engelse tekst werd gecorrigeerd door Dr. D. A. Curtis.

SOLLINGEN

De analyse van Verrey dat de veldmetrische relaties in kleine Tintinnaria met een ingesloten klein te vinden ook het Waalveld van het noordelijke P. en voldoende gemiddeld door de waarnemingen.

J. J. de Vries, J. A. Kruis, J. W. de Vries, A. J. van
Dijk, en C. J. Groot, *Verrey* 28 (1941) 22.
E. Verrey, *Verrey* 28 (1941) 22.

II

De het waalveld met zijn veldmetrische relaties in het gebied van
de veldmetrische relaties van Verrey, die van hoger op de 40's.

De veldmetrische relaties in het gebied van Verrey.

III

De veldmetrische relaties van Verrey met zijn veldmetrische relaties
van Verrey, die van Verrey met zijn veldmetrische relaties.

J. J. de Vries, J. A. Kruis, J. W. de Vries, A. J. van
Dijk, en C. J. Groot, *Verrey* 28 (1941) 22.

IV

De veldmetrische relaties van Verrey met zijn veldmetrische relaties
van Verrey, die van Verrey met zijn veldmetrische relaties.
De veldmetrische relaties van Verrey met zijn veldmetrische relaties.
De veldmetrische relaties van Verrey met zijn veldmetrische relaties.

J. J. de Vries, J. A. Kruis, J. W. de Vries, A. J. van
Dijk, en C. J. Groot, *Verrey* 28 (1941) 22.
E. Verrey, *Verrey* 28 (1941) 22.

Op verzoek van de faculteit der Wetenschappen vertaamt de beschrijver met hier een overzicht van zijn studie.

Na het behalen van het eindexamen H.B.S.-II aan het Duitse Instituut te Groningen in 1959 begon ik aan mijn studie aan de Rijksuniversiteit te Leiden. In april 1960 legde ik het kandidaatsexamen af in de Natuur- en Wiskunde met bijvak Sterrenkunde.

Sinds die tijd ben ik werkzaam op het Koninklijk Onderzoeksinstituut in de wiskgroep 'paradijgmatische relaties' onder de leiding van Prof. Dr. G. J. Groot. Aanvankelijk was ik bij betrokken met de Hattisberkryg, later begon ik omgaan met de methode van Dr. H. A. J. de Vries. Zijn meeningen die in dit proefschrift worden beschreven zijn met deze apparatus afgevoerd. Het is de samenwerking met Dr. H. A. J. de Vries bij ik de laatste van de experimentele Natuurkunde begin kennen.

Vanaf januari 1964 concentreerde ik op het natuurkundige practicum voor prekalculaten.

Eind 1962 begon ik het onderzoek naar 'isocorrelante' verschijnselen in vloeibare kristallen. Na twee jaarsverbanden in maart 1965 is deze zaak het verlaten ik op het gebied van de paradijgmatische optiek voor de laatste verlaten.

Na het vertrek van Dr. H. A. J. de Vries in oktober 1965 heb ik veel steun gehad aan de samenwerking met Dr. D. A. Curtis, de directeur van Dr. J. C. Verbeke en Dr. W. J. Huisman stelde ik altijd zeer op prijs. De meeningen welke verteld met assistentie van Drs. J. S. J. van der Wal, Dr. H. C. van der Meer van de heer H. M. C. F. de Boer en C. L. M. P. van der Wal, J. J. L. de Boer bestaande veel tijd en zorg aan de samenwerking van een computerprogramma om met vloeibare isocorrelante verschijnselen te werken. Het experimenteel onderzoek van de experimenten den werd verzorgd door de heren Dr. de Jong en W. de Boer. Alle preparaten zijn vervaardigd door mevr. J. C. B. van der Wal, J. J. L. de Boer en mevr. M. A. G. van der Wal. De heer W. F. T. van der Wal heeft de tekeningen van het proefschrift en mevr. S. M. J. van der Wal van het manuscript. De Engelse tekst werd gecorrigeerd door Dr. D. A. Curtis.

STELLINGEN

I

De conclusie van Verwey dat de spin-rooster relaxatie in koper Tutton zou-
ten toegeschreven dient te worden aan het Waller-Al'tshuler mechanisme, is
onvoldoende gemotiveerd door de waarnemingen.

A. J. de Vries, D. A. Curtis, J. W. M. Livius, A. J. van
Duyneveldt en C. J. Gorter, *Physica* 36 (1967) 91.
E. Verwey, proefschrift, Amsterdam 1969.

II

Bij het onderzoek naar spin-rooster relaxatieverschijnselen is het gewenst om
ook gebruik te maken van magneetvelden, die veel hoger zijn dan 4 kOe.

Dit proefschrift hoofdstukken III tot en met VI.

III

Het invoeren van een relaxatieparameter voor relatief hoge frequenties
($\rho_{h.f.}$), zoals door Van den Broek is voorgesteld, heeft weinig zin.

J. van den Broek, proefschrift, Leiden 1960.
A. J. de Vries, proefschrift, Leiden 1965.

IV

De relaxatietijden die Verwey opgeeft voor mangaan ammonium Tutton
zout, stemmen overeen met de resultaten van De Vries. De suggestie van
Verwey dat een gedeelte van de τ vs. H kromme toegeschreven dient te wor-
den aan het slechte warmtecontact tussen kristal en heliumbad, is dan ook
zeer aanvechtbaar.

A. J. de Vries, J. W. M. Livius, D. A. Curtis A. J. van
Duyneveldt, en C. J. Gorter, *Physica* 36 (1967) 65.
E. Verwey, proefschrift, Amsterdam 1969.

V

Het verdient aanbeveling om het onderzoek naar 'cross relaxaties' tussen paren koperionen in $\text{Cu}(\text{NO}_3)_2 \cdot 2\frac{1}{2}\text{H}_2\text{O}$ voort te zetten aan magnetisch verdunde kristallen. De door Amaya, c.s. voorgestelde 'cross-relaxatie' processen kunnen dan eenvoudig worden geverifieerd aan de hand van het verloop van de differentiële susceptibiliteit als functie van het uitwendig magneetveld.

K. Amaya, Y. Tokunaga, R. Yamada en T. Haseda, *Phys. letters* **28A** (1969) 732.

VI

De aanzienlijke verschillen tussen de waarden die de verschillende onderzoekers opgeven voor de magnetische term in de soortelijke warmte van koper kalium chloride, kunnen eenvoudig worden verklaard.

A. J. de Vries, proefschrift, Leiden 1965.

J. van den Broek, L. C. van der Marel en C. J. Gorter, *Physica* **27** (1961) 661.

A. R. Miedema, H. van Kempen en W. J. Huiskamp, *Physica* **29** (1963) 1266.

VII

De 'consistentie eis' die Barut en Malin invoeren bij de relativistisch quantummechanische beschrijving van elementaire deeltjes, is gebaseerd op een principiële inconsistentie.

A. O. Barut en S. Malin, *Rev. Mod. Phys.* **40** (1968) 632.

VIII

Als men bij het ontwerpen van een supergeleidende spoel met een homogeen magneetveld uitgaat van de berekeningen van B. Girard en M. Sauzade, verdient het aanbeveling uitsluitend de resultaten te gebruiken die deze auteurs in tabelvorm opgeven.

B. Girard en M. Sauzade, *Nucl. instr. and meth.* **25** (1964) 269.

IX

Kinderboeken waarin terloops het leven van mensen elders ter wereld in beeld wordt gebracht, kunnen onbewust een negatieve benadering van de vreemde medemens in de hand werken.

X

Om de relatie tussen weerstand en temperatuur van een geschikte germanium-thermometer zodanig vast te leggen dat tussen 4 en 14 K de temperatuur met een nauwkeurigheid van 1 mK kan worden bepaald, is het voldoende de thermometer in dit temperatuurgebied te ijken om de 2 K.

XI

'Kronig-Bouwkamp'- en 'cross'-relaxatieverschijnselen in sterk verdunde paramagnetische zouten die kristalwater bevatten, kunnen onderzocht worden door gebruik te maken van protonresonantie.

XII

Van der Molen vermeldt 'Kronig-Bouwkamp' relaxatietijden in chroomaluninen, waarbij de veldafhankelijkheid van τ_s afhankelijk is van de oriëntatie van het uitwendig magneetveld. Dit effect kan ten dele worden verklaard door rekening te houden met de veldafhankelijkheid van de energieverschillen die bij deze relaxaties een rol kunnen spelen.

K. van der Molen, proefschrift, Leiden 1969.

XIII

De kleuren van postzegels worden in catalogi met behulp van een zeer groot aantal namen aangeduid. Een systematische aanpak van het probleem der kleurbenamingen, waarbij een eenvoudige kleurtabel het subjectieve element grotendeels uitsluit, is uitvoerbaar.

A. J. van Duyneveldt

3 december 1969

De laatste wetten... (faint text)

H. G. van... (faint text)

De laatste wetten... (faint text)

H. G. van... (faint text)

De laatste wetten... (faint text)

H. G. van... (faint text)

De laatste wetten... (faint text)

De laatste wetten... (faint text)

De laatste wetten... (faint text)

H. G. van... (faint text)

De laatste wetten... (faint text)

